NSG-7369
JPL-954880

(NASA-CR-157465) EVALUATION OF THE PROPULSION CONTROL SYSTEM OF A PLANETARY ROVER AND DESIGN OF A MAST FOR AN ELEVATION SCANNING LASER/MULTI-DETECTOR SYSTEM (Rensselaer Polytechnic Inst., Troy, N. Y.) G3/14

N78-29131

Unclas
27170

Rensselaer Polytechnic Institute

Troy, New York 12181

RPI TECHNICAL REPORT MP-58

EVALUATION OF THE PROPULSION CONTROL SYSTEM OF A PLANETARY ROVER AND DESIGN OF A MAST FOR AN ELEVATION SCANNING LASER/MULTI-DETECTOR SYSTEM

by

D. Knaub
S. Yerazunis

A STUDY SUPPORTED BY THE
NATIONAL AERONAUTICS AND SPACE
ADMINISTRATION

Grant NSG-7369

School of Engineering
Rensselaer Polytechnic Institute
July 1978

CONTENTS

LIST OF FIGURES

SYMBOLIC NOTATION

A,B,	Points in a Kinematic link
a,b,c	Vehicle dimensions
C.G.	Center of Gravity
$\vec{F}$	Directed force on front wheel
$\vec{F}_H$	Horizontal component of F
$\vec{F}_N$	Normal component of F
$\vec{F}_T$	Tangential component of F
$\vec{F}_V$	Vertical component of F
I_F, I_R	Front and rear control systems
K_D, K_R	Front and rear feedback gains
M	Point of contact between rear wheel and ground
N	Point of contact between front wheel and ground
$\vec{P}$	Directed force
P_N	Normal component of P
$\vec{P}_T$	Tangential component of P
$\vec{R}$	Directed force on rear wheel
r	Wheel radius
$\vec{R}_H$	Horizontal component of R
$\vec{R}_N$	Normal component of R
$\vec{R}_T$	Tangential component of R
R_v	Vertical component of R
T	Torque
T_F, T_R	Torques required at front and rear wheels

T_m	Motor torque
T_s	Stall torque
$\vec{V}_A, \vec{V}_B$	Velocities of points A and B
$\vec{V}_{B/A}$	Velocity of point B with respect to point A
$\vec{V}_F, \vec{V}_R$	Velocities of front and rear wheels
$\vec{W}$	Directed force of total vehicle weight
α, β	Angles in velocity triangle
γ_F	Angle between F and F_V
γ_R	Angle between R and R_V
ρ_F	Angle between F and F_N
ρ_R	Angle between R and R_T
μ	Coefficient of static friction
μ_F, μ_R	Coefficients of static friction between ground and front and rear wheels
ϕ	Vehicle pitch
θ_F, θ_R	Angles of slopes under front and rear wheels
ω_{NL}	No load rotational speed

ACKNOWLEDGEMENT

The author wishes to express his appreciation to project advisor Dr. Stephen Yerazunis for his guidance and supervision. Thanks are also extended to several people who helped prepare this project: Mrs. Helen Hayes for the typing of the manuscript, Paul Sikora for the photographs, and Rich Lotti and Steve Markland for the drafting of most of the drawings in Appendix C. Lastly, the author would like to thank his parents, Donald and Charlotte Knaub, for their many years of encouragement and support.

ABSTRACT

Two major problems related to an autonomous rover were investigated. First, the issue of a propulsion control system capable of responding to steering, slope climbing, and irregular local terrains was addressed. An approach to this task was developed and is applied to the RPI Mars Roving Vehicle. Second, the design of the mechanical system required to implement the elevation laser scanning/multi-detector principle was undertaken and the system was constructed.

PART I

EVALUATION OF THE PROPULSION CONTROL SYSTEM OF A PLANETARY ROVER

CHAPTER 1

INTRODUCTION

1.1 Preface

A great deal of valuable scientific data and information has been obtained by the recent Viking missions to the surface of Mars. The photographs and scientific measurements taken thus far have provided the impetus for a more thorough investigation of the planet. Should a followup mission in the form of an unmanned exploration of Mars be undertaken, autonomous rovers of exceptional mobility over a broad range of terrain classes will be required.

For more than five years, studies related to autonomous roving have been conducted at Rensselaer. One of the products of this research is the present RPI Mars Roving Vehicle, or MRV. The primary function of this vehicle is to serve as a test bed for evaluating short-range hazard detection system concepts. The propulsion control system of the RPI MRV was originally designed with a degree of "softness," i.e., the ability to let the wheel speeds adjust to values appropriate for the local slopes encountered. While this type of propulsion control is entirely adequate for dealing with terrains of moderate irregularity, it may not be effective for extremely difficult terrains involving steps and other large variations of local slopes. A method of evaluating this propulsion control system has been conceived and applied to the RPI MRV.

1.2 The RPI Mars Roving Vehicle

The MRV developed at Rensselaer and shown in Figure 1 is a four-wheeled vehicle with a propulsion motor for each wheel. A gear train transfers

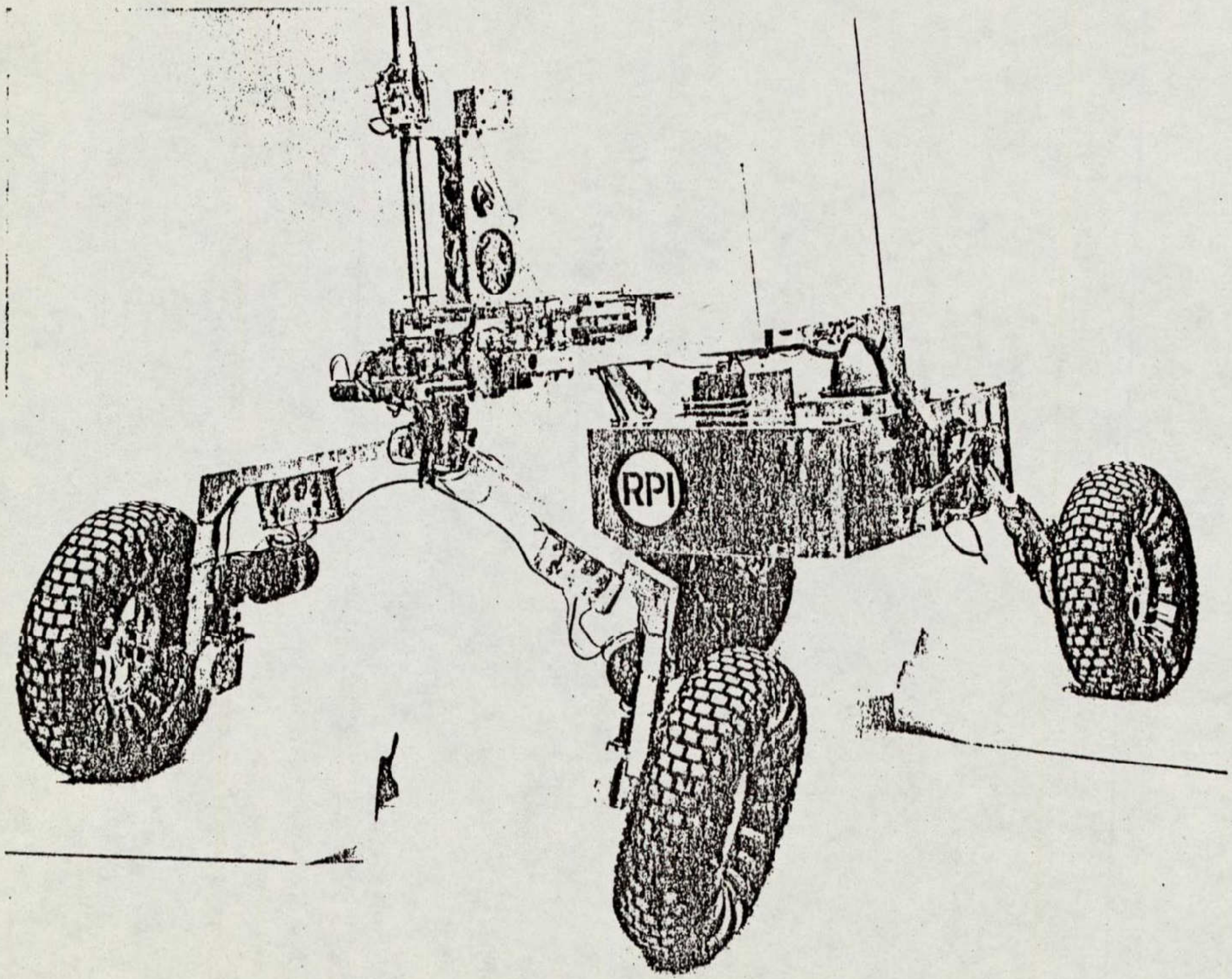

FIGURE 1

RPI Mars Roving Vehicle

power between the wheels and the motors, reducing the motors' speeds and increasing their torques. The propulsion motors are series wound DC electric motors powered by commercial electrochemical batteries carried in the vehicle's payload box.

The front axle unit of the MRV has two degrees of freedom with respect to the vehicle's main structure. The first is a pivoting motion about a vertical axis which allows the front axle unit to turn and thereby steer the vehicle. The second is a pivoting motion about a longitudinal axis of the rover which provides it with stable four-wheel contact even though the local terrain gradients under the front and rear wheels may differ by as much as 35°.

The propulsion control system is responsible for driving the individual motors at speeds which will prevent significant stretching or compressing forces on the vehicle wheel base. Any imbalance on the part of the speed of the four wheels will be to stress various rover structural components or to slip the wheels. The former can in time lead to fatigue failure of the vehicle structure whereas the latter will result in high energy consumption and unacceptable navigation errors. The control system must also provide sufficient torque to be applied to the wheels to negotiate the terrains encountered. These two conditions provide a basis for evaluating the propulsion control system.

1.3 Bicycle Model

For this initial analysis, the MRV will be constrained to move straight ahead, i.e., the vehicle will follow a specified heading vector. Although effects from turning the front axle unit to steer on irregular terrains will not be considered at this time, this aspect can later be added to the analysis. Since the vehicle is symmetric about a vertical-longitudinal plane, only one side of the vehicle need be examined. This simplification permits a two-dimensional, two-wheeled model of the rover which will henceforth be called the Bicycle Model.

It is useful to consider the wheel torques to be composed of three components. The first is the torque required to resist gravity and hold the vehicle stationary on non-level terrain. Without this torque component, a free-wheeling rover would roll backwards down a slope. The second component is the torque necessary to overcome the friction in the drive system which is manifested primarily in the bearings, gears, and soil-wheel interface. Lastly, a torque component exists which makes the transition from the case of a rover moving up a slope at constant speed to one of accelerating up the slope. In general, it will not be required to accelerate the vehicle up a slope, so this torque component and the added complexities from dynamic considerations will be ignored. A further simplification can be made since the frictional torque will be small compared to the torque component to resist gravity for the types of localized slope variations which pose the severest problems for the control system. The Bicycle Model will use only the gravity-resisting torque, which can be determined from a static analysis of the vehicle.

CHAPTER 2

MECHANICS OF THE BICYCLE MODEL

2.1 Bicycle Model as a Three Force Member

The two-wheeled Bicycle Model of the RPI MRV climbing a slope can be considered a three force member. Techniques of force analysis from classical machine dynamics can be applied to the Bicycle Model as if it were a member in some machine. This analysis provides the basis for the torque derivations in Chapter 3.

The Bicycle Model is shown climbing in Figure 2. If inertial and aerodynamic considerations are ignored, the vehicle is acted upon by only three forces: a gravitational force concentrated at the center of mass and a supporting force on each wheel. The gravitational force is equal to half of the vehicle's total weight due to symmetry. This force is completely defined at all times; its magnitude and direction are known and constant. On the other hand, the wheel forces, $\vec{R}$ and $\vec{F}$, are unknown, as their directions and magnitudes change as a function of the local terrain.

A useful relationship for these forces can be obtained by examining the case of the Bicycle Model located on an arbitrary slope with no motion. In this situation, the vehicle is in equilibrium, the vector sum of the three forces is zero, and a force triangle can be drawn as shown in Figure 3. Since only the $\frac{1}{2}W$ vector is known, there are an infinite number of ways in which a closed triangle can be formed. It will be shown in Chapter 3 that some limits can be applied to this triangle to obtain useful results.

2.2 Wheel Relationships

The soil-wheel interface is an exceedingly complex situation, as is shown in reference 1. For the sake of simplicity, phenomena such as wheel

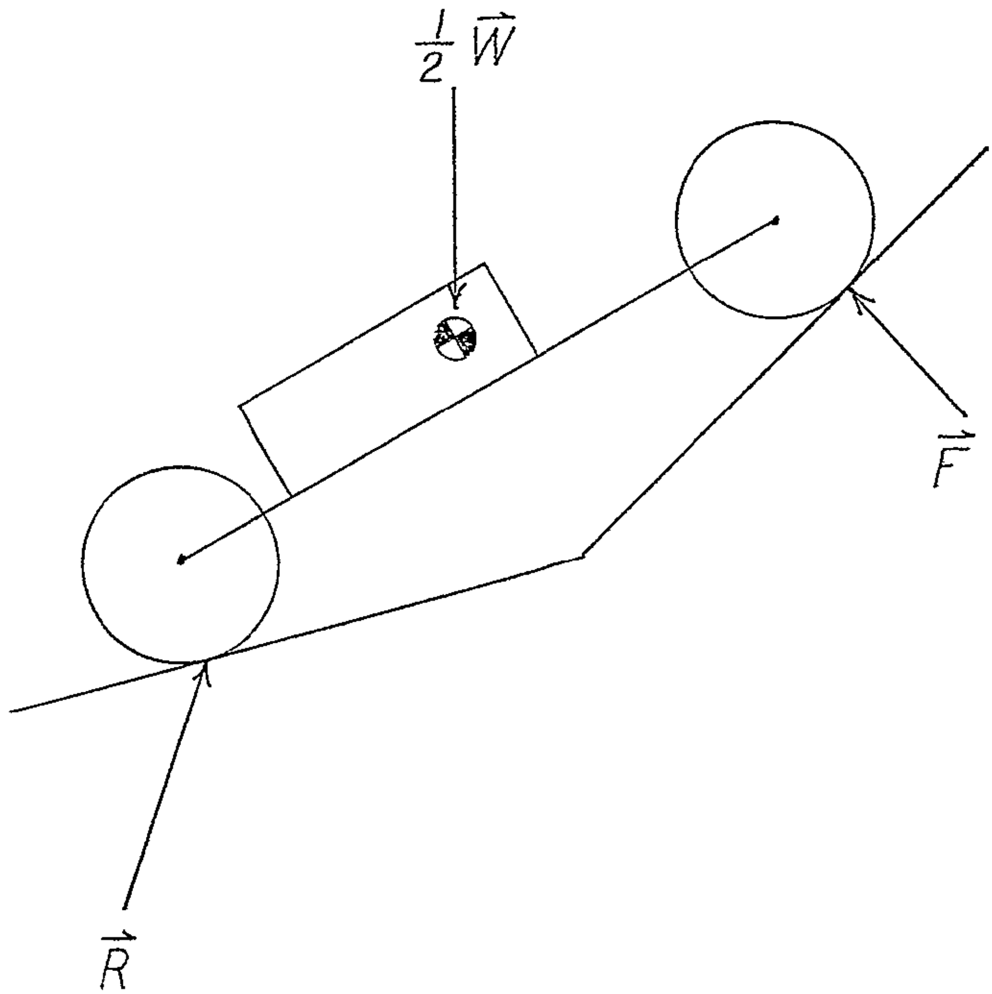

FIGURE 2

Bicycle Model Climbing a Slope

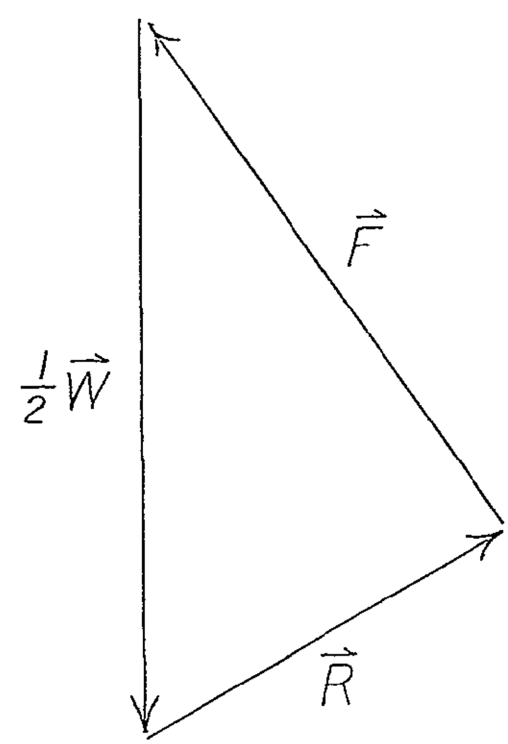

FIGURE 3

Force Triangle

bulldozing, soil compaction, and adhesion will be ignored. The Bicycle Model will be developed with wheels and terrain surfaces which are rigid and uniform. This should be adequate for a first look at the propulsion control system.

A generalized wheel is shown in Figure 4. A torque T is applied to the wheel by the motor and drive system. A force $\vec{P}$ is exerted on the wheel by the ground. This force may be broken into normal and tangential components, $\vec{P}_N$ and $\vec{P}_T$ respectively. $\vec{P}_N$ is normal to the local terrain, and its line of action passes through the wheel hub independent of the local terrain gradient. It is this component which supports the weight of the vehicle in a reference frame coincident to the sloped terrain. In contrast, $\vec{P}_T$ is parallel to the terrain, and opposes the force generated by the wheel torque. The torque and tangential force component are related by

$$T = P_T r \qquad 2.2.1$$

where r is the radius of the wheel. Note that P_T equals zero if the wheel is unpowered.

An important relationship exists between P_T and P_N. In order for the wheel not to slip with respect to the ground, the equation

$$P_T \leq \mu P_N , \qquad 2.2.2$$

where μ is the coefficient of static friction between the wheel and ground, must be satisfied. If the torque developed by the wheel is such that P_T exceeds μP_N, slippage occurs, kinetic friction is encountered, and the actual tangential force developed by the wheel on the ground is less than $\frac{T}{r}$. Slippage of a wheel not only wastes energy and torque, but it will also

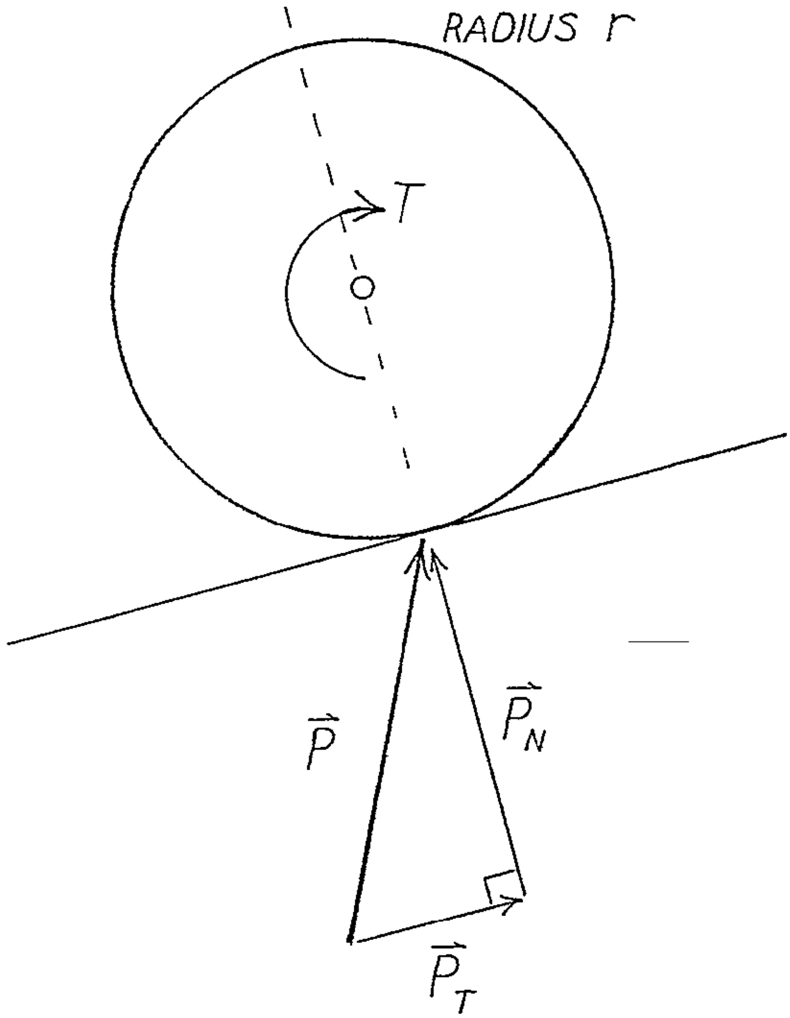

FIGURE 4

Generalized Wheel

add errors to the vehicle navigation and should be avoided.

2.3 Bicycle Model Parameters

A brief discussion of the parameters used in the Bicycle Model, Figure 5, follows.

The center of gravity, C.G., of the vehicle is defined by the distances a, b, and c. The horizontal distances of the C.G. from the wheel hubs are given by a and b, while the vertical distance above the wheel hubs is given by c. The vehicle wheel base is a+b. The radius of the wheels is r. Coefficients of static friction between the rear and front wheels and the ground are μ_R and μ_F, respectively. The magnitude of the force $\frac{1}{2}\vec{W}$ is one half of the vehicle's total weight. These parameters are all constants of the model.

Inputs to the model are the angles ϕ, θ_F, and θ_R. The pitch of the vehicle is given by ϕ, while θ_F and θ_R represent the local slope of the terrain under the front and rear wheels. All three angles can be either positive or negative, and are referenced to the horizontal in a gravity-oriented coordinate system. They are considered positive when measured in a counter-clockwise sense from the horizontal.

As before, $\vec{R}$ and $\vec{F}$ represent the total forces on the rear and front wheels. It will prove convenient to break these forces into two sets of components. The first set is relative to level ground. It gives horizontal and vertical components, denoted by the subscripts H and V respectively. The second set of components is taken with respect to the slope of the terrain immediately under the wheel. Force components normal and tangent to the ground are obtained, denoted by the subscripts N and T. Note that for the N and T components, the reference frames at the front and rear wheels will be different when θ_F and θ_R are different.

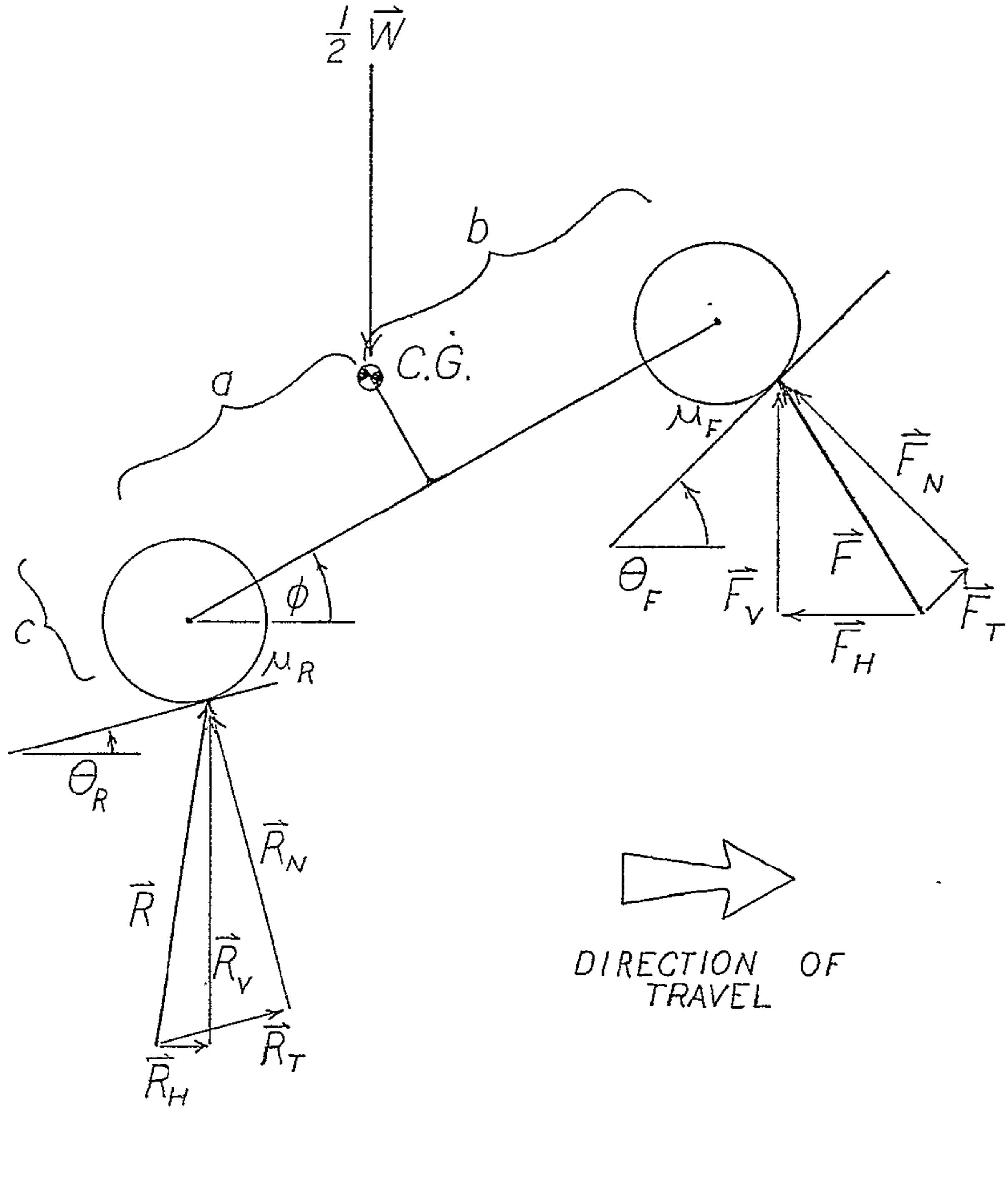

FIGURE 5

Bicycle Model Parameters

ORIGINAL PAGE IS
OF POOR QUALITY

CHAPTER 3

FORMULA DERIVATIONS

3.1 Vertical Wheel Loads

A relationship can be obtained that will help define the force triangle described in section 2.1. It involves the vertical components of the forces acting on the wheels. For any given position of the vehicle, these vertical components must sum to match one half of the total vehicle weight. In addition, these components must have values so that the overall moment on the vehicle is zero. These two conditions will completely define R_v and F_v, the vertical components of the wheel forces.

The bicycle model is shown in a generalized position in Figure 6. The wheels touch the ground at points M and N at which R_v and F_v act on the model. The value of F_v can be obtained by summing moments about point M:

$$\frac{1}{2} W(-r \sin \theta_R + a \cos \phi - c \sin \phi) - F_v(-r \sin \theta_R + (a+b)\cos \phi + r \sin \theta_F) = 0 \tag{3.1.1}$$

$$F_v = \frac{1}{2} W \frac{(a \cos \phi - c \sin \phi - r \sin \theta_R)}{((a+b)\cos \phi + r \sin \theta_F - r \sin \theta_R)} \ . \tag{3.1.2}$$

The value of R_v can now be found from

$$R_v = \frac{1}{2} W - F_v \ . \tag{3.1.3}$$

It can be seen that the components R_v and F_v are now known based solely on the geometry of the situation. Note that these equations are valid for both positive and negative slopes and vehicle pitches.

The values of R_v and F_v can be used as a check on the stability of the bicycle model on slopes. Should the model become tipped so that the

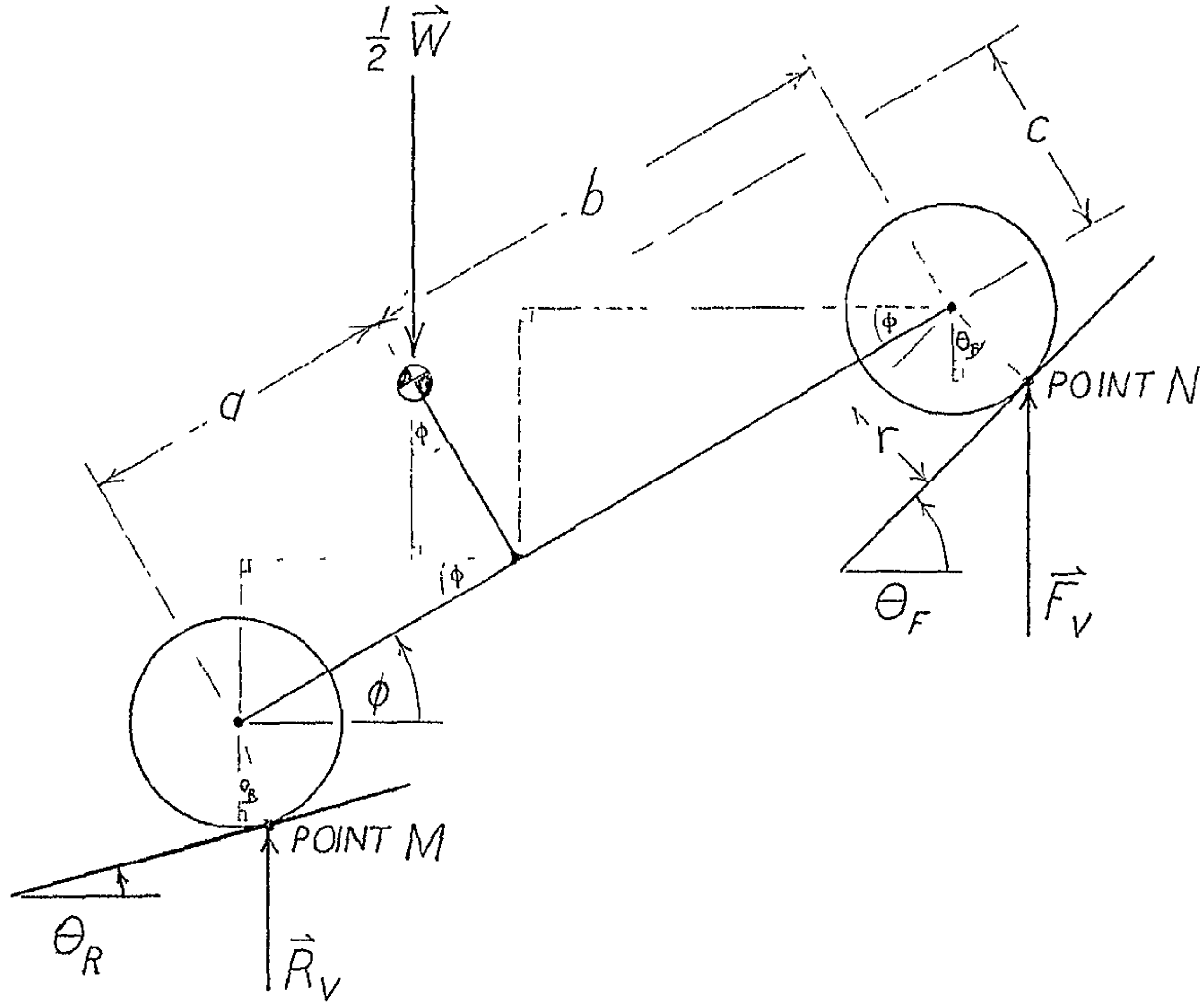

FIGURE 6

Bicycle Model in Generalized Position

center of gravity is directly above one of the wheel contact points, one component will support all the weight and the other will reduce to zero. If the model tips a little more, the zero component will have to become negative, or downward in direction, in order to maintain moment equilibrium. Since the ground can't exert a downward force on a wheel resting on it, an excess moment will result on the model and it will fall off the slope.

3.2 Wheel Speeds

An important consideration in the bicycle model is that of obtaining the correct ratio of front and rear wheel speeds when climbing obstacles. This ratio must change as different slopes are encountered; otherwise, excessive strains will be imposed on the vehicle's structure and wheels will slip. The mathematical analysis which follows relates the wheel velocity ratio to the geometry of the terrain.

A kinematic principle of mechanism analysis is that the velocity of one point in a link is equal to the velocity of another point in the link plus the relative velocity between the two points. In equation form with points A and B, this is

$$\vec{V}_B = \vec{V}_A + \vec{V}_{B/A} \qquad 3.2.1$$

where $\vec{V}_{B/A}$ is the velocity of point B with respect to point A. The frame of the Bicycle Model can be considered a link in some mechanism with the wheel hubs labeled points F and R as shown in Figure 7. As long as each wheel remains on its own constant slope, the linear velocity of a hub can represent the rotational velocity of a wheel. The rear hub velocity is $\vec{V}_R$, and it must be directed parallel to the ground under the rear wheel.

4. In like manner, the front hub velocity $\vec{V}_F$ must be directed parallel to the ground under the front wheel. The velocity of Point F with respect to Point R can be found by looking at the possible relative motions of the two points. Since they are connected by a rigid link, no relative motion of the two points along the link is allowed (they are separated by a constant distance). The only way that Point F can move relative to Point R is to rotate about it. Point F's instantaneous velocity is therefore perpendicular to the frame connecting Points F and R.

With the above information, the vector equation

$$\vec{V}_F = \vec{V}_R + \vec{V}_{F/R} \qquad 3.2.2$$

can be written. This equation is shown graphically in Figure 8. Two angles of this velocity triangle are known. The angle between the vectors $\vec{V}_F$ and $\vec{V}_R$ is $\theta_F - \theta_R$. The exterior angle between vectors $\vec{V}_{F/R}$ and $\vec{V}_R$ is $90° + \phi - \theta_R$. This is obtained by knowing the the direction of $V_{F/R}$ is $\phi + 90°$ from horizontal. The angles α and β of Figure 8 can now be determined as follows:

$$(\theta_F - \theta_R) + \alpha = 90° + \phi - \theta_R \qquad 3.2.3$$

$$\alpha = 90° + \phi - \theta_F \qquad 3.2.4$$

$$(\theta_F - \theta_R) + \alpha + \beta = 180° \qquad 3.2.5$$

$$\beta = 180° - (\theta_F - \theta_R) - \alpha \qquad 3.2.6$$

$$\beta = 180° - \theta_F + \theta_R - (90° + \phi - \theta_F) \qquad 3.2.7$$

$$\beta = 90° + \theta_R - \phi \qquad 3.2.8$$

The Law of Sines gives

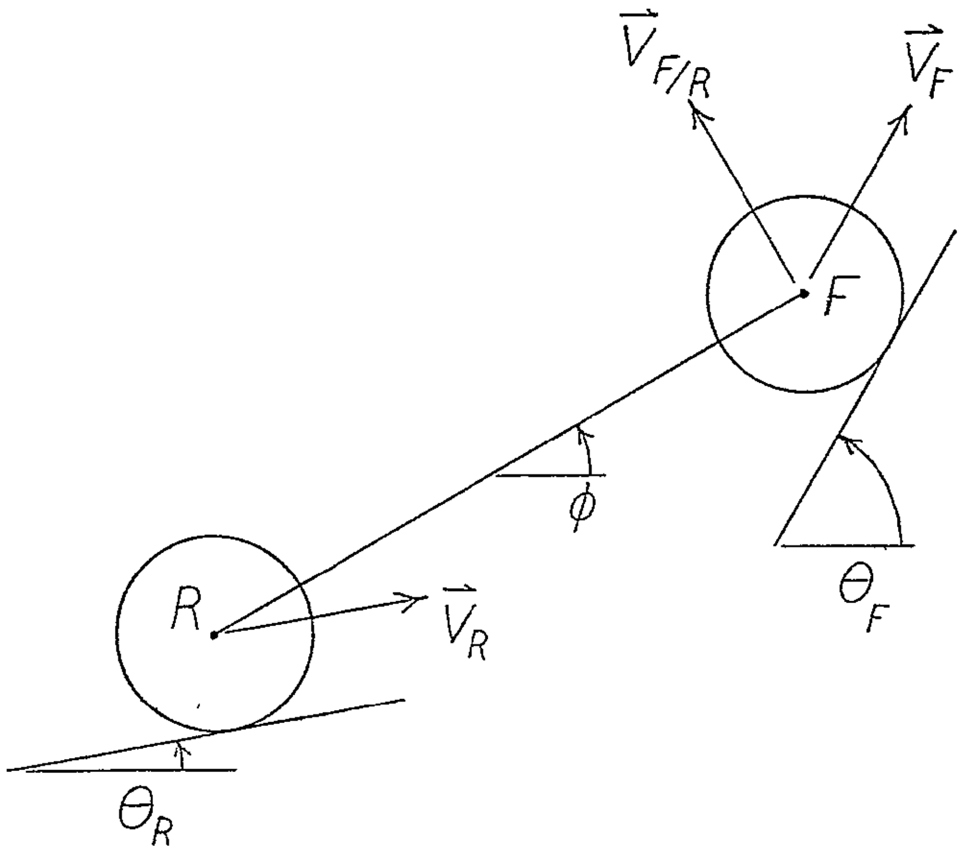

FIGURE 7

Bicycle Model Velocities

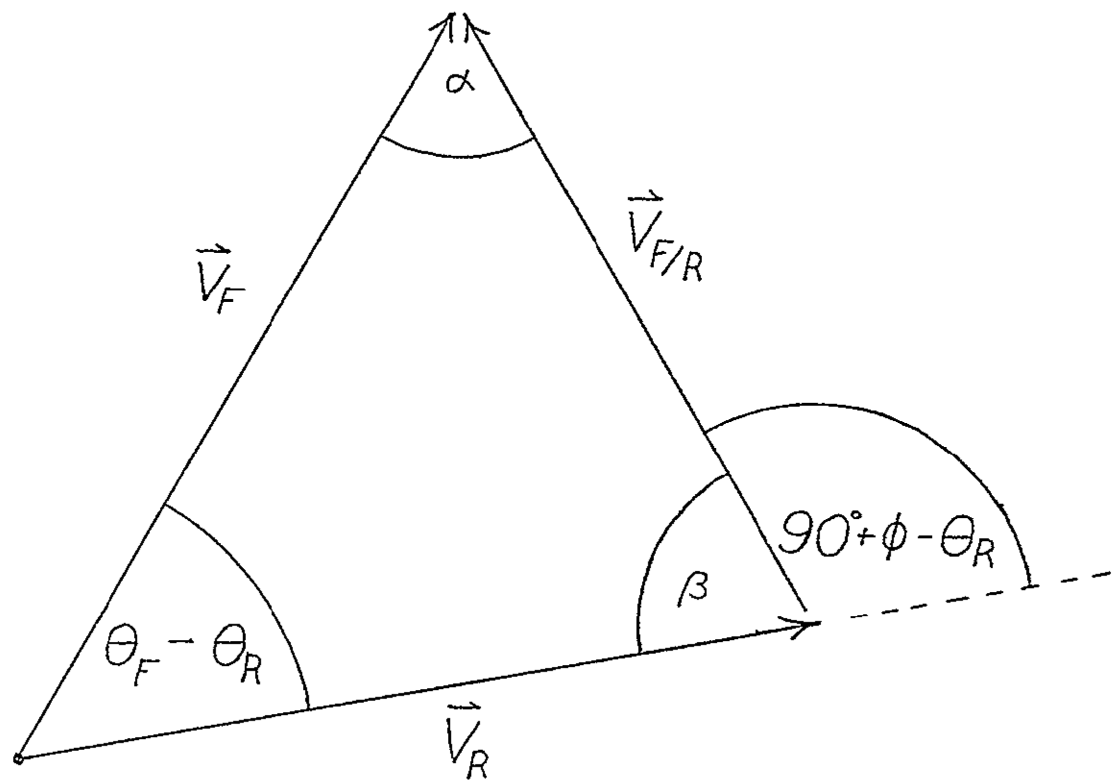

FIGURE 8

Velocity Triangle

$$\frac{V_F}{\sin\beta} = \frac{V_R}{\sin\alpha} \qquad 3.2.9$$

$$\frac{V_F}{V_R} = \frac{\sin\beta}{\sin\alpha} \qquad 3.2.10$$

$$\frac{V_F}{V_R} = \frac{\sin(90° - \phi + \theta_R)}{\sin(90° + \phi - \theta_F)} \qquad 3.2.11$$

This expression gives the ratio of the front to the rear wheel velocities in order for no wheel slipping to occur. It is dependent only on the terrain and the position of the vehicle.

3.3 Torque Relationships

It was shown in Section 2.1 that the bicycle model is acted upon by three forces only. A force triangle representing these forces can be drawn which has an infinite number of solutions. By applying the no-slip wheel conditions of Section 2.2, some limits can be placed on the solutions. The limits on the force solutions can then be used to find a range of possible wheel torques which will satisfy the given input requirements.

The equations derived in section 3.1 give the vertical components of the wheel loads, R_V and F_V, for any given position of the bicycle model. The sum of these components must equal $\frac{1}{2}W$ for equilibrium. Knowing the vertical components of the wheel loads allows a locus of possible solutions to be obtained for a given position, as shown in Figure 9. The locus is seen to be a straight line. A significant consequence of Figure 9 is that for every solution, the horizontal components of the two wheel forces are equal in magnitude but opposite in sign.

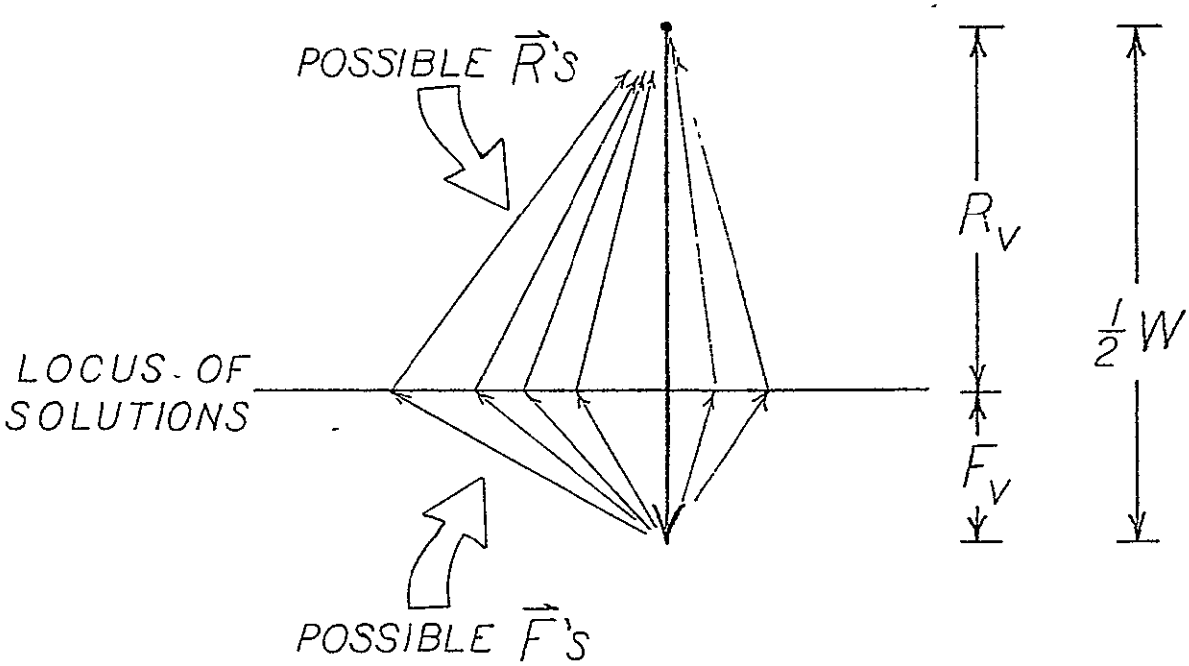

FIGURE 9

Force Triangle for a Given Position
of Bicycle Model

It will be useful now to relate the vertical-horizontal components of a wheel force to the normal-tangential components. This will be done with the aid of Figures 10 and 11. Let the angle γ be a measure of the H-V triangles. γ_R is the angle between $\vec{R}$ and $\vec{R}_V$, and γ_F is the angle between $\vec{F}$ and $\vec{F}_V$. It can be seen that

$$\gamma_R = \text{Arc Tan}\,\frac{R_H}{R_V} \qquad 3.3.1a$$

$$\gamma_F = -\,\text{Arc Tan}\,\frac{F_H}{F_V} \qquad 3.3.1b$$

A useful form of the second equation is

$$\gamma_F = -\,\text{Arc Tan}\,\frac{(-R_H)}{F_V} \qquad 3.3.2$$

$$\gamma_F = \text{Arc Tan}\,\frac{R_H}{F_V} \qquad 3.3.3$$

Let the angle ρ be a measure of the N-T triangles. ρ_R is the angle between $\vec{R}$ and $\vec{R}_T$, while ρ_F is the angle between $\vec{F}$ and $\vec{F}_N$. By introducing the slopes θ_R and θ_F into Figures 10 and 11, relationships between ρ and γ can be obtained:

$$\rho_R = 90° - \theta_R - \gamma_R \qquad 3.3.4a$$

$$\rho_F = \theta_F - \gamma_F \qquad 3.3.4b$$

Some trigonometric identities are needed:

$$\sin \rho_R = \frac{R_N}{R} \qquad 3.3.5a$$

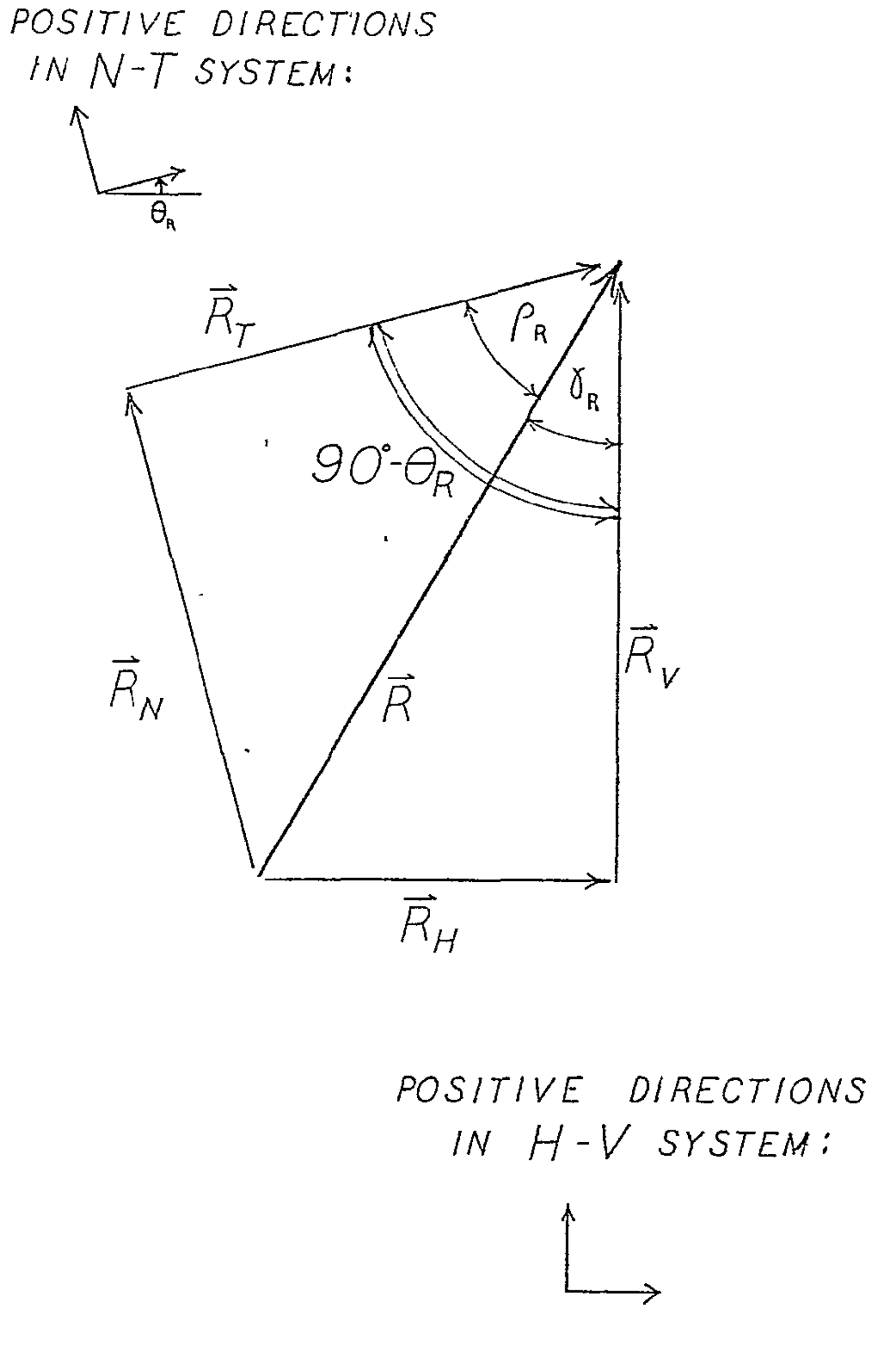

FIGURE 10

Rear Wheel Force Components

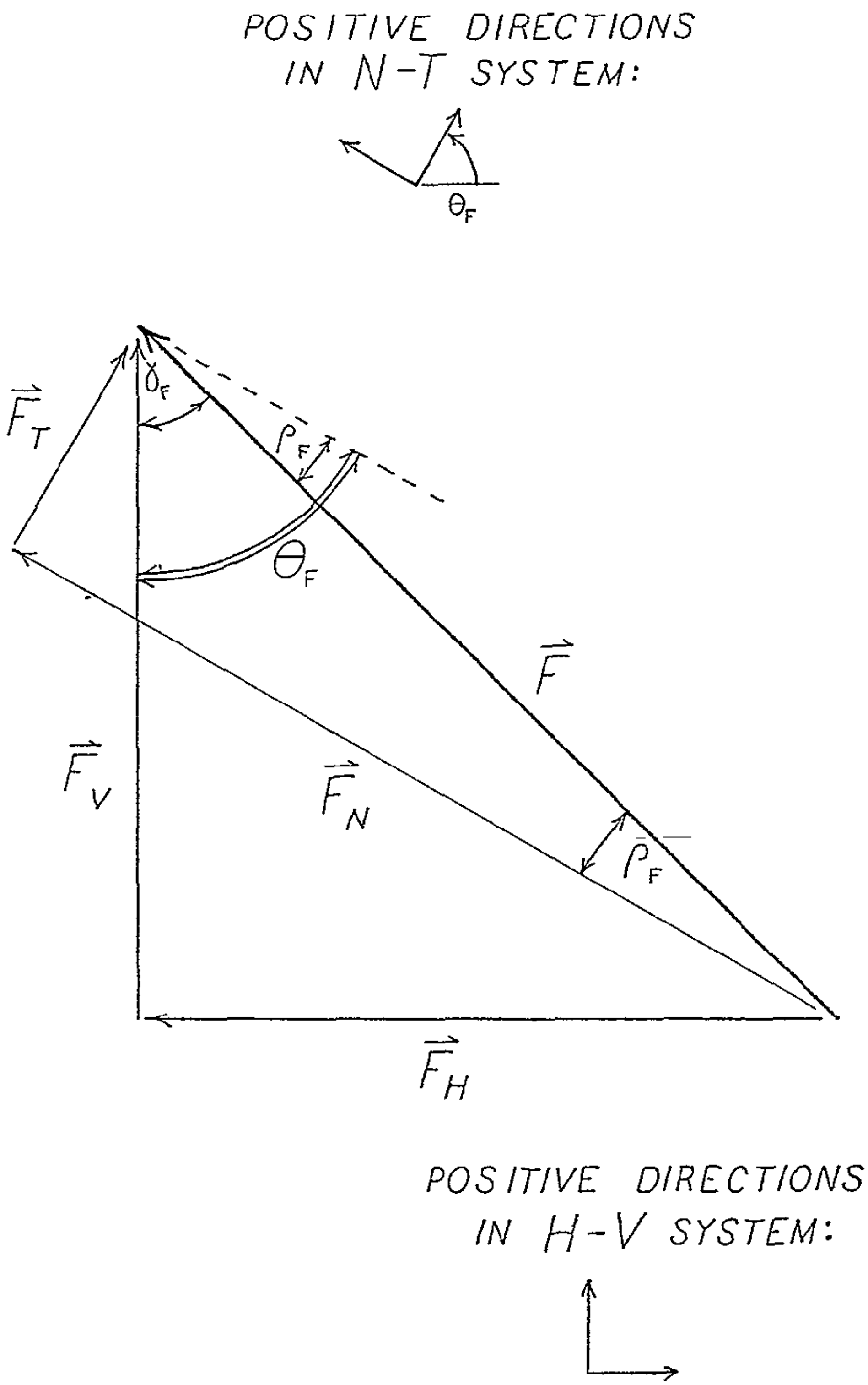

FIGURE 11

Front Wheel Force Components

$$\cos \rho_F = \frac{F_N}{F} \tag{3.3.5b}$$

$$\cos \rho_R = \frac{R_T}{R} \tag{3.3.6a}$$

$$\sin \rho_F = \frac{F_T}{F} \tag{3.3.6b}$$

$$\cos \gamma_R = \frac{R_V}{R} \tag{3.3.7a}$$

$$\cos \gamma_F = \frac{F_V}{F} \tag{3.3.7b}$$

Rearranging equations 3.3.5 through 3.3.7 gives

$$R_N = \sin \rho_R (R) \tag{3.3.8a}$$

$$F_N = \cos \rho_F (F) \tag{3.3.8b}$$

$$R_T = \cos \rho_R (R) \tag{3.3.9a}$$

$$F_T = \sin \rho_F (F) \tag{3.3.9b}$$

$$R = \frac{1}{\cos \gamma_R} R_V \tag{3.3.10a}$$

$$F = \frac{1}{\cos \gamma_F} F_V \tag{3.3.10b}$$

Substituting equation 3.3.10 into equations 3.3.8 and 3.3.9 gives

$$R_N = \frac{\sin \rho_R}{\cos \gamma_R} R_V \tag{3.3.11a}$$

$$F_N = \frac{\cos \rho_F}{\cos \gamma_F} F_V \tag{3.3.11b}$$

$$R_T = \frac{\cos \rho_R}{\cos \gamma_R} R_V \qquad 3.3.12a$$

$$F_T = \frac{\sin \rho_F}{\cos \gamma_F} R_V \ . \qquad 3.3.12b$$

Equations 3.3.11 and 3.3.12 give the normal and tangential force components in terms of angles and vertical components that are known from the terrain slopes, vehicle position, and vehicle geometry. The only unknown quantity in the above equations is R_H. By iterating on R_H, the infinite number of force triangle solutions can be generated.

Boundaries can be placed on the solutions by requiring that the wheels do not slip. For the rear wheel, this would require that

$$|R_T| \leq \mu_R R_N \ . \qquad 3.3.13$$

R_T can be either positive or negative while R_N must always be positive. For R_T positive,

$$R_T \leq \mu_R R_N \ . \qquad 3.3.14$$

$$\frac{\cos \rho_R}{\cos \gamma_R} R_V \leq \mu_R \frac{\sin \rho_R}{\cos \gamma_R} R_V \qquad 3.3.15$$

$$\cos \rho_R \leq \mu_R \sin \rho_R \qquad 3.3.16$$

$$\frac{\sin \rho_R}{\cos \rho_R} = \tan \rho_R - \frac{1}{\mu_R} \ . \qquad 3.3.17$$

For R_T negative,

$$- R_T \leq \mu_R R_N \ . \qquad 3.3.18$$

Following the same procedure as above, it can be shown that

$$\tan \rho_R \geq -\frac{1}{\mu_R} . \qquad 3.3.19$$

No slipping of the front wheel would require

$$|F_T| \leq \mu_F F_N . \qquad 3.3.20$$

For F_T positive,

$$F_T \leq \mu_F F_N \qquad 3.3.21$$

$$\frac{\sin \rho_F}{\cos \gamma_F} F_V \leq \mu_F \frac{\cos \rho_F}{\cos \gamma_F} F_V$$

$$\sin \rho_F = \mu_F \cos \rho_F \qquad 3.3.23$$

$$\frac{\sin \rho_F}{\cos \rho_F} = \tan \rho_F \leq \mu_F . \qquad 3.3.24$$

For F_T negative,

$$-F_T \leq \mu_F F_N . \qquad 3.3.25$$

Following the same procedure as above, it can be shown that

$$\tan \rho_F \geq -\mu_F . \qquad 3.3.26$$

Equations 3.3.17, 3.3.19, 3.3.24, and 3.3.26 give conditions which must be met if the wheels of the Bicycle Model are not to slip. The appropriate two-limit equations will give bounds to the possible values of R_H.

If a solution satisfies the limit equations, the wheel torques required to hold the vehicle stationary on the terrain can be calculated. As shown in Section 2.2, it is the tangential force of the N-T system which given the torque. Once the tangential force components are calculated from equations 3.3.12, the values of the required torques are found from

$$T_R = R_T\, r \qquad 3.3.27a$$

$$T_F = F_T\, r\,. \qquad 3.3.27b$$

A front and rear torque can be found for each possible force triangle solution.

CHAPTER 4

PROPULSION CONTROL SYSTEM ANALYSIS

4.1 General Strategy

A method has been conceived to evaluate the propulsion control system and it will now be described. For a given vehicle position ϕ and terrain characterized by θ_F and θ_R, a series of possible torque solutions can be calculated. The required ratio of front to rear wheel speeds can also be determined If the control system is capable of driving the wheels at the required ratio and at the same time satisfy one of the torque solutions, it is judged satisfactory for the specific vehicle position, ϕ. By using the procedure for the range of ϕ's between θ_R and θ_F, the ability of the control system to negotiate the terrain characterized by θ_R and θ_F can be evaluated.

4.2 Computer Analysis of Bicycle Model

Because of the iteration which is required to obtain possible torque solutions of the Bicycle Model, the use of a computer program is suggested. Such a program was written and is listed in Appendix A with its output. The program takes a specified terrain and calculated possible torque solutions and required speed ratios for incremented vehicle positions. A brief description of the program follows.

The program starts by reading and printing the inputs which remain constant throughout the calculations. These inputs are:

a) THF, THR: the slopes under the wheels θ_F and θ_R

b) A,B,C: vehicle dimensions a,b, and c as shown in Figure 5.

c) MUF, MUR: coefficients of static friction μ_F and μ_R

d) RHI, RHF: initial and final values of R_H

e) DELTR ; change in R_H between successive iterations

f) HALFW: half of the total vehicle weight

g) R: wheel radius r.

After this is done, the program goes about indexing the position of the vehicle, ϕ. The successive values of ϕ give the sequence of positions that the Bicycle Model goes through as it climbs the specified terrain. In the example given in Appendix A, ϕ starts at 0^o, which corresponds to the point where the front wheel rests entirely on θ_F. By increments of 5^o, ϕ increases to 40^o, which corresponds to just before the rear wheel moves from θ_R to θ_F These two conditions are illustrated in Figure 12.

At each value of ϕ, subroutine BICYCL is called. The first step in BICYCL is to calculate the vertical wheel force components for the given from equations 3.1.3 and 3.1.4. A check is made on the stability of the vehicle by the method described in Section 3.1. If the vehicle is unstable, the subroutines prints VEHICLE WILL TIP OVER. BICYCL next calculates VRAT. the required ratio of front to rear wheel speeds, from equation 3.2.11. After some comparison values are calculated and headings printed, the iteration process over R_H is begun. For each value of R_H between RHI and RHF, the tangential force components are determined from equations 3.3.12. The two appropriate limit conditions are selected from among equations 3.3.17, 3.3.19, 3.3.24 and 3.3.26, and the solution is checked for wheel slipping. If no slipping occurs, the wheel torques are calculated from equations 3.3.27 and printed. If slipping does occur, the subroutine will print WHEEL SLIPS. After either case, R_H is incremented and the next possible solution is calculated and checked. This is repeated until RHF is reached.

A few general remarks about the program are in order. Due to the way that the equations were derived, they will be valid for negative θ's and

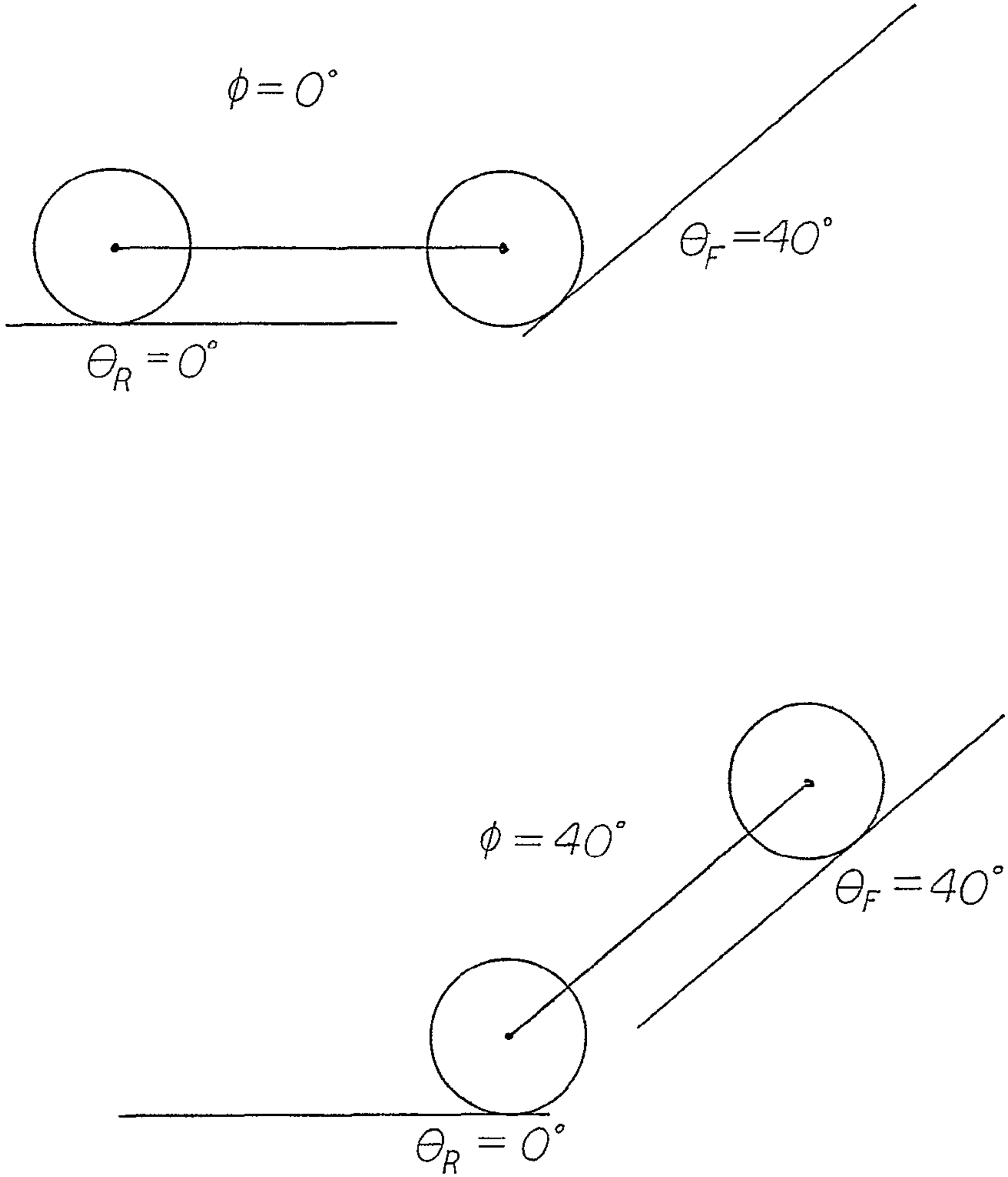

FIGURE 12

Terrain of Example in Appendix A

ϕ 's as well as positive ones. This will allow many different terrain situations to be examined. A warning should be given for the θ's to not exceed $\pm 90^o$, as the equations then break down.

The $R_H = 15.0$ solution for $\phi = 40^o$ is shown in Figure 13. Note that a negative torque is required of the front wheel. From force considerations, this case would be satisfactory for resisting gravity and maintaining the vehicle's position on the terrain. However, it is absurd to apply a negative torque to one wheel and a positive torque to the second, as they oppose and fight against each other. For this reason, all possible solutions giving torques with opposite signs will be discarded. Note that both torques should be negative when the vehicle is moving down a slope.

4.3 Speed-Torque Diagrams

The final information required to analyze the control system of the Bicycle Model is the speed-torque curve of each motor-wheel system. For a given input current from the motor drivers, a definite relationship exists between the speed of the wheel and the wheel torque developed. This relationship is often expressed in a plot of the torque versus speed. There will be a different speed-torque curve for each input current to the motor-wheel system.

The speed-torque relationship can be derived analytically. However, the expressions are very complex and involve parameters such as the feedback gains, the gear reductions, the efficiency of the gears, and the currents, voltages, resistances, and inductances of the motor's armature and field. The derivation of the equations and measurements of the necessary quantities is outside the scope of this investigation.

An alternate method for obtaining the speed-torque relationship is by experiment. A dynamometer is a device which is used for this measurement. For a

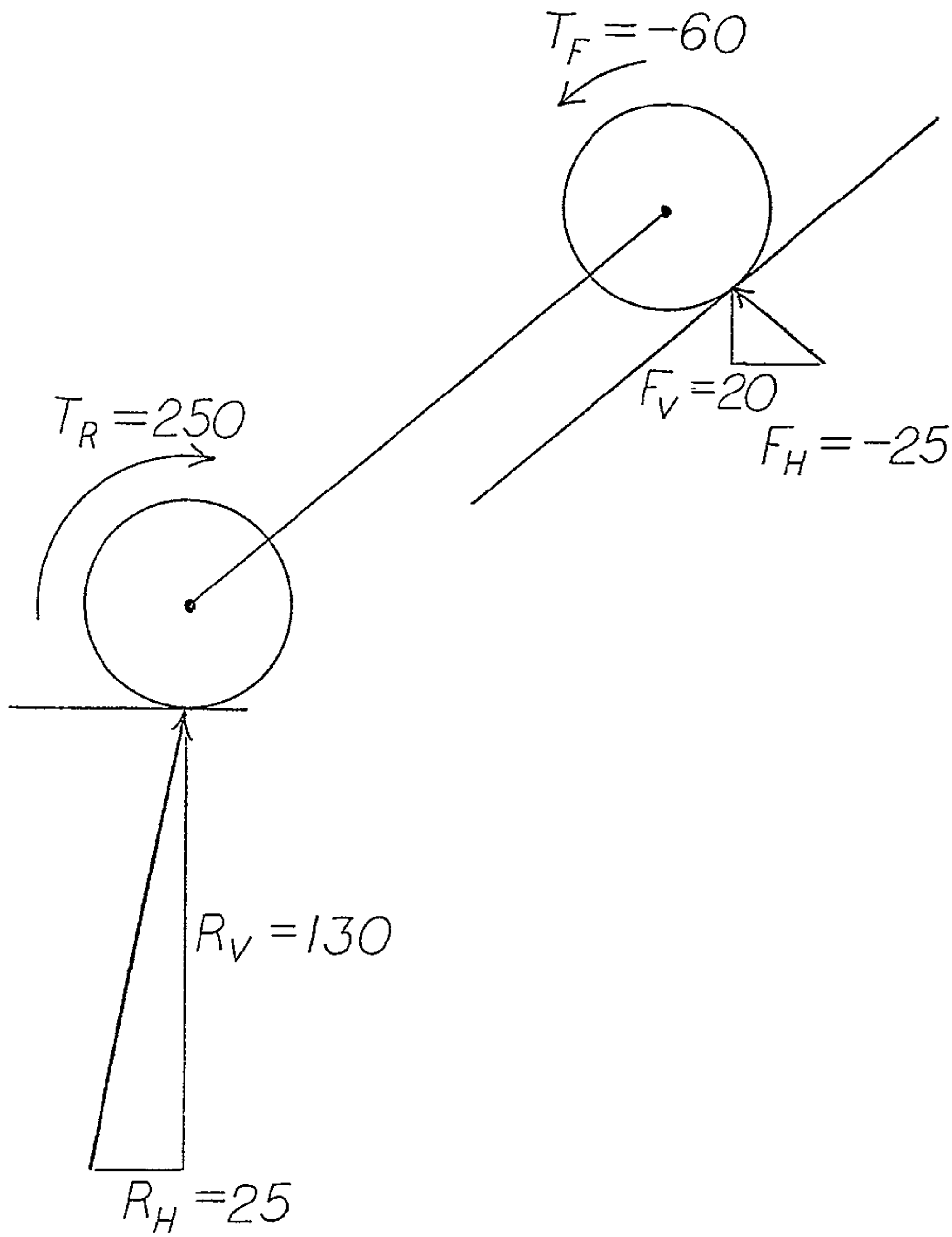

FIGURE 13

Solution for $R_H = 25.0$, $\phi = 40°$

constant motor input, the dynamometer puts a series of load torques on the motor and measures the resulting speeds. Reference 4 explains a speed-torque experiment conducted by the RPI Mars Roving Vehicle Project in 1974. Measurements similar to this should be taken of the present motor-wheel systems on the MRV to obtain accurate speed-torque curves.

Although the refinements described above will eventually be required to develop an effective control system, the purpose at hand is equally well served by employing a rather simple concept to gain a first order appreciation of the control problem. Approximate speed-torque curves can be obtained by using information supplied by the motor manufacturers. The speed-torque curve of a permanent magnet D.C. motor is well represented by a straight line between the motor's no-load speed and its stall torque. This straight line form was assumed to hold for the armature-field, series wound D.C. motors used on the RPI MRV. A gear train efficiency of 87% was estimated in Reference 4, and thus will be assumed to hold for the front as well as the rear gear trains. These allow approximate speed-torque curves to be drawn.

For the rear motor-wheel system, a gear reduction of 413:1 is used. The motor is a surplus aircraft motor rated at 7500 rpm and 1/8 horsepower. This would correspond to a motor torque of

$$T_m = 63{,}000\left(\frac{\text{h.p.}}{\text{rpm}}\right) = 1.05 \text{ in-lb.} \qquad 4.2.1$$

It will be assumed that this is the motor's stall torque, and that 7500 rpm is the motor's no-load speed. When put through the rear drive train, these become the wheel values of

$$W_{NL} = \left(\frac{1}{413}\right)(7500) = 18.2 \text{ rpm} \qquad 4.2.2$$

$$T_S = (.87)(413)(1.05) = 377 \text{ in-lb} \qquad 4.2.3$$

The approximate speed-torque curve for the rear wheel is drawn in Figure 14 using the valus in equations 4.2.2 and 4.2.3.

A gear reduction of 12.5:1 is used in the front motor-wheel system. The motor is a Boehm gear motor rated at 30 in-lb torque and 166 rpm at full load. Assume that 30 in-lb is the gear motor's stall torque, and that 200 rpm is its no-load speed. When put through the front drive train, these become the wheel values of

$$W_{NL} = \left(\frac{1}{11.4} \right) (200) = 16.0 \text{ rpm} \qquad 4.2.4$$

$$T_s = (.87)(12.5)(30) = 326 \text{ in-lb} \qquad 4.2.5$$

The approximate speed-torque curve for the front wheel is also drawn in Figure 14 using the values in equations 4.2.4 and 4.2.5.

4.4 Control System Evaluation

It is now possible to make a first order evaluation of the propulsion control system of the RPI MRV. The evaluation will be made for the Bicycle Model of the vehicle encountering a 40° slope. The computer output of Appendix A and the speed-torque curves of Figure 14 are used. A brief description of the propulsion control system is given first to clarify the evaluation.

The control system, shown in simplified form in Figure 15, is a passive one in that it functions automatically regardless of the local terrain. When roving, the Motor Drivers are told to move the vehicle forward at a specified cruising speed. The Drivers send out constant control currents I_R and I_F that would cause the front and rear wheels to propel the vehicle at the desired speed on level ground. These currents are unaffected by any load torques or

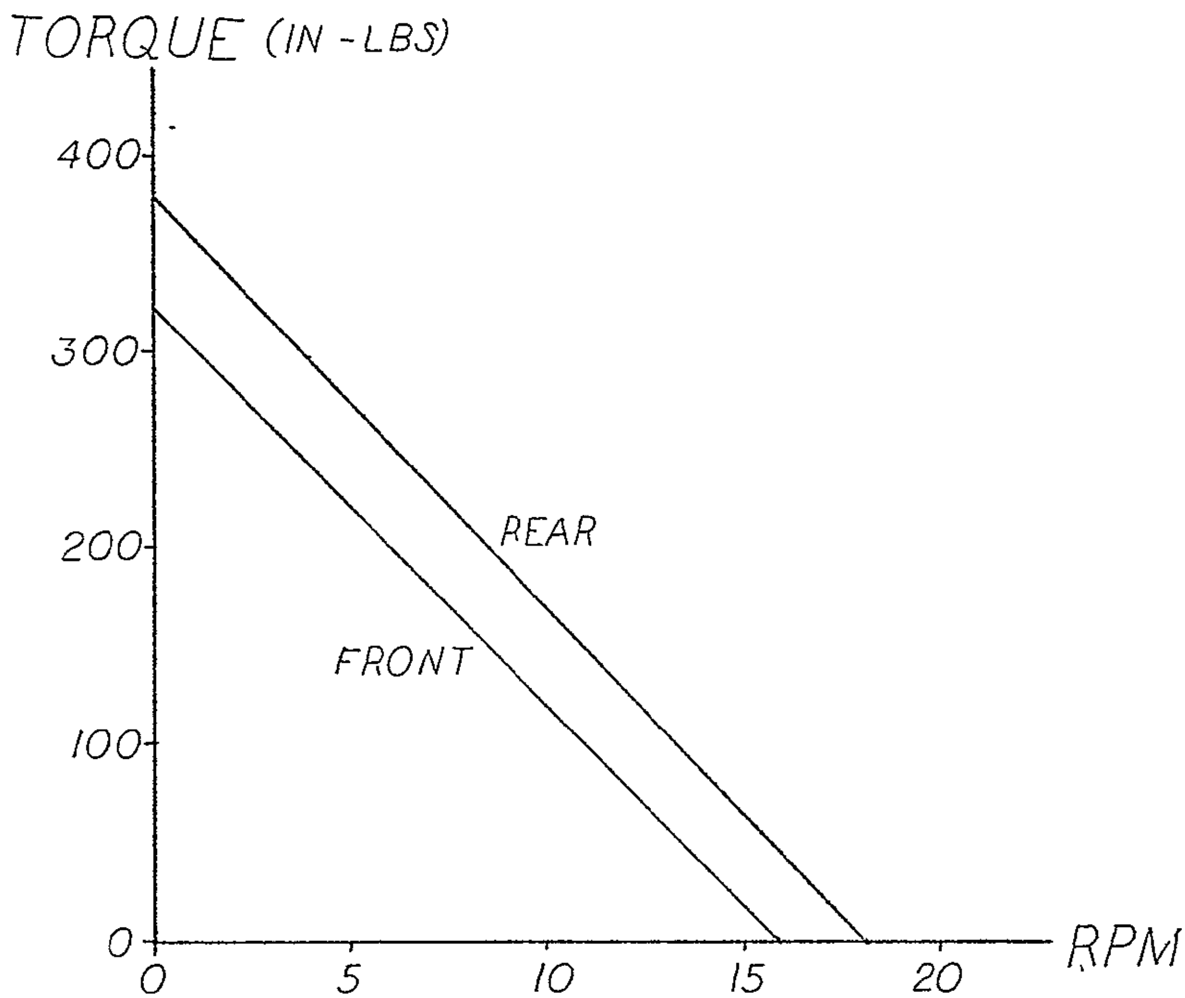

FIGURE 14

Approximate Speed-Torque Curves

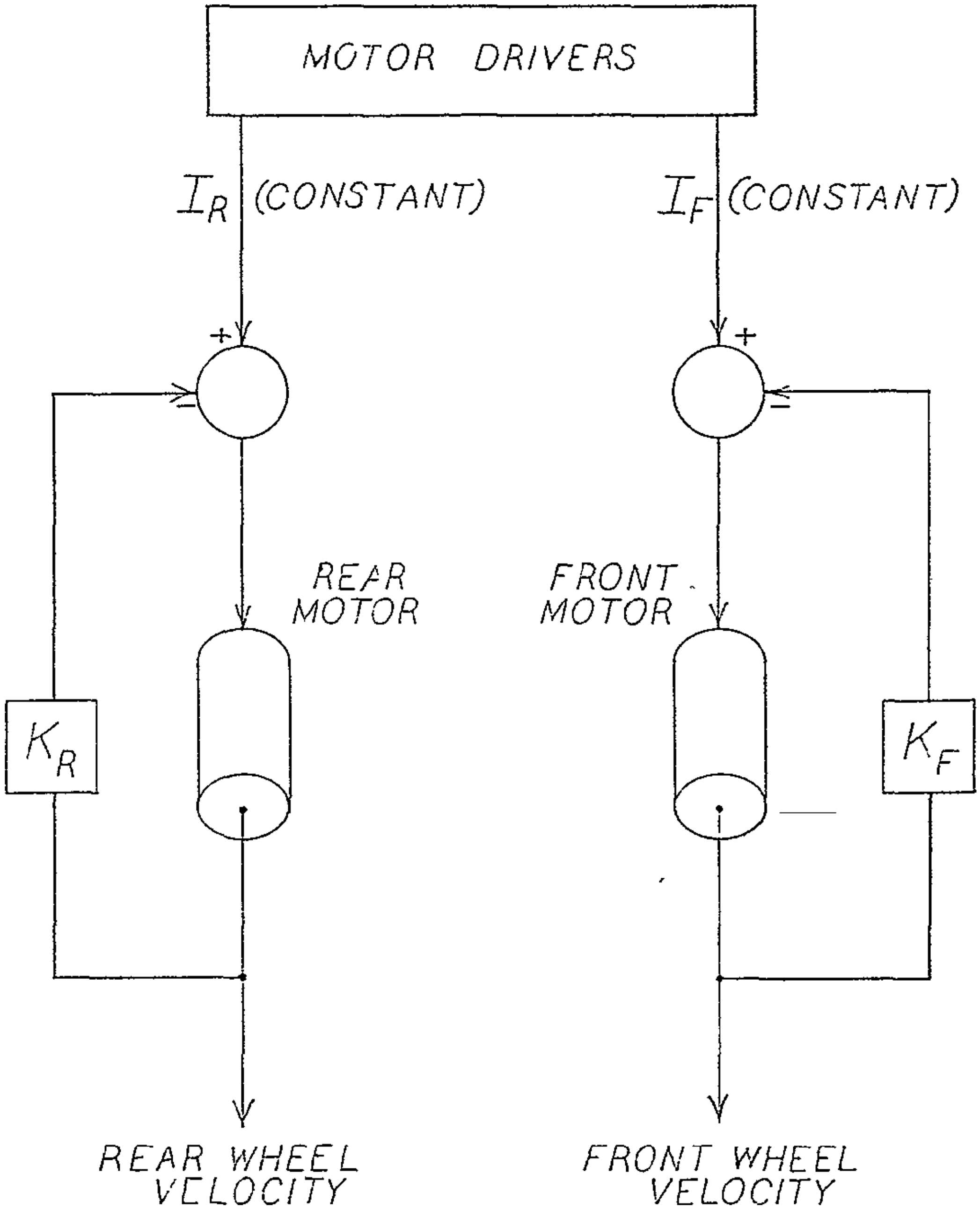

FIGURE 15

Propulsion Control System

speed fluctuations imposed on the wheels by obstacles. The control currents are fed into velocity monitored negative feedback loops where the effects of obstacles encountered enter the control system. Any changes in the load torques that occur on the wheels cause the velocities to change according to the speed-torque curves obtained for the constant control currents I_R and I_F. The speed-torque curves are the physical manifestation of the propulsion control system and express the allowed relationship between wheel speeds and torques.

The strategy for making the evaluation is as follows. For the first position of the Bicycle Model at $\phi = \theta_R$ the possible solutions calculated by the computer which involve wheel slipping or opposing torques are eliminated. One of the remaining solutions is then used as a starting point. The values of T_F and T_R for this solution are found in the front and rear speed-torque curves respectively. Corresponding speeds V_F and V_R are then determined from the curves and their ratio is calculated and compared to VRAT. This process is repeated with other solutions until a solution is found which gives velocities in the ratio of VRAT. If a solution which results in a velocity ratio of VRAT is found, this is the condition of torques and speeds which the control system will automatically execute in the given vehicle position ϕ. The control system will be adequate for this position. If no solution can be found which will give wheel velocities in the ratio VRAT, the control system is incapable of getting the vehicle to the specified position ϕ. By examining each incremented ϕ position of the vehicle up to $\phi = \theta_F$ in a similar fashion, it can be determined if the control system will allow the vehicle to climb the specified terrain.

The specific case of $\theta_R = 0^o$ and $\theta_F = 40^o$ will now be examined. The first position of the Bicycle Model is $\phi = 0^o$. The computer output of

Appendix A shows that no wheel slippage occurs in the range of R_H's over which the iteration takes place. The remaining task is to see if one of the possible solutions satisfies the velocity requirements. A first guess of R_H = 25.0 will be examined. The rear torque for R_H = 25.0 is 250 in-lbs. Using this in the rear wheel speed-torque curve of Figure 14, a value of V_R = 6.1 rpm is found. Taking the front torque calculated of 219 in-lbs into the front wheel speed-torque curve gives a value of V_F = 5.1 rpm. The speed ratio for this solution is

$$\frac{V_F}{V_R} = \frac{5.1}{6.1} = .84 \qquad 4.3.1$$

This is less than the required ratio VRAT = 1.305, so the R_H = 29.0 solution is tried. Entering the speed-torque curves with the solution torques of T_R = 290 and T_F = 189 in-lbs gives the speeds V_R = 4.8 and V_F = 6.1 rpm. The ratio V_F/V_R here is 1.63, which is greater than VRAT. It can be shown that for R_H = 27.5, the torques T_R = 255 and T_F = 200 in-lbs have corresponding velocities V_R = 4.8 and V_F = 6.1 rpm. The ratio V_F/V_R equals 1.27 which is close to the required VRAT = 1.305. For some R_H between 27.5 and 28.0, there will be a solution which converges to the exact value of VRAT.

This procedure can be repeated for the other Bicycle Model positions to locate their correct solutions. A summary of the computer solutions which are closest to VRAT for each position is shown in Figure 16. Again, there exist exact solutions which will converge to VRAT that could be found by reducing the size between successive iterations of R_H. Since all the ϕ positions in Figure 16 can be satisfied, the present control system, as modeled, is capable of propelling the MRV from a level surface onto a 40° slope.

(degrees)	R_H (lbs)	T_F (in-lbs)	V_F (rpm)	T_R (in-lbs)	V_R (rpm)	Solutions V_F/V_R	VRAT
0	27.5	200	6.1	275	4.8	1.27	1.305
5	26.0	183	6.9	260	5.6	1.23	1.216
10	24.0	163	7.6	240	6.6	1.15	1.137
15	21.5	157	8.2	215	7.8	1.05	1.066
20	19.0	144	8.8	190	9.0	.98	1.000
25	16.5	129	9.6	165	10.2	.94	.938
30	13.5	115	10.2	135	11.6	.88	.879
35	10.0	100	11.0	100	13.4	.82	.822
40	6.5	82	11.8	65	15.1	.78	.766

FIGURE 16

Control System Solutions

CHAPTER 5

DISCUSSION AND CONCLUSIONS

5.1 Bicycle Model as an Analytical Tool

It has been shown that because of symmetry, the four-wheel RPI Mars Roving Vehicle can be modeled in a two-wheel bicycle configuration. By applying principles of mechanics to this model, possible solutions of the torques required of the wheels to hold the vehicle stationary on slopes can be found. These torques are relevant if vehicle accelerations and friction are ignored. With no acceleration, the frictional torque is small compared to the gravity resisting torque, and the assumptions are valid. In addition, friction is accounted for to some extent by assigning efficiencies to the gear trains.

Once possible propulsion control system outputs have been calculated with the Bicycle Model, the required speed ratio conditions can be applied. These conditions are dependent on the geometry of the vehicle and terrain. It can be seen that the output of the control system must satisfy both torque requirements to climb the slope, and wheel speed requirements to prevent wheel slipping and excessive strains in the vehicle structure. The speed-torque curve, which is a function of the control system, is a useful way of checking these requirements.

The analysis technique described above has been used to make a first order evaluation of the present propulsion control system of the RPI MRV. The specific case of moving from a 0° slope to a 40° slope was examined. With the estimated speed-torque curves of the system, the present control system was found adequate. It has the capability to move the vehicle from the 0° to the 40° slope.

5.2 Future Work

Before any intensive analysis work is done, a better determination of the front and rear speed-torque curves should be made. As mentioned in Section 4.3, it would probably be best to measure the curves directly with some sort of dynamometer than to trust a whole series of measurements to use in an analytic expression. With accurate curves, a thorough examination of many terrains should be conducted to determine the strengths and limitations of the propulsion control system.

An attempt should be made to extend the two dimensional Bicycle Model to a three dimensional model of a Four-wheeled vehicle. This would permit the analysis of the important case of turning the vehicle on various slopes. It is known that wheel speeds must be adjusted when making turns. The question of how the control system correspondingly adjusts the torques, and thereby the climbing ability, should be addressed. New control system concepts may be required which might involve monitoring torques or incorporating vehicle strains into the feedback loops.

PART II

DESIGN OF A MAST FOR AN ELEVATION SCANNING LASER/MULTI-DETECTOR SYSTEM

CHAPTER 6

INTRODUCTION

6.1 Preface

In order to travel in an autonomous manner, a planetary rover must have the capability of detecting obstacles and hazardous terrains in its path. The RPI MRV is equipped with a first order short range hazard detection system, i.e., the one laser/one detector concept, which is effective for simple obstacles and terrains involving moderate gradients. The chief draw-back to the current system lies in its conservative characteristics. While the system can detect and avoid all real hazards, the detection and avoidance system interprets many possible terrains as hazardous because of the lack of sufficiently accurate data. An elevation scanning laser/multi-detector system which provides more data of increased accuracy for discriminating between hazardous and non-hazardous terrains is under development. It was the objec-tive of this task to design and construct the mechanical systems required to implement this advanced data acquisition system.

6.2 Laser Triangulation

The hazard detection system for the RPI Rover is based on the concept of laser triangulation. This is illustrated in Figure 17 for the one laser/one detector system. If Terrain A is scanned, the laser beam is reflected from Point A. This is below the detector's cone of vision and is not "seen" by the detector. Similarly for Terrain C, the laser spot is at Point C, above the cone of vision, and is also not "seen". However, for Terrain B, the laser beam strikes the ground at Point B. The spot is within the cone of vision and a positive response is registered by the detector. By sweeping the laser beam

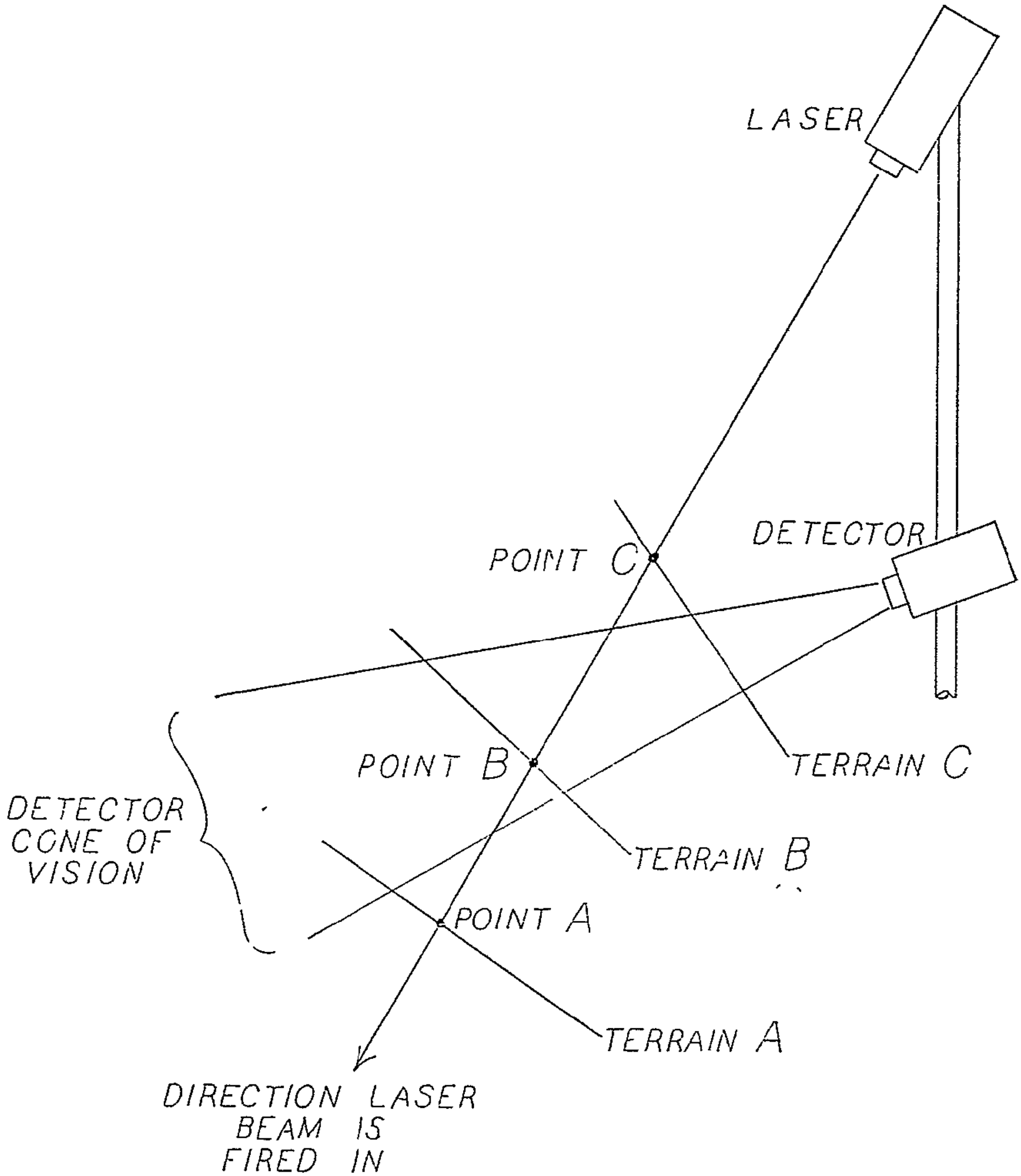

FIGURE 17

Laser Triangulatron

and detector cone of vision in front of a planetary rover, information can be gathered for an artificial intelligence to interpret. By knowing the angles that the Laser and Detector are pointed in and the angle of the cone of vision, some judgments on unobstructed paths for the rover can be made. The RPI MRV presently employs a single laser/single detector system similar to that just described.

It is felt that a more refined and accurate picture of terrain features can be obtained by using many different detectors and laser shots at each position in the most sweep. This increases the amount of data available to the hazard detection algorithm, which can now provide more detailed information on the immediate terrain. The succeeding chapters document mechanical aspects of the design of such a multi-laser, multi-detector system.

6.3 Design Criteria

Many parameters such as scanning speeds and pointing angles were already determined by computer simulations and electronic component speed considerations. These also led to the decisions on selection of slip rings and position encoders, and on using a rotating 8-sided mirror.

Since a totally new mast had to be designed, it was decided to abandon the oscillating type in favor of a continuously rotating mast. There were three major reasons for this decision. First, the power requirement would be reduced. This oscillating mast continuously requires power to accelerate and decelerate it at the ends of its sweep. The continuously rotating mast would only require a small amount of power to overcome friction once it reached its sweeping speed. Secondly, since it isn't accelerating and decelerating, the continuously rotating mast will impart smaller vibrations to the vehicle. Lastly, the rotating mast can have its center of scan moved by starting the laser firing sequence at a different position. The reliability problems which arose from the tracking mechanism of the oscillating mast which physically pointed it in various directions can be avoided.

A number of general requirements for the multi-laser, multi-detector system were defined. The design had to be flexible to allow experiments in hazard detection with different parameters. Critical components in the design had to be accurately positioned, as only small deviations in the locations of the laser spots can be tolerated. Simple adjustments had to be made to line up the system initially. Lastly, the weight had to be kept as low as possible to prevent any adverse effects on the vehicle's performance. These considerations led to the design of the multi-laser/multi-detector system shown being bench tested in Figure 18 without the Detector.

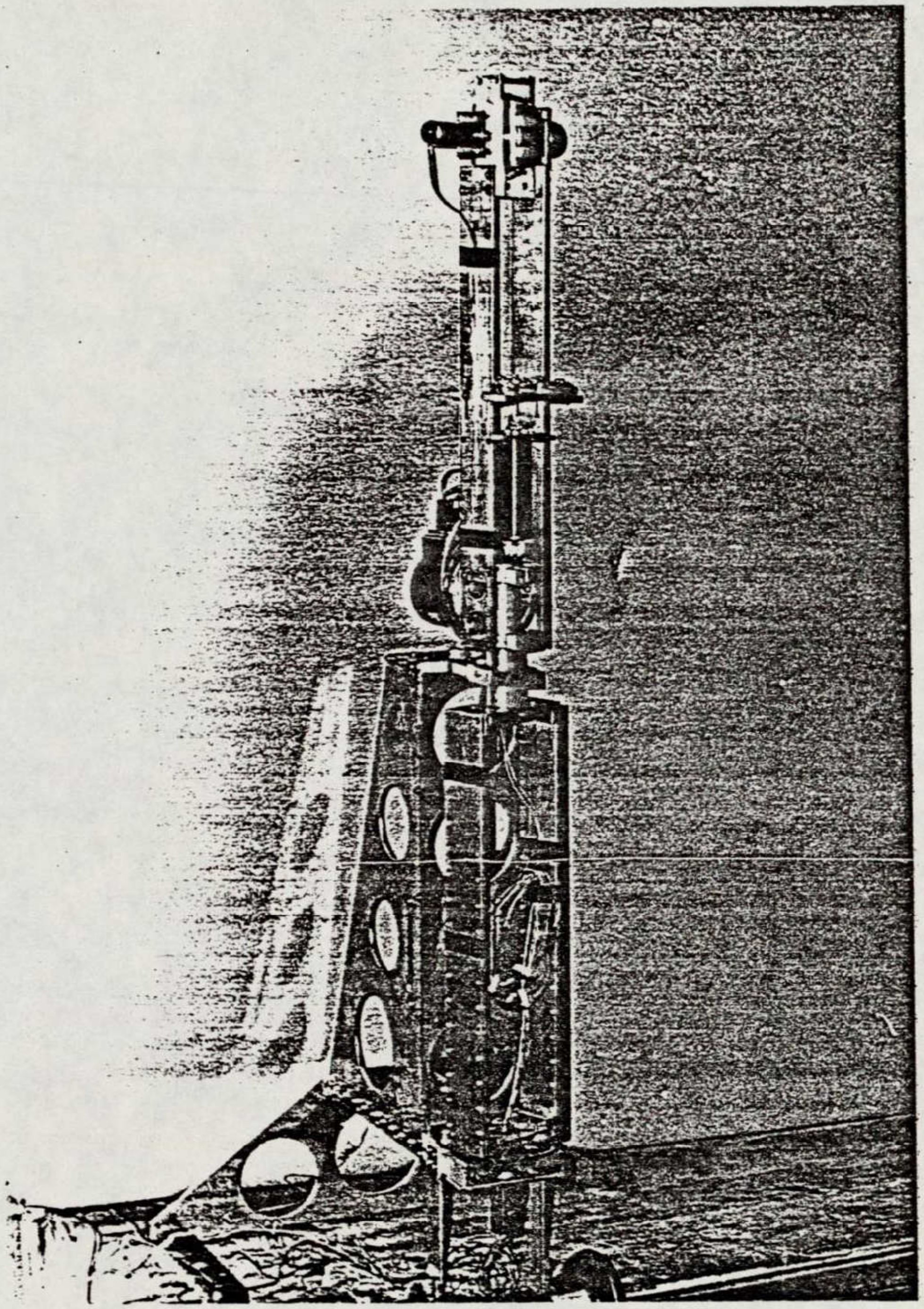

FIGURE 18

Multi-Laser/Multi-Detector System

CHAPTER 7

SELECTION OF MAJOR MECHANICAL COMPONENTS

7.1 Motors

The new mast required two motors, one to rotate the mirror and one to turn the mast. The two quantities used to evaluate motor candidates were their starting torque and time to come up to full speed. The approximate running speeds were again determined by electronic timing considerations related to the hazard detection system.

7.1.1 Mirror Motor

The first step in considering a mirror motor was to calculate the load inertia and starting torque. The value of the mirror's inertia penciled on its brochure by the manufacturer was found to be incorrect. By assuming the mirror to be a cylinder instead of the suggested value of .03 in-oz-sec^2 was calculated and used instead of the suggested value of .002 in-oz-sec^2. The total inertia of the mirror flanges, bearings, couplings and encoder were calculated to be .001 in-oz-sec^2, making the load inertia

$$J_L = .03 + .001 = .031 \text{ in-oz-sec}^2 \qquad 7.1.1$$

The starting torque for two ball bearings was estimated by a method outlined in Reference 5. This was found to be small compared to the starting torque of the Elevation Encoder, so the encoder's value of .15 oz-in was used.

Micro Mo Electronics of Cleveland is a distributor with a wide selection of miniature motors and seed reducers. Their 330/D09 motor with a 54:1 reduction 03/2 gear head looked like a good candidate. With a no-load speed of 1690 rpm and a starting torque of 9.2 oz-in, it seemed to operate at the right speed and provide a healthy margin of safety for the torque calculation. Using an equation from Reference 3 with the motor and gear head data, an acceleration time of 60 milliseconds was calculated. A small time such as this was felt to be beneficial, as the mirror must rotate at a very precise speed and be adjusted back to the speed very quickly when it strays. This motor and gear head was ordered and appears satisfactory.

7.1.2 Mast Motor

The mast motor was selected in a similar manner. The inertia of the mast was estimated by assuming all its components to be cylinders or slabs, and summing inertias of each piece. A total inertia of 1.0 oz-in-sec^2 was estimated. The total starting torque was estimated at 1.6 oz-in by the method used previously. There is a greater uncertainty in these estimates than in those for the mirror motor, as cylinder-slab assumptions and estimates of sleeve bearing characteristics were required.

The motor selected was a Globe 168A229-2 gearmotor rated at 140 oz-in stall torque and a no-load speed between 68 and 83 rpm. Again, a large margin of safety is employed to account for errors in the analysis. The time to accelerate to full speed was calculated at 1.2 seconds, which would seem adequate.

7.2 Gears

Since the slip rings had to be put at the bottom of the mast, motor couldn't be coupled directly to the mast. The motor had to be separate and transfer power to the mast by some mechanisms. Spur gearing was selected as the transfer mechanism for the new mast.

The Browning Power Transmission Equipment catalog recommends using the finest pitch gears possible for the smoothest, most economical operation. A larger pressure angle will generally allow a finer pitch to be used. W. M. Berg, Inc. had a wider selection of small size gears with 20° pressure angles than Browning did so gears were selected from Berg.

In order to allow as much room for the detector as possible, the mast motor is required to be as far away from the mast as possible. This would mean that the gear diameters should be as large as possible. The largest gears available from Berg have a pitch diameter of 4.0000 inches. For hubbed gears, the finest pitch available with 4.0000 inch pitch diameter is 64 pitch. It was decided to purchase 64 pitch gears with pitch diameters of 4.0000 inches.

All of Berg's gears are A.G.M.A. Quality 10 with Class C Backlash. The technical section of the Berg manual gives the worst case of backlash for these gears as .0015 inches. For the gears selected above with 2 inch radii, the angular play between the gears is

$$\text{Arc Tan}\ \frac{(.0015\ \text{inch})}{2\ \text{inch}} = .043^{\circ} = 2.6\ \text{minutes} \qquad 7.2.1$$

This appears to be an acceptable value.

7.3 Mast Bearings

The previous system of supporting the mast with a sleeve bearing in the middle and a ballbearing on the bottom has proven to be a good design, and is used on the new mast. The ball bearing on the bottom supports the entire mast weight as a thrust load, and any rotational imbalance as a radial load. The imbalance load is generally smaller than the weight, The sleeve bearing at the middle encounters only a radial load which again is usually small. The low load and slow rotational speed of the mast justifies the use of a simple sleeve bearing.

Since the thrust load on the ball bearing is the larger load, the bearing was selected according to this parameter. The literature from Federal Bearings Co. gave the most complete information on thrust loadings so a Federal bearing was selected. The thrust load, or mast weight, was calculated as a by-product in the mast inertia estimate of Section 6.1.2. A weight of 10 lbs was found. The Lower Mast Tube which would fit into the bearing was .75 inches in diameter. This size was determined by the diameter of the slip ring shaft which must fit inside the Lower Mast Tube. A ball bearing was found whose critical thrust load was above 10 lbs, the R12 FF bearing, and it was ordered.

The sleeve bearing selection was very straightforward. The Upper Mast Tube which it was to support had a diameter of 1.25 inches. The size just below this, a Randall SH-419 sleeve bearing, was purchased. The inside of this bearing was bored accurately to size to provide a tight slide fit over the Upper Mast Tube. This will eliminate a good deal of play which was present here on the old mast.

7.4 Couplings

Flexible couplings are used to connect two shafts that may be slightly out of line. They are especially desirable if accurate positioning of the shafts with respect to each other is required. This is the case for the optical encoders in the new mast system.

7.4.1 Mirror Assembly

Couplings were needed for connecting the mirror shafts to the gear motor and to the encoder. It was beneficial to use as small a coupling as possible to minimize rotating imbalance in the mast. The smallest found were Helical Products 4042 one piece couplings which were ordered and are operating properly.

7.4.2. Mast Encoder

The mast encoder is positioned directly under the mast motor, and a coupling was again needed. Since the shafts being connected were rotating at slow speeds and were not being rotated on the mast, a standard coupling could be used. A Berg CC9-20-4 Flex-E-Grip coupling was found and installed.

7.4.3 Slip Rings

At first glance, the connection between the slip rings and the bottom of the mast would seem like an application requiring a flexible coupling. However, there is no reason for the slip ring shaft to rotate precisely with the mast. The slip ring manufacturer even stated that the slip ring shaft could be left unconnected to the mast so that the electrical wires running out of the shaft transmitted the torque to the rings in a haphazard fashion. This seemed like asking for trouble, so an intermediate design was used. The slip ring shaft would be held firmly in the Lower Mast Tube by set screws, and the main body of the slip rings would be loosely attached to the structure of the mast support. This would prevent any bearing stresses being transmitted to the main body of the slip rings by misalignment of the mast and slip ring shaft.

The mechanical components purchased are listed in Appendix B along with the vendors from which they were obtained.

CHAPTER 8

FINAL DESIGN

8.1 Elevation Scanner

The purpose of the Elevation Scanner is to rotate the 8-sided mirror in a precisely controlled manner. This is essential for the multi-laser/multi-detector hazard detection system to function properly. The position of the mirror must be known within an acceptable tolerance in order to obtain the desired elevation angle for the laser.

The elevation scanner is shown in Figure 19. The 8-sided mirror is fastened to two mirror flanges with shafts that pass through the bearings. These shafts are connected by flexible couplings to the mirror motor and the elevation encoder shafts. The problem of lining up all the shafts and the requirement of exact position relationships forced the use of flexible couplings. The bearings were located as close to the mirror as possible to minimize bending of the mirror's supporting shafts. Slots were provided in the elevation encoder mounting plate to allow the body of the encoder to be moved for zeroing. Once zeroed, the screws through the slots could be tightened to hold the encoder firmly in position.

8.2 Optics Rack

The Optics Rack, shown in Figure 20, contains the laser and the lens required to focus the laser beam. The optics frame is the main structural member, supporting the elevation scanner at its top on to the upper most tube at its bottom. Within the frame, mounting plates for the laser and lens were fastened. They can be adjusted as described below.

The laser is firmly fastened to the laser mounting plate, which can slide forward and backward $\pm$ 3/16 of an inch about the center position.

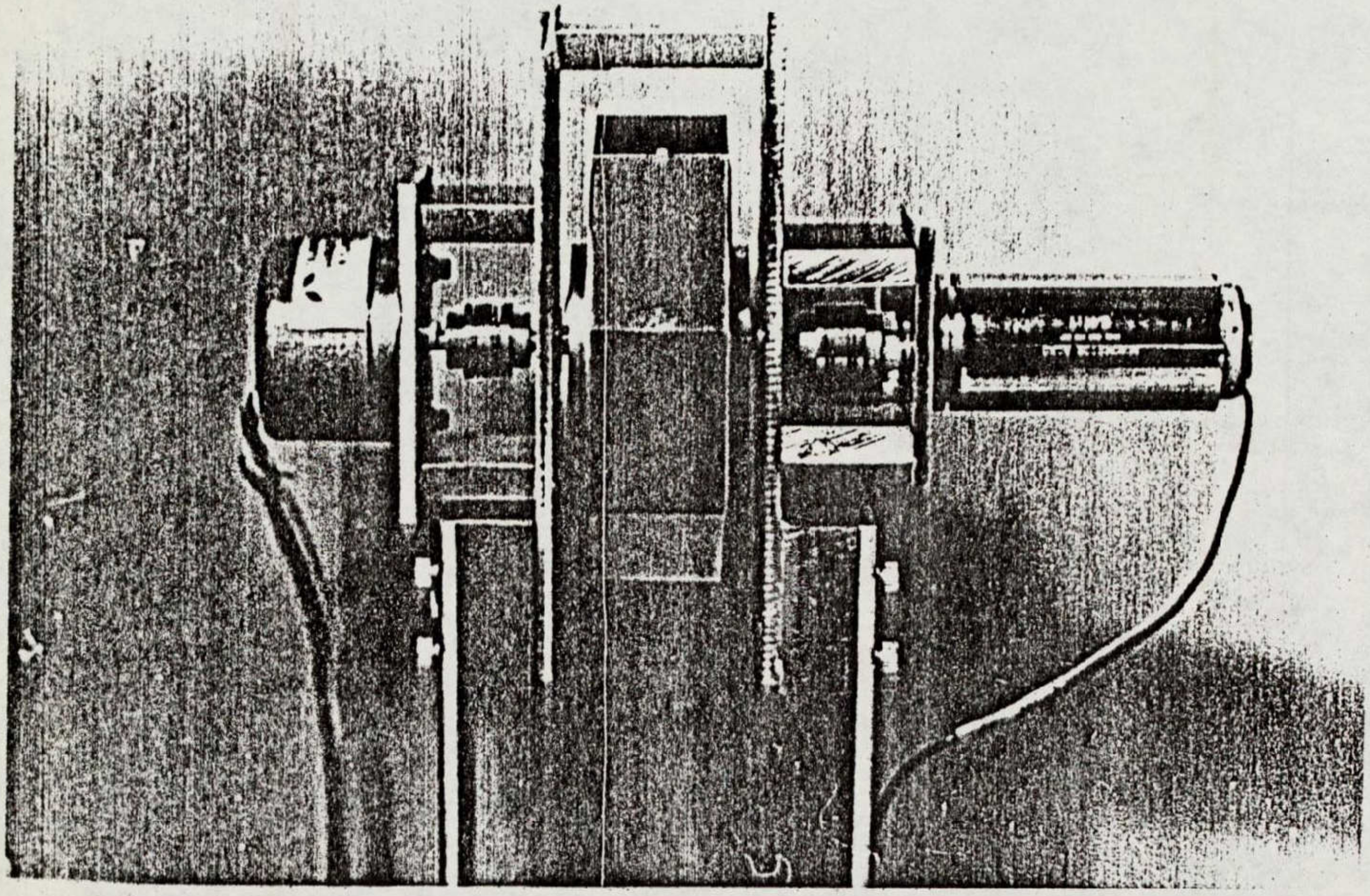

FIGURE 19

Elevation Scanner

ORIGINAL PAGE IS
OF POOR QUALITY

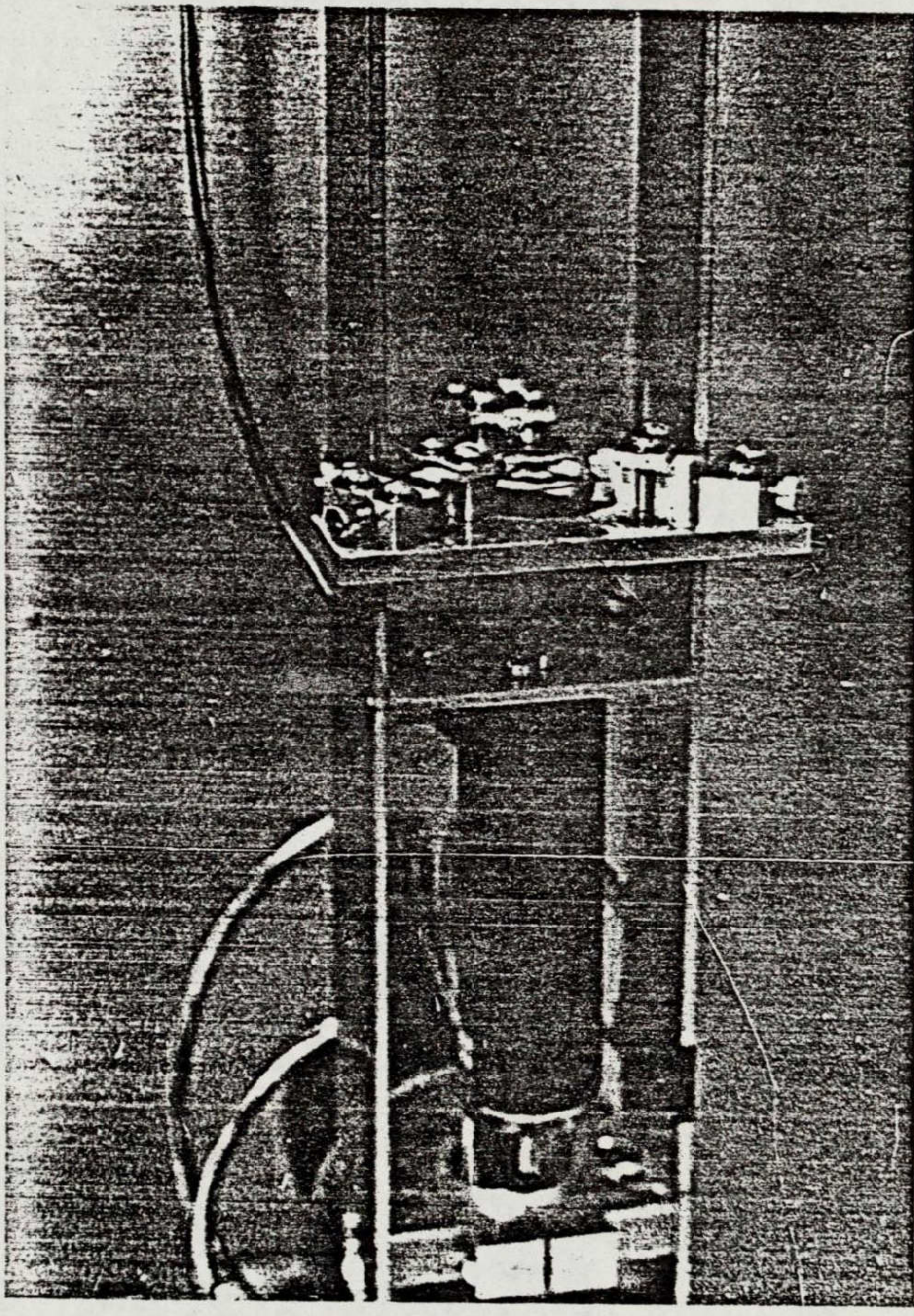

FIGURE 20

Optics Rack

This center position is directly below the forward edge of the bottom mirror face when it is horizontal. The forward and backward adjustment of the laser was judged to be the important motion. A side to side adjustment would have made the design much more complicated and was ignored. It is believed that this adjustment can be accomplished equally well by adjusting the lens position.

The position of the lens can be adjusted in all three directions. Motions with respect to the two major dimensions of the lens plate can be accomplished by using the adjusting screws. These screws move the three lens feet which hold the lens. When a satisfactory position in these two directions has been found, the feet holders can be tightened down to clamp the feet in place. The entire lens plate can be moved up and down to make the third adjustment. The plate will move $\pm$ 3/4 inches about the center position. The center position puts the lens 4 centimeters above the laser and either 10 or 15 inches below the mirror, depending on whether Optics Frame "A" or "B" is used. Two frames of different lengths were made due to the uncertainty in the optical specifications.

The bottom of the optics rack is attached to the upper most tube by two mast clamps spaced 2-1/2 apart. It was felt that two clamps would be required to get the necessary stiff support of the upper part of the mast. An electronics package for the Elevation Encoder is supported on the back of the clamps. It is out of the way at this location and close to a bearing so that the effect of its rotating imbalance on the mast is minimized.

8.3 Lower Mast

The Lower Mast is composed of a detector rack adapted to the lower mast tube, Figure 21. The detector and detector pointing mechanism are mounted inside the rack. Holes are drilled every 1 inch in the detector frame, allowing the detector to be mounted at many discrete heights. The upper detector frame support makes the transition from the top of the rack to the upper mast tube. Similarly, the lower detector frame support adapts the rack to the lower mast tube. These circular tube sections are necessary to fit into the mast's bearings.

The lower mast tube has three important functions. The tube's shoulder rests on the upper edge of the lower mast bearing's inner race. This transfer the weight of the mast to the ball bearings. Secondly, the mast gear is slide fitted onto the tube in order to align it accurately at the center of rotation. The gear is subsequently bolted to the lower detector frame support. Lastly, the shaft of the slip rings fits into the bottom of the tube and is anchored there by set screws. The wires from the slip ring shaft pass through the hollow lower mast tube into the detector rack area.

8.4 Detector Pointing Mechanism

A critical requirement of the new hazard detection system is that the detector must be accurately pointed. With the previous one laser/one detector system, a greater degree of "slop" could be tolerated in the pointing mechanism than now. Careful consideration of the causes of the previous system's inaccuracies led to the design shown in Figures 22 and 23.

The Detector Pointing Mechanism is controlled by a worm and worm gear system. A single threaded worm and a 120 tooth worm gear are used resulting in a reduction of 120:1. This means that one-third of a turn of the input worm will produce a 1^{o} change in the pointing angle of the detector.

ORIGINAL PAGE IS
OF POOR QUALITY

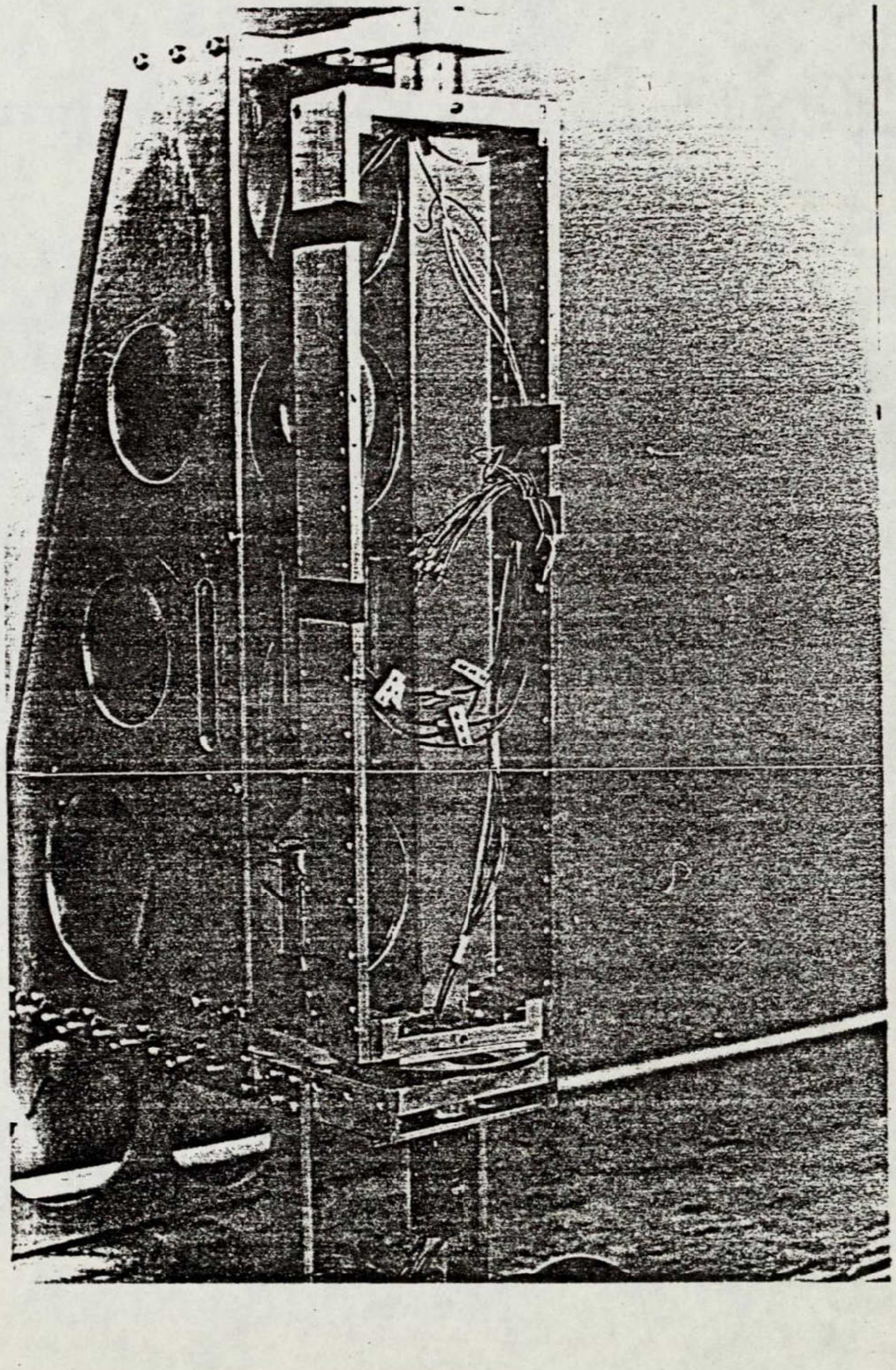

FIGURE 21

Lower Mast

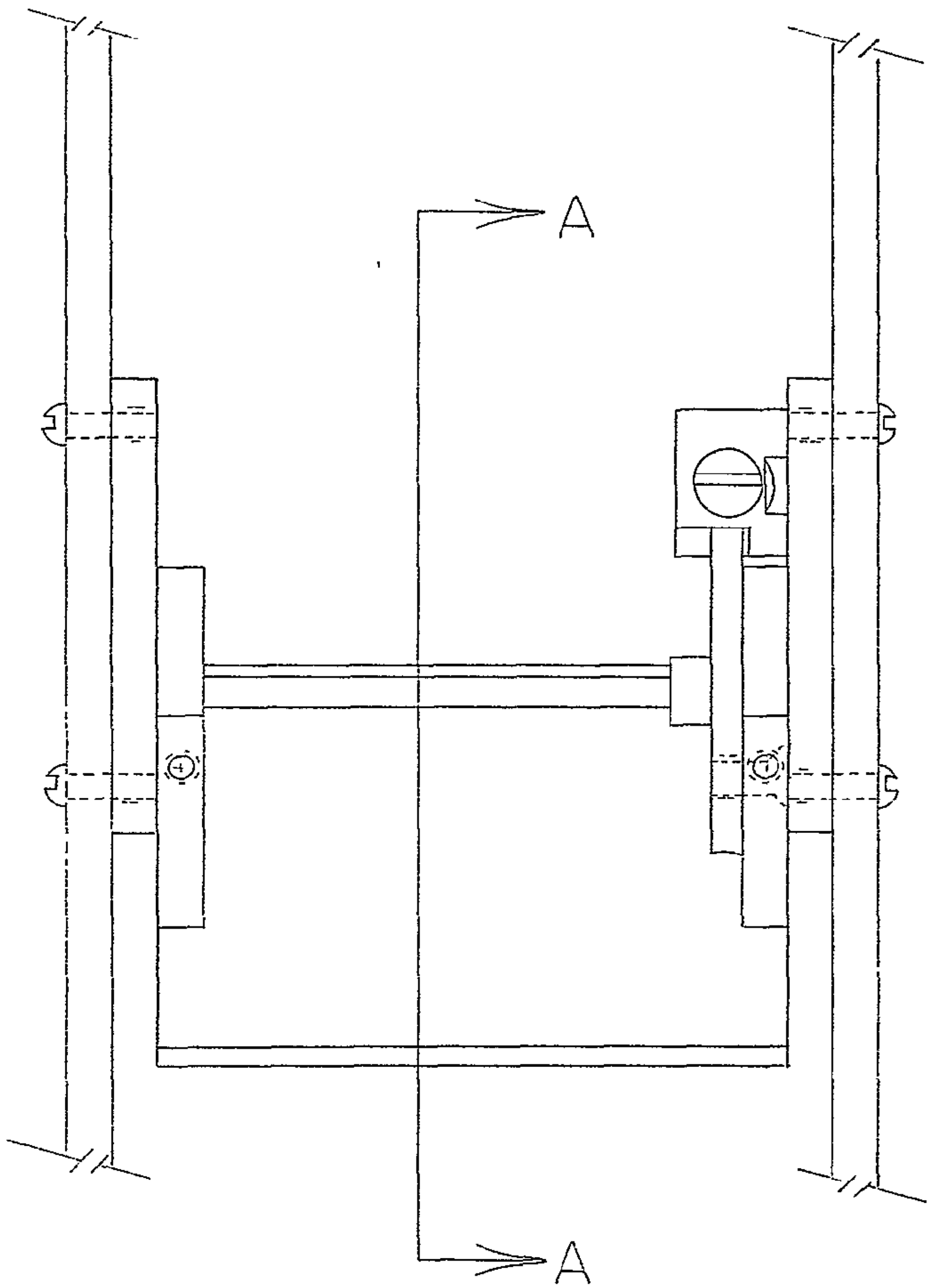

FIGURE 22

Detector Pointing Mechanism (Front View)

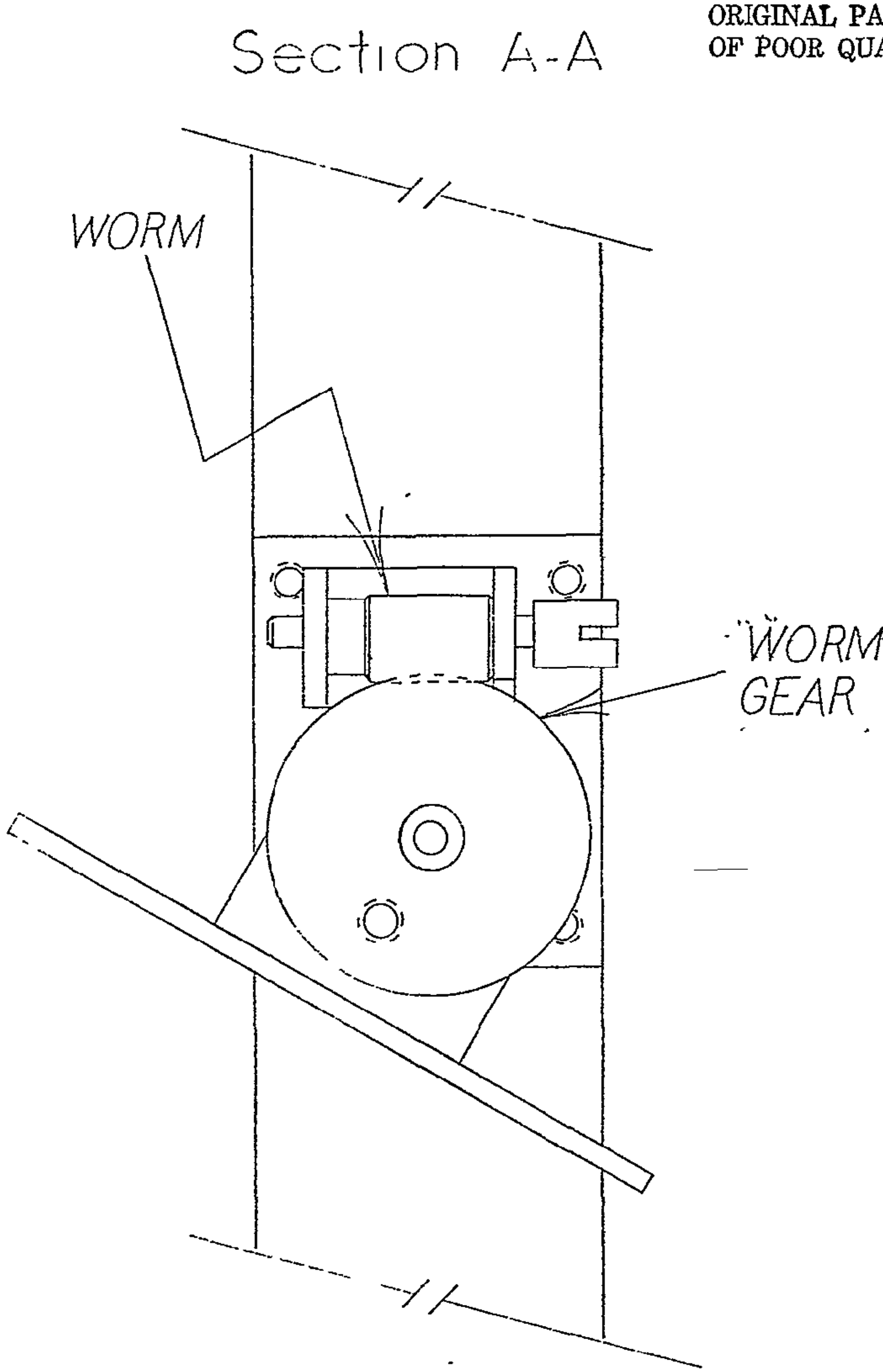

FIGURE 23

Detector Pointing Mechanism (Section View)

Note that this high reduction makes it impossible for the worm gear to turn the worm.

It was felt that the inaccuracies in the pointing of the detector of the old system arose from two sources. The first was the motion of the detector shaft in the holes of the blocks which supported it. There seemed to be an excessive amount of radial clearance of the shaft in the holes. This most likely was not present when originally built, but gradually developed from wear. To prevent this from occurring in the new design, the detector shaft is supported by ball bearings which should keep the shaft in a single axis of rotation.

The other source of play in the previous detector's positioning is believed to be caused by the method of attaching the worm gear and detector to the shaft. This was done by set screws over flat spots on the shaft. Since these set screws were very small, it was impossible to get them torqued down as tightly as necessary. There always seemed to be some relative motion possible between the worm gear and the detector. The new system does use set screws and flat spots, but also employs a direct connection between the worm gear and Detector Face Plate Holder. This direct connection is achieved by screwing the face plate holder to the outside face of the worm gear. These two measures should greatly increase the "stiffness" of the detector.

Two different face plates were designed since there at still some questions concerning the detector. Either of the mounting arrangements can be used. Design A mounts the Face Plate vertically before being aimed, while Design B mounts it horizontally. Design B is shown in Figures 22 and 23.

8.5 Mast Support Structure

The design for the structure to support the new mast shown in Figure 24 is rather similar to the previous design. An Upper Mast Bearing Block holds the sleeve bearing and extends back forming the top of the structure. The front mast support and mast side supports hold the bearing block firmly on three surfaces. These supports are tied into the mast main frames to which the slip rings, moast encoder, and lower bearing block are also fastened. The new mast is fastened to the MRV via the main frame.

The mast motor and motor gear are contained within the mast support structure. Space has been left around the motor in case a larger motor is needed. Provisions have also been made for mounting 3 electronic circuit cards inside the support structure. Slots have been cut at various locations to allow easy access to the pins of the card holders.

Drawings of all the components of the new mast are included in Appendix C.

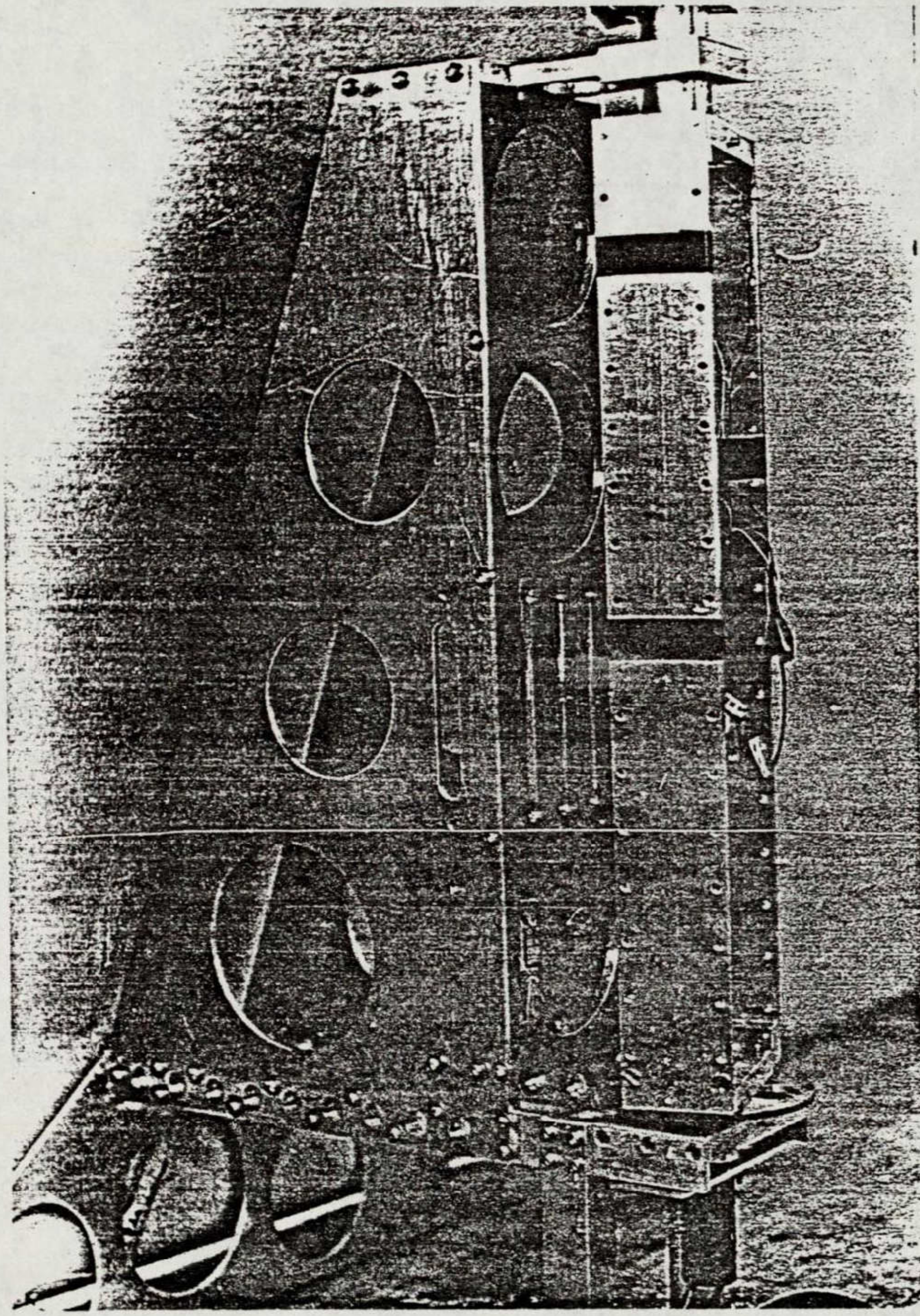

FIGURE 24

Mast Support Structure

CHAPTER 9

DISCUSSION AND CONCLUSIONS

9.1 Summary

A mechanical design for implementing the elevation scanning laser/multi-detector hazard detection system has been completed and the system has been fabricated. Close attention has been given to positioning accurately critical components and maintaining tight tolerances. Flexibility of the system was also considered to make important adjustments and vary the parameters for research in hazard detection. Lastly, an attempt was made to design a sturdy yet light weight system which wouldn't impede the performance of the RPI Rover.

9.2 Suggested Maintenance

A few comments concerning system maintenance are in order. Components requiring lubrication should be watched carefully. Specifically, grease should be kept on the mast and motor gears, and a film of oil should be maintained on top of the sleeve bearing and touching the upper mast tube. It would be a good idea to periodically check the set screws on the system. Set screws are located on the Elevation Scanner's couplings, the Detector Frame Supports, the Lower Mast Tube, and the Mast Encoder coupling.

9.3 Future Work

A careful evaluation of the new mast design should be conducted. This can best be done by testing the system and noting any problems that develop. Of particular interest are the Mast Motor and the Mast and Support Structure stiffnesses. Due to the assumptions required in calculating mast inertia and starting torques, the motor selected could be too small to do the job. Also, the lightening holes cut into some of the structural members may have weakened them to the point where too much movement and vibration of the mast might be experienced.

The final task will be to mount the multi-laser/multi-detector system on the Rover. Footings and tapped holes have been provided in the design, but specific connections to the vehicle have not been devised. The final mounting arrangement will depend on exactly where the mast is to be mounted on the Rover.

REFERENCES

1. Mabie, Hamilton H., and Ocvirk, Fred W., Mechanisms and Dynamics and Dynamics of Machinery, John Wiley and Sons, Inc., 1975.

2. Lipowicz, Robert F., "A Wheel Design Analysis and Locomotion Study for the RPI-Mars Roving Vehicle, Master's Project, Rensselaer Polytechnic Institute, May, 1976.

3. Truxal, John G., ed., Control Engineers' Handbook, McGraw-Hill Book Co., 1958.

4. Kern, Daniel S., "Mars Roving Vehicle Dimensional Considerations and Main Drive System Design," Master's Thesis, Rensselaer Polytechnic Institute, June 1974.

5. FMC Corp., Bearing Technical Journal, 1977.

6. Browning Manufacturing, Division of Emerson Electric Co., Browning Catalog No. 8, 1975.

7. W.M. Berg Inc., Manual A8, 1977.

APPENDIX A

BICYCLE MODEL COMPUTER PROGRAM AND OUTPUT

MAIN PROGRAM

```
C
      REAL MUF,MUR
      COMMON A,B,C,MUF,MUR,RHI,DELTRH,RHF,PHI,HALFW,R,THFRAD,THRRAD,
     1PHIRAD,PI,THF,THR
C
C        READ INPUTS
      READ(5,10) THF,THR
10    FORMAT(2F10.0)
      READ(5,20) A,B,C
20    FORMAT(3F10.0)
      READ(5,10) MUF,MUR
      READ(5,20) RHI,DELTRH,RHF
      READ(5,25) HALFW
25    FORMAT(F10.0)
      READ(5,25) R
C
C        PRINT INPUTS
      WRITE(6,30)
30    FORMAT('1',10X,'*PROGRAM INPUTS*')
      WRITE(6,40) THF,THR
40    FORMAT('-',' THF=',F6.1,10X,'THR=',F6.1,30X,'(IN DEGREES)')
      WRITE(6,50) A,B,C
50    FORMAT('-','A=',F5.1,13X,'B=',F5.1,13X,'C=',F5.1,13X,'(IN INCHES)
     1')
      WRITE(6,60) MUF,MUR
60    FORMAT('-','MUF=',F5.3,11X,'MUR=',F5.3,31X,'(NC UNITS)')
      WRITE(6,70) RHI,DELTRH,RHF
70    FORMAT('-','RHI=',F6.1,10X,'DELTRH=',F4.1,9X,'RHF=',F6.1,10X,'(IN
     1LBS.)')
      WRITE(6,80) HALFW
80    FORMAT('-','HALFW=',F5.1,49X,'(IN LBS.)')
      WRITE(6,90) R
90    FORMAT('-','R=',F4.1,54X,'(IN INCHES)')
C
C        CALCULATE ANGLES IN RADIANS
      PI=3.14159
      THFRAD=THF*PI/180.
      THRRAD=THR*PI/180.
C
C        SET UP CONTROL OF PHI
      PHI=0.0
      DO 100 I=1,9
      PHIRAD=PHI*PI/180
      CALL BICYCL
      PHI=PHI+5.
100   CONTINUE
      STOP
      END
```

SUBROUTINE BICYCL

```
C**********************************************************************
C          SUBROUTINE BICYCL
C
      SUBROUTINE BICYCL
      REAL MUF,MUR
      COMMON A,B,C,MUF,MUR,RHI,DELTRH,RHF,PHI,HALFW,R,THFRAD,THRRAD,
     1PHIRAD,PI,THF,THR
C
C          CALCULATE RV AND FV AND CHECK VEHICLE STABILITY
      FV=HALFW*(A*COS(PHIRAD)-C*SIN(PHIRAD)-R*SIN(THRRAD))/((A+B)*COS
     1(PHIRAD)+R*SIN(THFRAD)-R*SIN(THRRAD))
      RV=HALFW-FV
      IF(FV.LT.0.) GO TO 230
      IF(RV.LT.0.) GO TO 230
C
C          CALCULATE RATIO OF WHEEL SPEEDS, VF/VR
      VRAT=(SIN(PI/2.-PHIRAD+THRRAD))/(SIN(PI/2.+PHIRAD-THFRAD))
C
C          CALCULATE COMPARISON QUANTITIES
      COMP1=0.-MUF
      COMP2=MUF
      COMP3=0.-1./MUR
      COMP4=1.-MUR
C
C          PRINT HEADING
      WRITE(6,100) PHI,FV,RV,VRAT
100   FORMAT('1','PHI=',F6.1,' DEGREES',5X,'FV=',F5.1,' LBS.',5X,'RV=',
     1F5.1,' LBS.',5X,'VRAT=',F7.3)
      WRITE(6,110)
110   FORMAT('-',10X,'RH(LBS.)',10X,'TF(IN.-LBS.)',10X,'TR(IN.-LBS.)')
C
C          START ITERATIVE PROCESS TO FIND RANGE OF RH'S:
      RH=RHI
C
C          CALCULATE INTERMEDIATE PARAMETERS
120   FGAM=ATAN(RH/FV)
      RGAM=ATAN(RH/RV)
      FRHO=THFRAD-FGAM
      RRHO=PI/2.-THRRAD-RGAM
      TNFRHO=TAN(FRHO)
      TNRRHO=TAN(RRHO)
C
C          CALCULATE TANGENTIAL COMPONENTS
      FT=(SIN(FRHO)/COS(FGAM))*FV
      RT=(COS(RRHO)/COS(RGAM))*RV
C
C          CHECK SIGN OF FT AND GO TO APPROPRIATE LIMIT EQUATION
      IF(FT.GE.0.0) GO TO 130
      IF(TNFRHO.LT.COMP1) GO TO 180
      GO TO 140
130   IF(TNFRHO.GT.COMP2) GO TO 180
C
C          CHECK SIGN OF RT AND GO TO APPROPRIATE LIMIT EQUATION
140   IF(RT.GE.0.0) GO TO 150
      IF(TNRRHO.LT.COMP3) GO TO 188
```

```
      GO TO 160
150   IF(TNRRHO.LT.COMP4) GO TO 188
C
C        CALCULATE TORQUES IF LIMIT EQUATIONS ARE SATISFIED
160   TF=FT*R
      TR=RT*R
C
C        PRINT RESULTS IF LIMIT EQUATIONS ARE SATISFIED
      WRITE(6,170) RH,TF,TR
170   FORMAT(' ',10X,F6.1,13X,F7.2,15X,F7.2)
      GO TO 200
C
C        SEE IF REAR WHEEL SLIPS GIVEN THAT FRONT WHEEL DOES
180   IF(RT.GE.0.0) GO TO 182
      IF(TNRRHO.LT.COMP3) GO TO 192
      GO TO 184
182   IF(TNRRHO.LT.COMP4) GO TO 192
C
C        PRINT RESULTS IF ONLY FRONT WHEEL SLIPS
184   TR=RT*R
      WRITE(6,186) RH,TR
186   FORMAT(' ',10X,F6.1,14X,'WHEEL SLIPS',13X,F7.2)
      GO TO 200
C
C        PRINT RESULTS IF ONLY REAR WHEEL SLIPS
188   TF=FT*R
      WRITE(6,190) RH,TF
190   FORMAT(' ',10X,F6.1,13X,F7.2,16X,'WHEEL SLIPS')
      GO TO 200
C
C        PRINT RESULTS IF BOTH WHEELS SLIP
192   WRITE(6,194) RH
194   FORMAT(' ',10X,F6.1,13X,'* * * * *BOTH WHEELS SLIP* * * * *')
C
200   IF(RH.GE.RHF) GO TO 260
      RH=RH+DELTRH
      GO TO 120
C
230   WRITE(6,240) PHI,FV,RV
240   FORMAT('1','PHI=',F6.1,' DEGREES',5X,'FV=',F5.1,' LBS.',5X,'RF=',
     1F5.1,' LBS.')
      WRITE(6,250)
250   FORMAT('-','***VEHICLE WILL TIP OVER***')
      GO TO 200
260   RETURN
      END
```

COMPUTER OUTPUT

PROGRAM INPUTS

THF= 40.0	THR= 0.0		(IN DEGREES)
A= 30.0	B= 34.0	C= 24.0	(IN INCHES)
MUF=0.900	MUR=0.900		(NO UNITS)
RHI= 0.0	DELTRH= 0.5	RFF= 35.0	(IN LBS.)
HALFW=150.0			(IN LBS.)
R=10.0			(IN INCHES)

PHI= 0.0 DEGREES FV= 63.9 LBS. RV= 86.1 LBS. VRAT= 1.305

RH(LBS.)	TF(IN.-LBS.)	TR(IN.-LBS.)
0.0	410.71	0.00
0.5	406.88	5.00
1.0	403.05	10.00
1.5	399.22	15.00
2.0	395.39	20.00
2.5	391.56	25.00
3.0	387.73	30.00
3.5	383.90	35.00
4.0	380.07	40.00
4.5	376.24	45.00
5.0	372.41	50.00
5.5	368.58	55.00
6.0	364.75	60.00
6.5	360.92	65.00
7.0	357.09	70.00
7.5	353.26	75.00
8.0	349.43	80.00
8.5	345.60	85.00
9.0	341.77	90.00
9.5	337.94	95.00
10.0	334.10	100.00
10.5	330.27	105.00
11.0	326.44	110.00
11.5	322.61	115.00
12.0	318.78	120.00
12.5	314.95	125.00
13.0	311.12	130.00
13.5	307.29	135.00
14.0	303.46	140.00
14.5	299.63	145.00
15.0	295.80	150.00
15.5	291.97	155.00
16.0	288.14	160.00
16.5	284.31	165.00
17.0	280.48	170.00
17.5	276.65	175.00
18.0	272.82	180.00
18.5	268.99	185.00
19.0	265.16	190.00
19.5	261.33	195.00
20.0	257.50	200.00
20.5	253.67	205.00
21.0	249.84	210.00
21.5	246.01	215.00
22.0	242.18	220.00
22.5	238.35	225.00
23.0	234.52	230.00
23.5	230.69	235.00
24.0	226.86	240.00
24.5	223.03	245.00
25.0	219.20	250.00
25.5	215.37	255.00
26.0	211.54	260.00
26.5	207.71	265.00
27.0	203.88	270.00
27.5	200.05	275.00
28.0	196.22	280.00
28.5	192.39	285.00
29.0	188.56	290.00
29.5	184.73	295.00
30.0	180.90	300.00
30.5	177.07	305.00
31.0	173.24	310.00
31.5	169.41	315.00
32.0	165.58	320.00
32.5	161.74	325.00
33.0	157.91	330.00
33.5	154.08	335.00
34.0	150.25	340.00
34.5	146.42	345.00
35.0	142.59	350.00

PHI= 5.0 DEGREES FV= 59.4 LBS. RV= 90.6 LBS. VRAT= 1.216

RH(LBS.)	TF(IN.-LBS.)	TR(IN.-LBS.)
0.0	381.83	0.00
0.5	378.00	5.00
1.0	374.17	10.00
1.5	370.34	15.00
2.0	366.51	20.00
2.5	362.68	25.00
3.0	358.85	30.00
3.5	355.02	35.00
4.0	351.19	40.00
4.5	347.36	45.00
5.0	343.53	50.00
5.5	339.70	55.00
6.0	335.87	60.00
6.5	332.04	65.00
7.0	328.21	70.00
7.5	324.38	75.00
8.0	320.55	80.00
8.5	316.72	85.00
9.0	312.89	90.00
9.5	309.06	95.00
10.0	305.23	100.00
10.5	301.40	105.00
11.0	297.57	110.00
11.5	293.74	115.00
12.0	289.91	120.00
12.5	286.07	125.00
13.0	282.24	130.00
13.5	278.41	135.00
14.0	274.58	140.00
14.5	270.75	145.00
15.0	266.92	150.00
15.5	263.09	155.00
16.0	259.26	160.00
16.5	255.43	165.00
17.0	251.60	170.00
17.5	247.77	175.00
18.0	243.94	180.00
18.5	240.11	185.00
19.0	236.28	190.00
19.5	232.45	195.00
20.0	228.62	200.00
20.5	224.79	205.00
21.0	220.96	210.00
21.5	217.13	215.00
22.0	213.30	220.00
22.5	209.47	225.00
23.0	205.64	230.00
23.5	201.81	235.00
24.0	197.98	240.00
24.5	194.15	245.00
25.0	190.32	250.00
25.5	186.49	255.00
26.0	182.66	260.00
26.5	178.83	265.00
27.0	175.00	270.00
27.5	171.17	275.00
28.0	167.34	280.00
28.5	163.51	285.00
29.0	159.68	290.00
29.5	155.85	295.00
30.0	152.02	300.00
30.5	148.19	305.00
31.0	144.36	310.00
31.5	140.53	315.00
32.0	136.70	320.00
32.5	132.87	325.00
33.0	129.04	330.00
33.5	125.21	335.00
34.0	121.38	340.00
34.5	117.54	345.00
35.0	113.71	350.00

PHI= 10.0 DEGREES   FV= 54.8 LBS.   RV= 95.2 LBS.   VRAT= 1.137

RH(LBS.)	TF(IN.-LBS.)	TR(IN.-LBS.)
0.0	352.28	0.00
0.5	348.45	5.00
1.0	344.62	10.00
1.5	340.79	15.00
2.0	336.96	20.00
2.5	333.13	25.00
3.0	329.30	30.00
3.5	325.47	35.00
4.0	321.64	40.00
4.5	317.81	45.00
5.0	313.98	50.00
5.5	310.15	55.00
6.0	306.32	60.00
6.5	302.49	65.00
7.0	298.66	70.00
7.5	294.82	75.00
8.0	290.99	80.00
8.5	287.16	85.00
9.0	283.33	90.00
9.5	279.50	95.00
10.0	275.67	100.00
10.5	271.84	105.00
11.0	268.01	110.00
11.5	264.18	115.00
12.0	260.35	120.00
12.5	256.52	125.00
13.0	252.69	130.00
13.5	248.86	135.00
14.0	245.03	140.00
14.5	241.20	145.00
15.0	237.37	150.00
15.5	233.54	155.00
16.0	229.71	160.00
16.5	225.88	165.00
17.0	222.05	170.00
17.5	218.22	175.00
18.0	214.39	180.00
18.5	210.56	185.00
19.0	206.73	190.00
19.5	202.90	195.00
20.0	199.07	200.00
20.5	195.24	205.00
21.0	191.41	210.00
21.5	187.58	215.00
22.0	183.75	220.00
22.5	179.92	225.00
23.0	176.09	230.00
23.5	172.26	235.00
24.0	168.43	240.00
24.5	164.60	245.00
25.0	160.77	250.00
25.5	156.94	255.00
26.0	153.11	260.00
26.5	149.28	265.00
27.0	145.45	270.00
27.5	141.62	275.00
28.0	137.79	280.00
28.5	133.96	285.00
29.0	130.13	290.00
29.5	126.30	295.00
30.0	122.46	300.00
30.5	118.63	305.00
31.0	114.80	310.00
31.5	110.97	315.00
32.0	107.14	320.00
32.5	103.31	325.00
33.0	99.48	330.00
33.5	95.65	335.00
34.0	91.82	340.00
34.5	87.99	345.00
35.0	84.16	350.00

PHI= 15.0 DEGREES FV= 50.0 LBS. RV=100.0 LBS. VRAT= 1.066

RH(LBS.)	TF(IN.-LBS.)	TR(IN.-LBS.)
0.0	321.63	0.00
0.5	317.80	5.00
1.0	313.97	10.00
1.5	310.14	15.00
2.0	306.31	20.00
2.5	302.48	25.00
3.0	298.65	30.00
3.5	294.82	35.00
4.0	290.99	40.00
4.5	287.16	45.00
5.0	283.33	50.00
5.5	279.50	55.00
6.0	275.67	60.00
6.5	271.84	65.00
7.0	268.01	70.00
7.5	264.18	75.00
8.0	260.35	80.00
8.5	256.52	85.00
9.0	252.69	90.00
9.5	248.86	95.00
10.0	245.03	100.00
10.5	241.20	105.00
11.0	237.37	110.00
11.5	233.54	115.00
12.0	229.71	120.00
12.5	225.88	125.00
13.0	222.05	130.00
13.5	218.22	135.00
14.0	214.39	140.00
14.5	210.56	145.00
15.0	206.73	150.00
15.5	202.90	155.00
16.0	199.07	160.00
16.5	195.24	165.00
17.0	191.41	170.00
17.5	187.58	175.00
18.0	183.75	180.00
18.5	179.92	185.00
19.0	176.09	190.00
19.5	172.26	195.00
20.0	168.43	200.00
20.5	164.60	205.00
21.0	160.77	210.00
21.5	156.93	215.00
22.0	153.10	220.00
22.5	149.27	225.00
23.0	145.44	230.00
23.5	141.61	235.00
24.0	137.78	240.00
24.5	133.95	245.00
25.0	130.12	250.00
25.5	126.29	255.00
26.0	122.46	260.00
26.5	118.63	265.00
27.0	114.80	270.00
27.5	110.97	275.00
28.0	107.14	280.00
28.5	103.31	285.00
29.0	99.48	290.00
29.5	95.65	295.00
30.0	91.82	300.00
30.5	87.99	305.00
31.0	84.16	310.00
31.5	80.33	315.00
32.0	76.50	320.00
32.5	72.67	325.00
33.0	68.84	330.00
33.5	65.01	335.00
34.0	61.18	340.00
34.5	57.35	345.00
35.0	53.52	350.00

PHI= 20.0 DEGREES FV= 45.0 LBS. RV=105.0 LBS. VRAT= 1.000

RH(LBS.)	TF(IN.-LBS.)	TR(IN.-LBS.)
0.0	289.43	0.00
0.5	285.60	5.00
1.0	281.76	10.00
1.5	277.93	15.00
2.0	274.10	20.00
2.5	270.27	25.00
3.0	266.44	30.00
3.5	262.61	35.00
4.0	258.78	40.00
4.5	254.95	45.00
5.0	251.12	50.00
5.5	247.29	55.00
6.0	243.46	60.00
6.5	239.63	65.00
7.0	235.80	70.00
7.5	231.97	75.00
8.0	228.14	80.00
8.5	224.31	85.00
9.0	220.48	90.00
9.5	216.65	95.00
10.0	212.82	100.00
10.5	208.99	105.00
11.0	205.16	110.00
11.5	201.33	115.00
12.0	197.50	120.00
12.5	193.67	125.00
13.0	189.84	130.00
13.5	186.01	135.00
14.0	182.18	140.00
14.5	178.35	145.00
15.0	174.52	150.00
15.5	170.69	155.00
16.0	166.86	160.00
16.5	163.03	165.00
17.0	159.20	170.00
17.5	155.37	175.00
18.0	151.54	180.00
18.5	147.71	185.00
19.0	143.88	190.00
19.5	140.05	195.00
20.0	136.22	200.00
20.5	132.39	205.00
21.0	128.56	210.00
21.5	124.73	215.00
22.0	120.90	220.00
22.5	117.07	225.00
23.0	113.24	230.00
23.5	109.40	235.00
24.0	105.57	240.00
24.5	101.74	245.00
25.0	97.91	250.00
25.5	94.08	255.00
26.0	90.25	260.00
26.5	86.42	265.00
27.0	82.59	270.00
27.5	78.76	275.00
28.0	74.93	280.00
28.5	71.10	285.00
29.0	67.27	290.00
29.5	63.44	295.00
30.0	59.61	300.00
30.5	55.78	305.00
31.0	51.95	310.00
31.5	48.12	315.00
32.0	44.29	320.00
32.5	40.46	325.00
33.0	36.63	330.00
33.5	32.80	335.00
34.0	28.97	340.00
34.5	25.14	345.00
35.0	21.31	350.00

PHI= 25.0 DEGREES FV= 39.7 LBS. RV=110.3 LBS. VRAT= 0.938

RH(LBS.)	TF(IN.-LBS.)	TR(IN.-LBS.)
0.0	255.09	0.00
0.5	251.26	5.00
1.0	247.43	10.00
1.5	243.60	15.00
2.0	239.77	20.00
2.5	235.94	25.00
3.0	232.11	30.00
3.5	228.28	35.00
4.0	224.45	40.00
4.5	220.62	45.00
5.0	216.79	50.00
5.5	212.96	55.00
6.0	209.13	60.00
6.5	205.30	65.00
7.0	201.47	70.00
7.5	197.64	75.00
8.0	193.81	80.00
8.5	189.98	85.00
9.0	186.15	90.00
9.5	182.31	95.00
10.0	178.48	100.00
10.5	174.65	105.00
11.0	170.82	110.00
11.5	166.99	115.00
12.0	163.16	120.00
12.5	159.33	125.00
13.0	155.50	130.00
13.5	151.67	135.00
14.0	147.84	140.00
14.5	144.01	145.00
15.0	140.18	150.00
15.5	136.35	155.00
16.0	132.52	160.00
16.5	128.69	165.00
17.0	124.86	170.00
17.5	121.03	175.00
18.0	117.20	180.00
18.5	113.37	185.00
19.0	109.54	190.00
19.5	105.71	195.00
20.0	101.88	200.00
20.5	98.05	205.00
21.0	94.22	210.00
21.5	90.39	215.00
22.0	86.56	220.00
22.5	82.73	225.00
23.0	78.90	230.00
23.5	75.07	235.00
24.0	71.24	240.00
24.5	67.41	245.00
25.0	63.58	250.00
25.5	59.75	255.00
26.0	55.92	260.00
26.5	52.09	265.00
27.0	48.26	270.00
27.5	44.43	275.00
28.0	40.60	280.00
28.5	36.77	285.00
29.0	32.94	290.00
29.5	29.11	295.00
30.0	25.28	300.00
30.5	21.45	305.00
31.0	17.62	310.00
31.5	13.79	315.00
32.0	9.95	320.00
32.5	6.12	325.00
33.0	2.29	330.00
33.5	-1.54	335.00
34.0	-5.37	340.00
34.5	-9.20	345.00
35.0	-13.03	350.00

PHI= 30.0 DEGREES FV= 33.9 LBS. RV=116.1 LBS. VRAT= 0.879

RH(LBS.)	TF(IN.-LBS.)	TR(IN.-LBS.)
0.0	217.93	0.00
0.5	214.10	5.00
1.0	210.27	10.00
1.5	206.44	15.00
2.0	202.61	20.00
2.5	198.78	25.00
3.0	194.95	30.00
3.5	191.12	35.00
4.0	187.29	40.00
4.5	183.46	45.00
5.0	179.63	50.00
5.5	175.80	55.00
6.0	171.97	60.00
6.5	168.14	65.00
7.0	164.31	70.00
7.5	160.48	75.00
8.0	156.65	80.00
8.5	152.82	85.00
9.0	148.99	90.00
9.5	145.16	95.00
10.0	141.33	100.00
10.5	137.50	105.00
11.0	133.67	110.00
11.5	129.84	115.00
12.0	126.01	120.00
12.5	122.18	125.00
13.0	118.35	130.00
13.5	114.52	135.00
14.0	110.69	140.00
14.5	106.86	145.00
15.0	103.03	150.00
15.5	99.20	155.00
16.0	95.37	160.00
16.5	91.54	165.00
17.0	87.71	170.00
17.5	83.88	175.00
18.0	80.05	180.00
18.5	76.22	185.00
19.0	72.39	190.00
19.5	68.56	195.00
20.0	64.73	200.00
20.5	60.89	205.00
21.0	57.06	210.00
21.5	53.23	215.00
22.0	49.40	220.00
22.5	45.57	225.00
23.0	41.74	230.00
23.5	37.91	235.00
24.0	34.08	240.00
24.5	30.25	245.00
25.0	26.42	250.00
25.5	22.59	255.00
26.0	18.76	260.00
26.5	14.93	265.00
27.0	11.10	270.00
27.5	7.27	275.00
28.0	3.44	280.00
28.5	-0.39	285.00
29.0	-4.22	290.00
29.5	-8.05	295.00
30.0	-11.88	300.00
30.5	-15.71	305.00
31.0	-19.54	310.00
31.5	-23.37	315.00
32.0	-27.20	320.00
32.5	-31.03	325.00
33.0	-34.86	330.00
33.5	-38.69	335.00
34.0	-42.52	340.00
34.5	-46.35	345.00
35.0	-50.18	350.00

PHI= 35.0 DEGREES FV= 27.5 LBS. RV=122.5 LBS. VRAT= 0.822

RH(LBS.)	TF(IN.-LBS.)	TR(IN.-LBS.)
0.0	177.08	0.00
0.5	173.25	5.00
1.0	169.42	10.00
1.5	165.59	15.00
2.0	161.76	20.00
2.5	157.93	25.00
3.0	154.09	30.00
3.5	150.26	35.00
4.0	146.43	40.00
4.5	142.60	45.00
5.0	138.77	50.00
5.5	134.94	55.00
6.0	131.11	60.00
6.5	127.28	65.00
7.0	123.45	70.00
7.5	119.62	75.00
8.0	115.79	80.00
8.5	111.96	85.00
9.0	108.13	90.00
9.5	104.30	95.00
10.0	100.47	100.00
10.5	96.64	105.00
11.0	92.81	110.00
11.5	88.98	115.00
12.0	85.15	120.00
12.5	81.32	125.00
13.0	77.49	130.00
13.5	73.66	135.00
14.0	69.83	140.00
14.5	66.00	145.00
15.0	62.17	150.00
15.5	58.34	155.00
16.0	54.51	160.00
16.5	50.68	165.00
17.0	46.85	170.00
17.5	43.02	175.00
18.0	39.19	180.00
18.5	35.36	185.00
19.0	31.53	190.00
19.5	27.70	195.00
20.0	23.87	200.00
20.5	20.04	205.00
21.0	16.21	210.00
21.5	12.38	215.00
22.0	8.55	220.00
22.5	4.72	225.00
23.0	0.89	230.00
23.5	-2.94	235.00
24.0	-6.77	240.00
24.5	-10.60	245.00
25.0	-14.43	250.00
25.5	-18.27	255.00
26.0	-22.10	260.00
26.5	-25.93	265.00
27.0	-29.76	270.00
27.5	-33.59	275.00
28.0	-37.42	280.00
28.5	-41.25	285.00
29.0	-45.08	290.00
29.5	-48.91	295.00
30.0	-52.74	300.00
30.5	-56.57	305.00
31.0	-60.40	310.00
31.5	-64.23	315.00
32.0	-68.06	320.00
32.5	-71.89	325.00
33.0	-75.72	330.00
33.5	-79.55	335.00
34.0	-83.38	340.00
34.5	-87.21	345.00
35.0	-91.04	350.00

PHI= 40.0 DEGREES FV= 20.4 LBS. RV=129.6 LBS. VRAT= 0.766

RH(LBS.)	TF(IN.-LBS.)	TR(IN.-LBS.)
0.0	131.35	0.00
0.5	127.52	5.00
1.0	123.69	10.00
1.5	119.86	15.00
2.0	116.03	20.00
2.5	112.20	25.00
3.0	108.37	30.00
3.5	104.54	35.00
4.0	100.71	40.00
4.5	96.88	45.00
5.0	93.05	50.00
5.5	89.22	55.00
6.0	85.38	60.00
6.5	81.55	65.00
7.0	77.72	70.00
7.5	73.89	75.00
8.0	70.06	80.00
8.5	66.23	85.00
9.0	62.40	90.00
9.5	58.57	95.00
10.0	54.74	100.00
10.5	50.91	105.00
11.0	47.08	110.00
11.5	43.25	115.00
12.0	39.42	120.00
12.5	35.59	125.00
13.0	31.76	130.00
13.5	27.93	135.00
14.0	24.10	140.00
14.5	20.27	145.00
15.0	16.44	150.00
15.5	12.61	155.00
16.0	8.78	160.00
16.5	4.95	165.00
17.0	1.12	170.00
17.5	-2.71	175.00
18.0	-6.54	180.00
18.5	-10.37	185.00
19.0	-14.20	190.00
19.5	-18.03	195.00
20.0	-21.86	200.00
20.5	-25.69	205.00
21.0	-29.52	210.00
21.5	-33.35	215.00
22.0	-37.18	220.00
22.5	-41.01	225.00
23.0	-44.84	230.00
23.5	-48.67	235.00
24.0	-52.50	240.00
24.5	-56.33	245.00
25.0	-60.16	250.00
25.5	-63.99	255.00
26.0	-67.82	260.00
26.5	-71.65	265.00
27.0	-75.48	270.00
27.5	-79.31	275.00
28.0	-83.14	280.00
28.5	-86.97	285.00
29.0	-90.81	290.00
29.5	-94.64	295.00
30.0	-98.47	300.00
30.5	-102.30	305.00
31.0	-106.13	310.00
31.5	-109.96	315.00
32.0	-113.79	320.00
32.5	-117.62	325.00
33.0	-121.45	330.00
33.5	-125.28	335.00
34.0	-129.11	340.00
34.5	-132.94	345.00
35.0	-136.77	350.00

APPENDIX B

MECHANICAL COMPONENTS PURCHASED

COMPONENT	MANUFACTURER AND STOCK NUMBER	VENDOR
Mirror Motor	Micro Mo 330/D09 motor with 03/2 gear head of 5.4:1 reduction	Micro Mo Electronics Inc 3691 Lee Rd. Cleveland, OH 44120
Mirror Bearings	Fafnir 33KDD3	Bearing Distributors 1 Spring Ave. Troy, N.Y. 12181
Motor-Mirror Coupling	Helical 4042-5-4	Helical Products Inc. 901 McCoy Lane P.O.Box 2296 Santa Maria, CA. 93454
Mirror-Encoder Coupling	Helical 4042-4-4	Helical Products Inc.
Sleeve Bearing	Randall SH-419	TEK Bearing Co. Inc. 776 Watervliet-Shaker Rd. Latham, N.Y.
Lower Mast Ball Bearing	Federall R12-FF	Bearing Distributors
Detector Worm Gear	Berg W64B21-S120	W.M. Berg, Inc. 499 Ocean Ave. East Rockaway,L.I.,N.Y.
Detector Worm	Berg W64S-4S	W.M. Berg, Inc.
Mast Gear	Berg F64S3-256	W.M. Berg, Inc.
Mast Motor Gear	Berg P64S19X-256	W.M. Berg, Inc.
Mast Motor	Globe 168A229-2	Jaco Electronics Inc. 145 Oser Ave. Hauppauge, L.I., N.Y. 11787
Mast Encoder Coupling	Berg CC9-20-4	W.M. Berg, Inc.

APPENDIX C

DRAWINGS OF MAST COMPONENTS

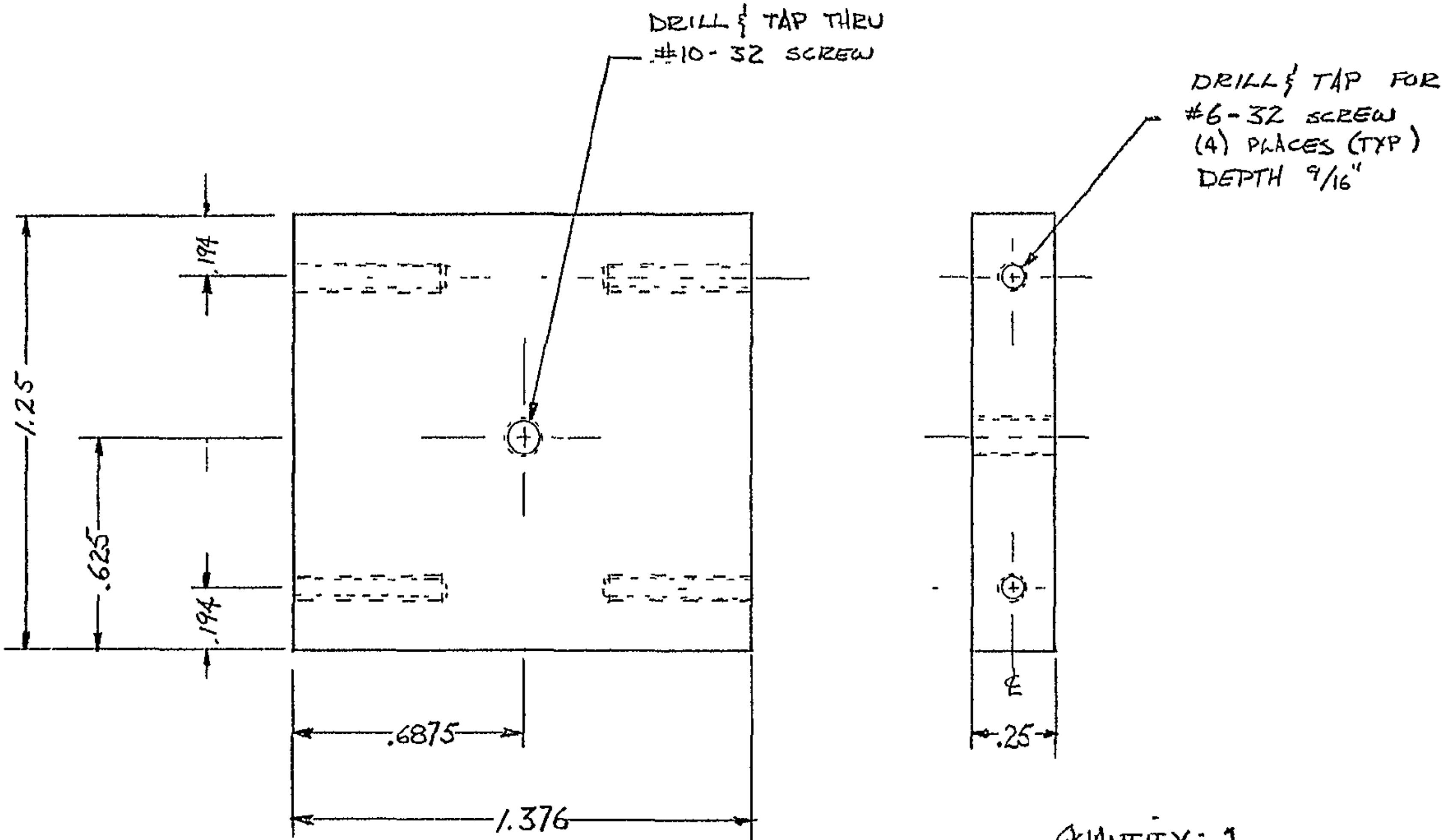

QUANTITY: 1

TOLERANCES (EXCEPT AS NOTED)	REVISIONS			UPPER SUPPORT		
	NO	DATE	BY	Mars Rover		
DECIMAL ± .005	1					
	2					
FRACTIONAL ±	3			DRAWN BY RAL	SCALE	MATERIAL ALUM
	4			CHK'D	DATE 2-6-78	DRAWING NO
ANGULAR ±	5			TRACED	APP D	

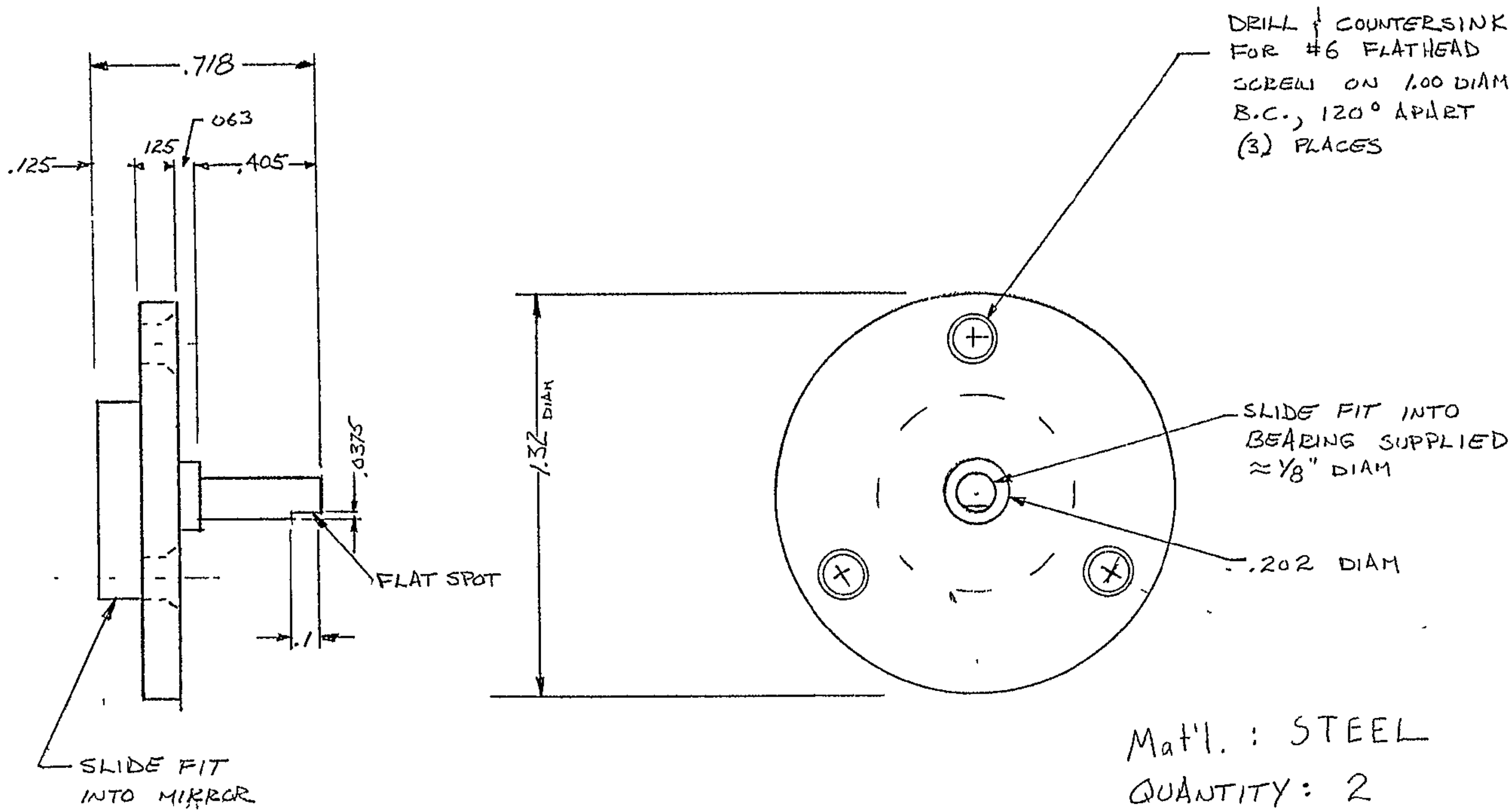

Mat'l. : STEEL
QUANTITY : 2

TOLERANCES (EXCEPT AS NOTED)	REVISIONS			MARS ROVER		
	NO	DATE	BY	MIRROR FLANGE		
DECIMAL ± .005	1					
	2					
FRACTIONAL ±	3			DRAWN BY K.L.L	SCALE 3" = 1"	MATERIAL STEEL
ANGULAR ±	4			CHK'D	DATE 2/24/78	DRAWING NO
	5			TRACED	APP D	

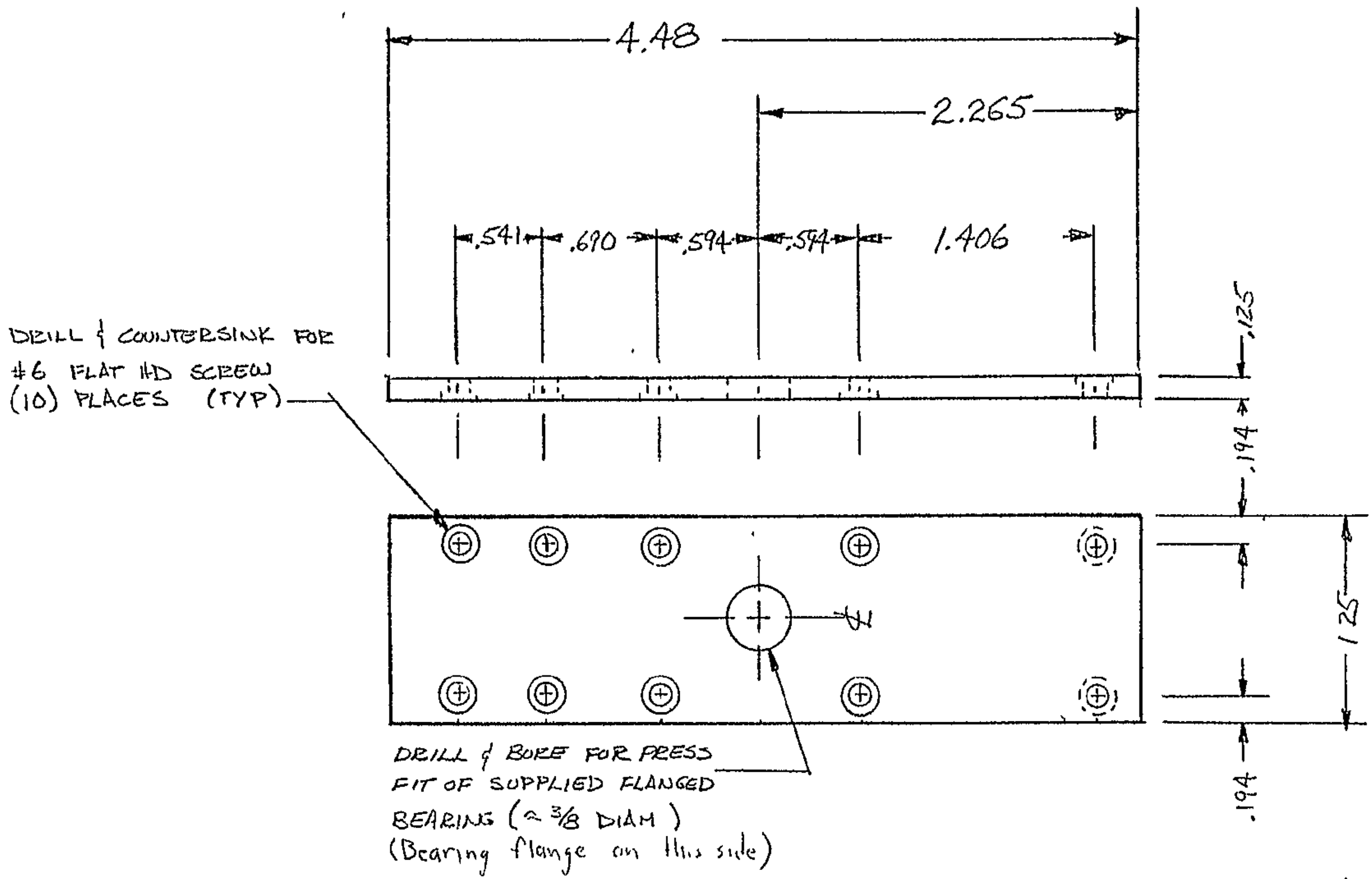

QUANTITY: 1

TOLERANCES (EXCEPT AS NOTED)	REVISIONS NO	DATE	BY	MARS ROVER		
DECIMAL	1			RIGHT SCANNER FRAME		
± .005	2					
FRACTIONAL	3			DRAWN BY RAL	SCALE 1" = 1"	MATERIAL Al 011
±	4			CHK'D	DATE 3-27-78	DRAWING NO
ANGULAR ±	5			TRACED	APP'D	

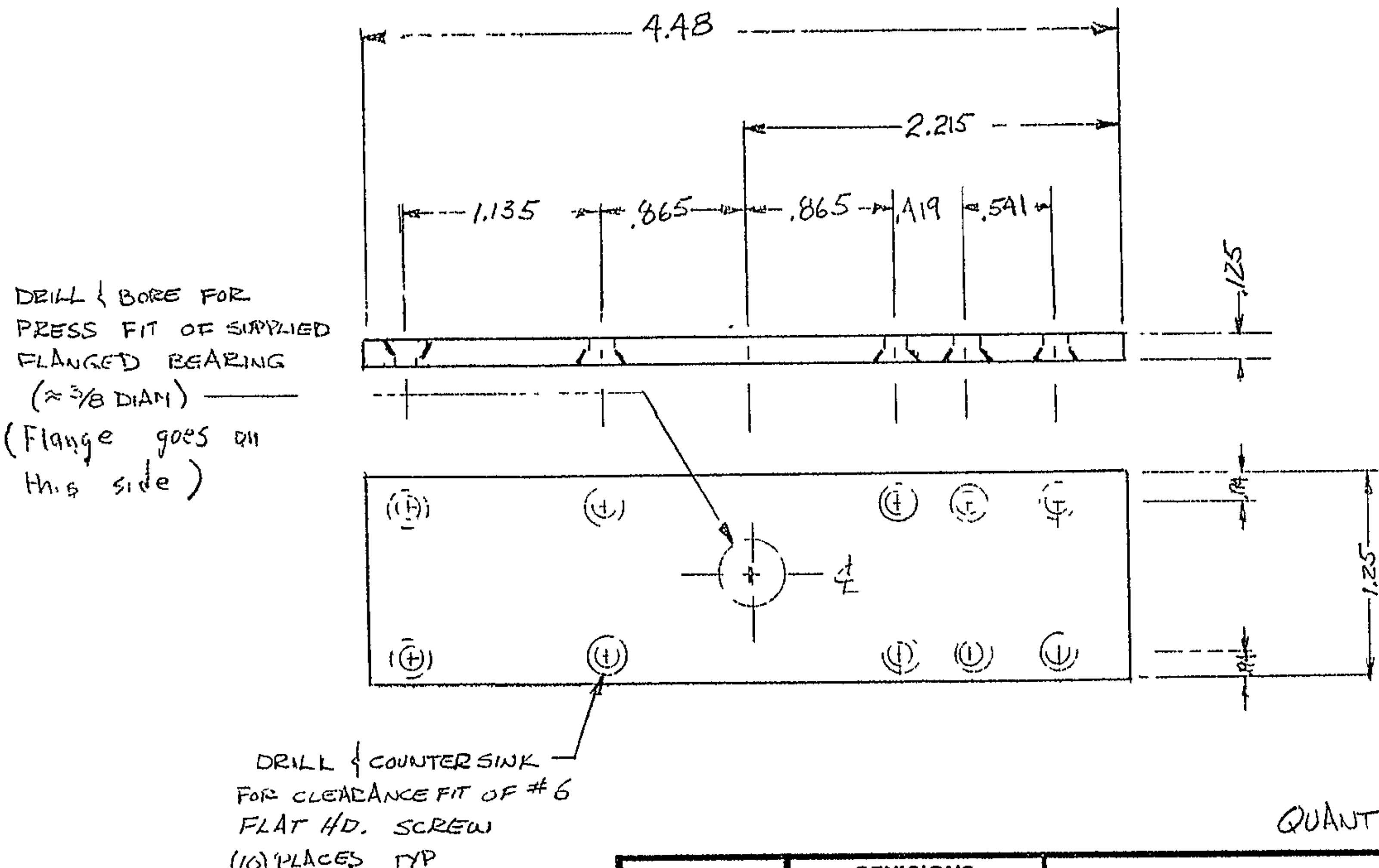

QUANTITY : 1

TOLERANCES (EXCEPT AS NOTED)	REVISIONS NO	DATE	BY	
DECIMAL ± .005	1			LEFT SCANNER FRAME
	2			MARS ROVER
FRACTIONAL ±	3			DRAWN BY: [illegible] — SCALE: 1" - 1" — MATERIAL: [illegible]
	4			CHK D — DATE: / - — DRAWING NO
ANGULAR ±	5			TRACED — APP D

TELEDYNE POST 18AE-01E—8½X11

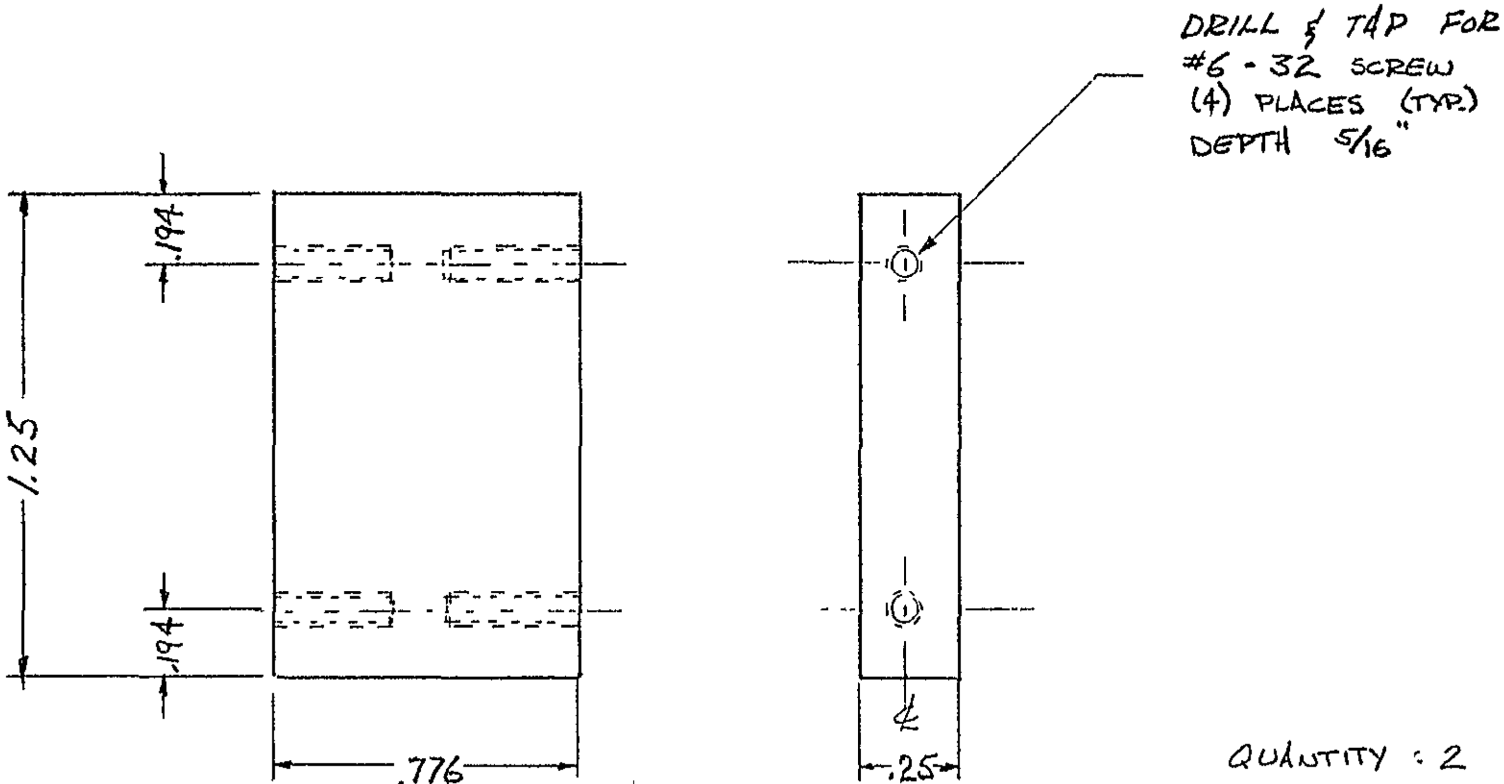

QUANTITY : 2

TOLERANCES (EXCEPT AS NOTED)	REVISIONS		
	NO	DATE	BY
DECIMAL ± .005	1		
	2		
FRACTIONAL ±	3		
	4		
ANGULAR ±	5		

ENCODER SUPPORT

Mars Rover

DRAWN BY RAL	SCALE 2" = 1"	MATERIAL ALUM.
CHK'D	DATE 2-6-78	DRAWING NO
TRACED	APP D	

TELEDYNE POST 18AE-01E–8½X11

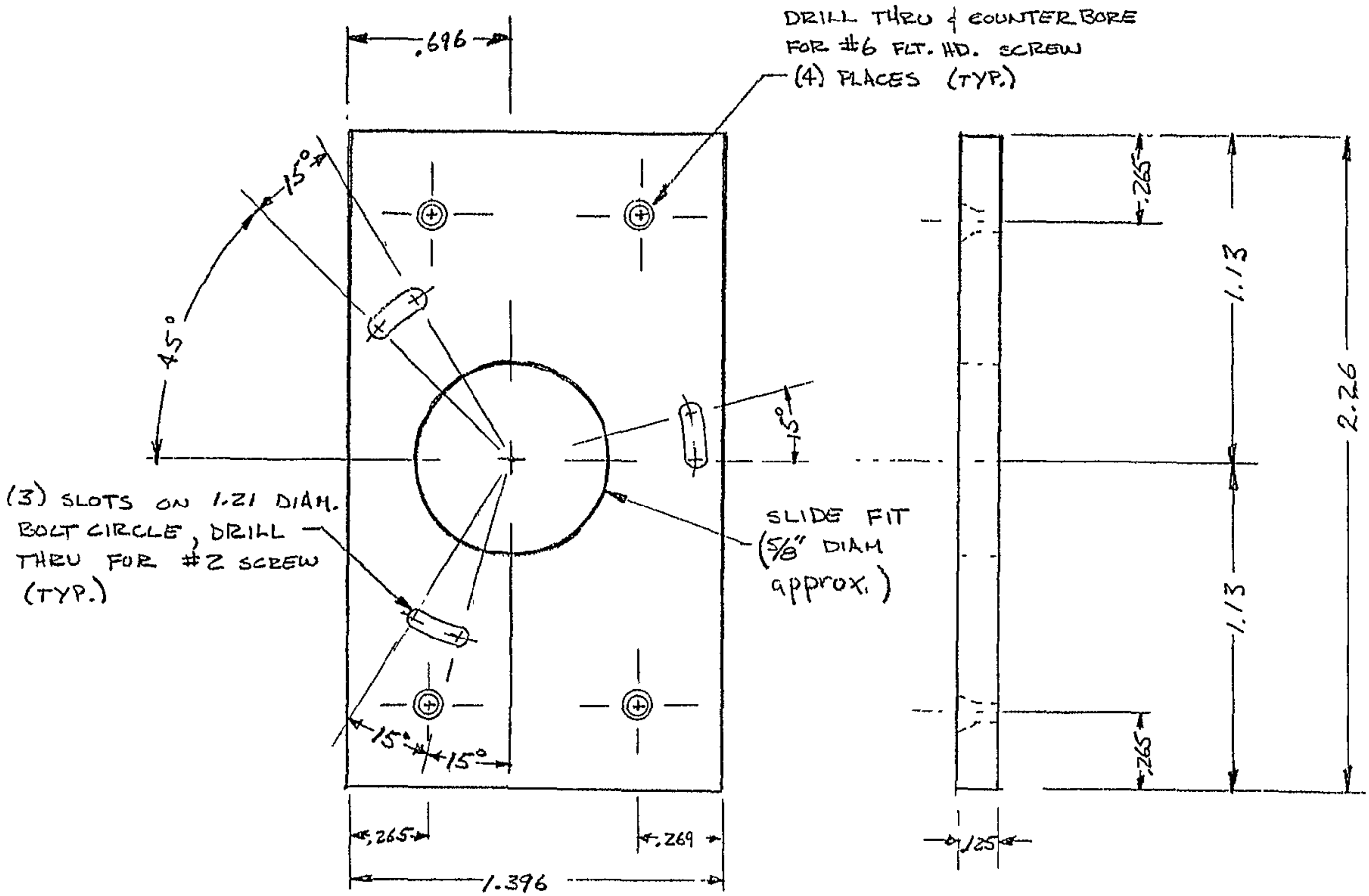

TOLERANCES (EXCEPT AS NOTED)	REVISIONS			ENCODER MOUNTING PLATE	
	NO	DATE	BY	Mars Rover	
DECIMAL ± .005	1			DRAWN BY R.A.L	SCALE 2" = 1"
FRACTIONAL ±	2			CHK'D	DATE 2-13-78
	3			TRACED	APP'D
ANGULAR ±	4			MATERIAL ALUM.	DRAWING NO
	5				

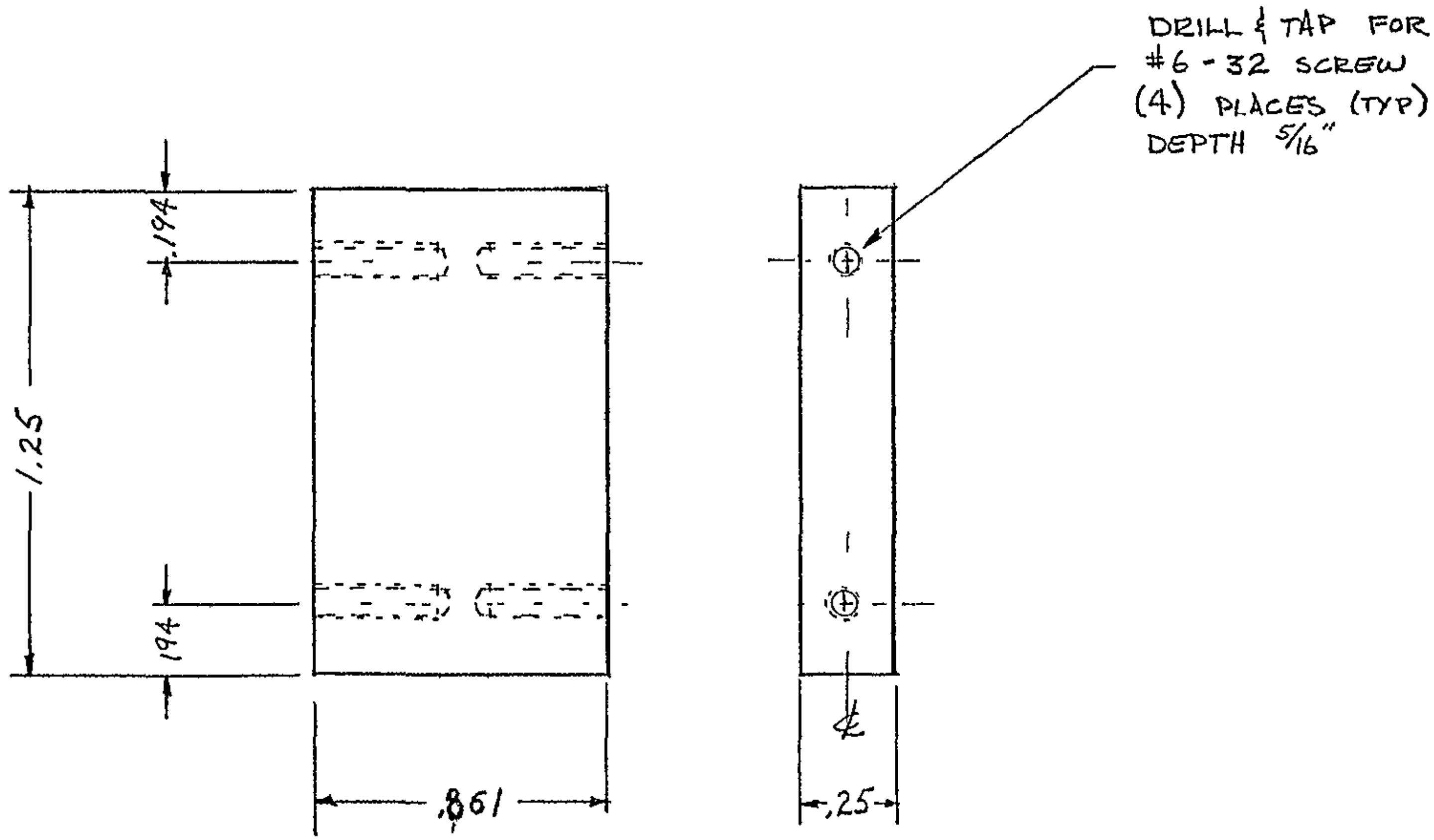

QUANTITY : 2

TOLERANCES (EXCEPT AS NOTED)	REVISIONS			MOTOR SUPPORT		
	NO	DATE	BY	Mars Rover		
DECIMAL ± .005	1					
	2					
FRACTIONAL ±	3			DRAWN BY RAL	SCALE 2" : 1"	MATERIAL ALUM
	4			CHK'D	DATE 2-8-78	DRAWING NO
ANGULAR ±	5			TRACED	APP D	

TELEDYNE POST 18AE-01E-8½X11

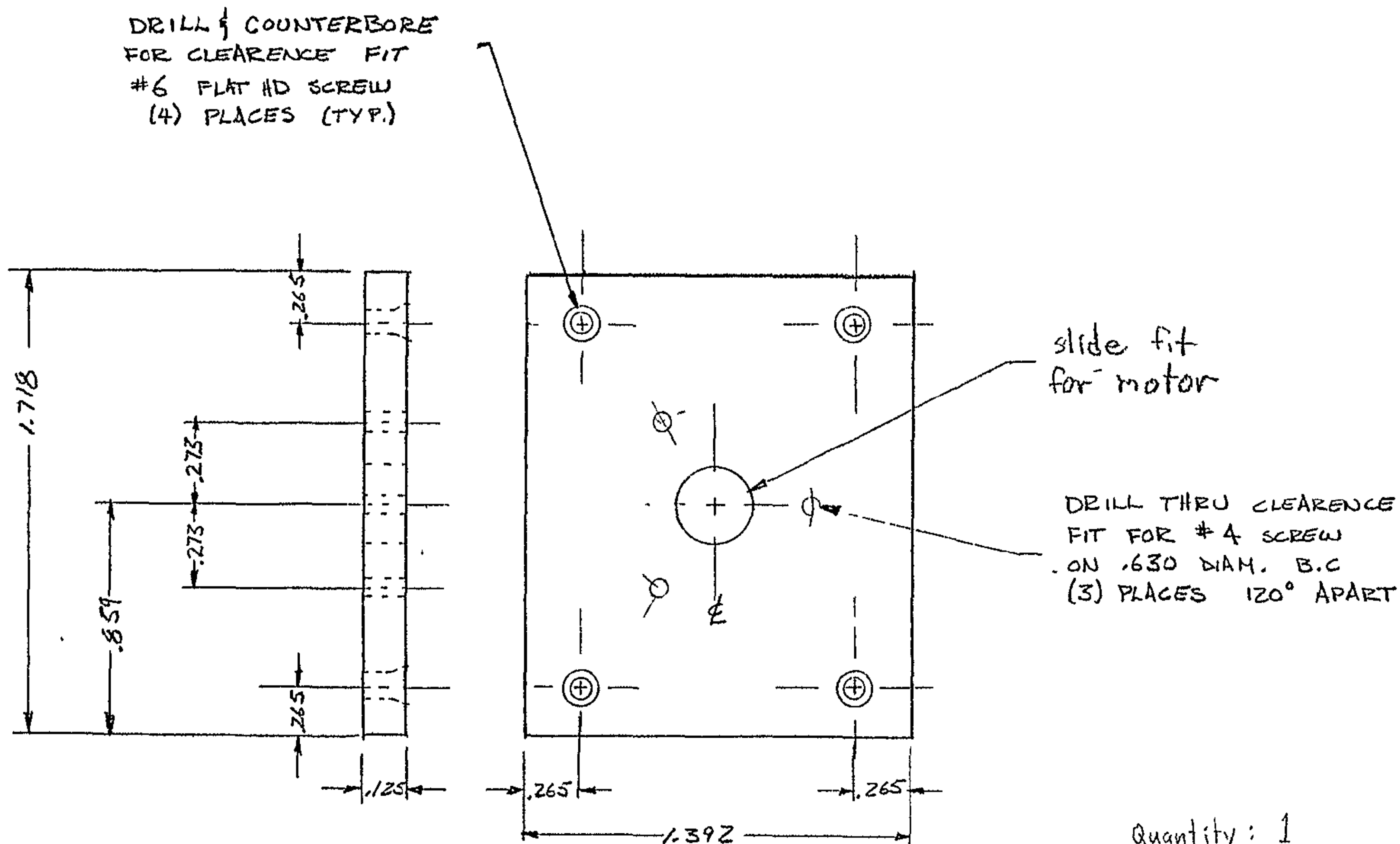

Quantity: 1

TOLERANCES (EXCEPT AS NOTED)	REVISIONS NO	DATE	BY	
DECIMAL ± .005	1			MOTOR MOUNTING PLATE
	2			Mars Rover
FRACTIONAL ±	3			DRAWN BY R.A.L · SCALE NONE · MATERIAL ALUM
ANGULAR ±	4			CHK'D · DATE 6-8-78 · DRAWING NO
	5			TRACED · APP'D

TELEDYNE POST 18AE 01E–8½X11

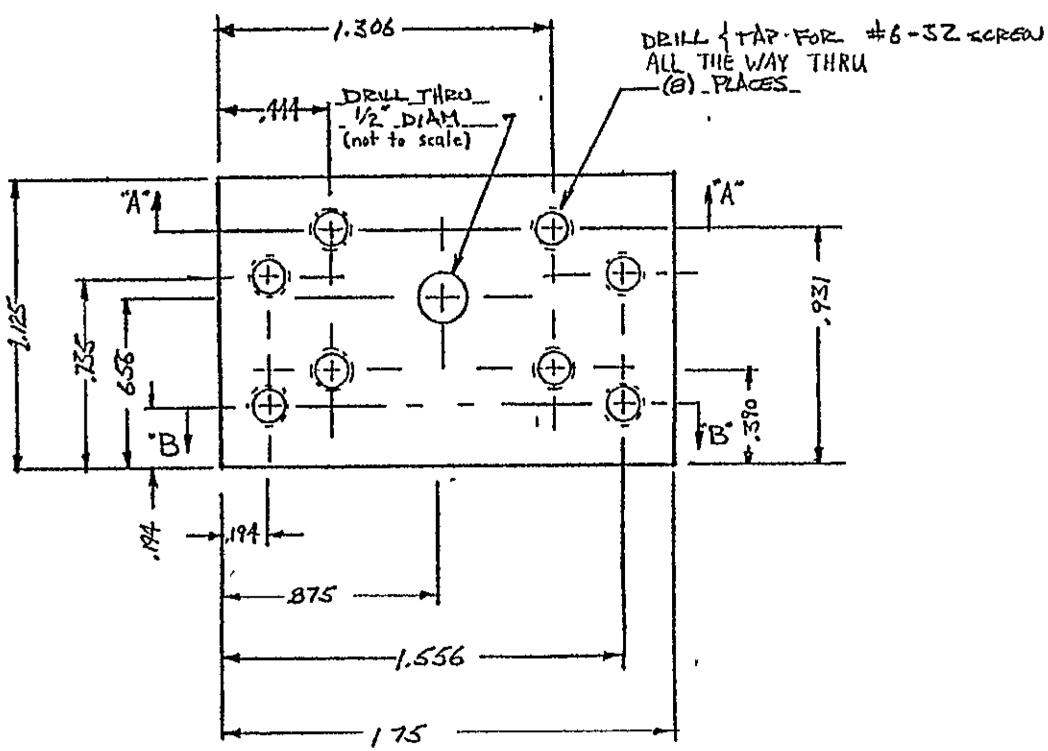

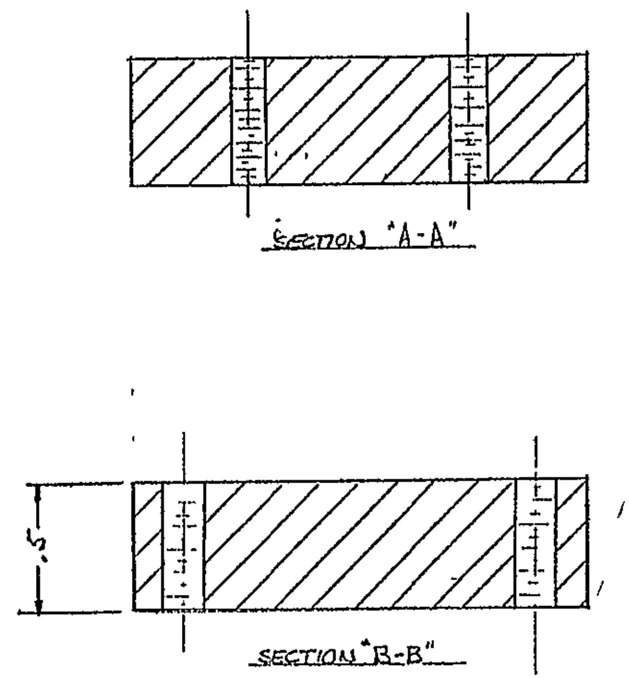

QUANTITY : 2

TOLERANCES (EXCEPT AS NOTED)	REVISIONS NO	DATE	BY	MARS ROVER		
DECIMAL ±	1			SCANNER SPACING BLOCKS		
	2					
FRACTIONAL ±	3			DRAWN BY RAL	SCALE 1" = 1/2"	MATERIAL ALUM
	4			CHK D	DATE 3-31-78	DRAWING NO
ANGULAR ±	5			TRACED	APP D	

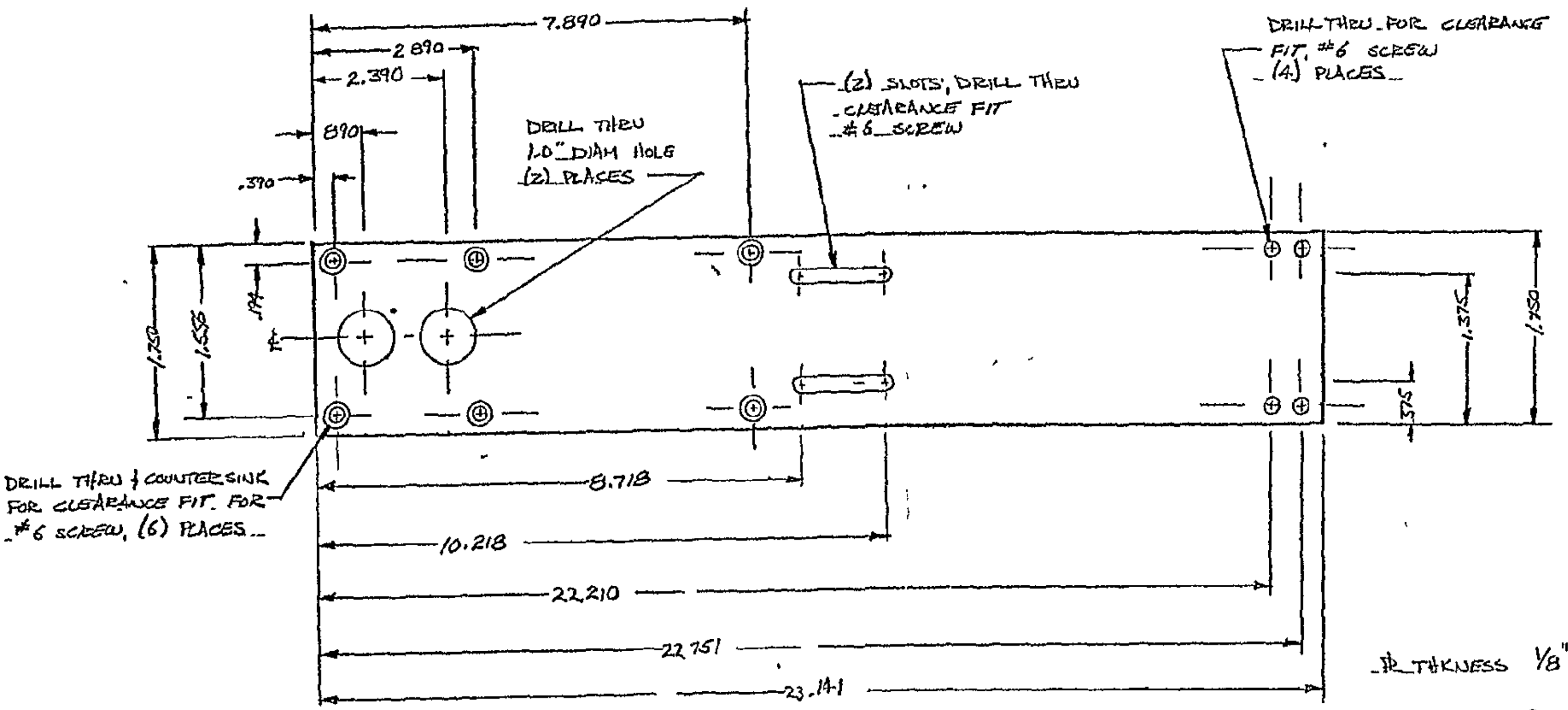

(Lengths not to scale)

THKNESS 1/8"

QUANTITY : 2

TOLERANCES (EXCEPT AS NOTED)	REVISIONS			MARS ROVER
	NO	DATE	BY	OPTICS FRAME
DECIMAL ±	1			DRAWN BY RAL — SCALE N.T.S — MATERIAL ALUM
FRACTIONAL ±	2			CHK D — DATE 3-31-78 — DRAWING NO
ANGULAR ±	3			TRACED — APP D
	4			
	5			

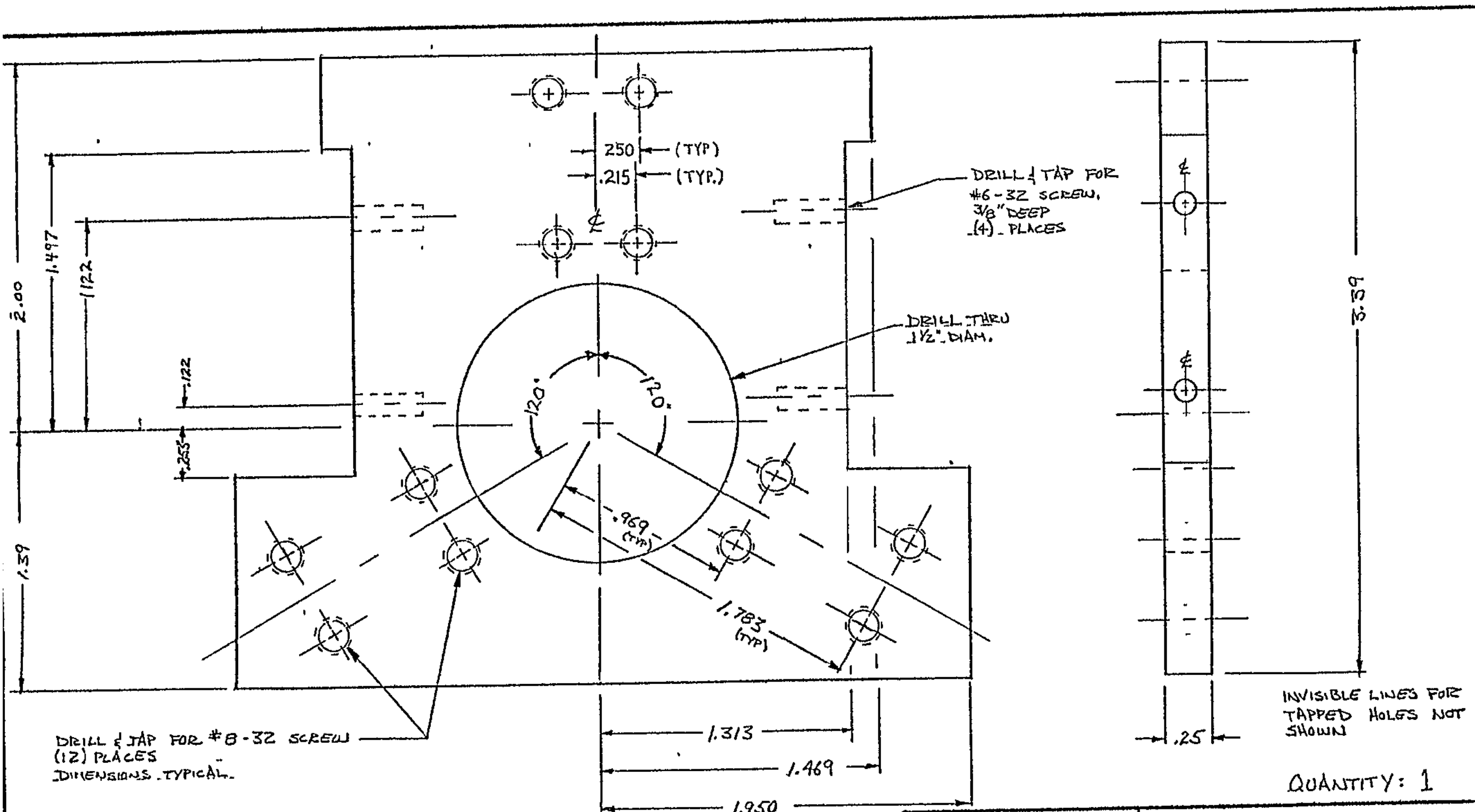

QUANTITY: 1

TOLERANCES (EXCEPT AS NOTED)	REVISIONS			MARS ROVER		
	NO	DATE	BY	LENS PLATE		
DECIMAL ±	1			DRAWN BY RJL	SCALE 1" = ½"	MATERIAL ALUM
FRACTIONAL ±	2			CHK'D	DATE 4-7-78	DRAWING NO
ANGULAR ±	3			TRACED	APP'D	
	4					
	5					

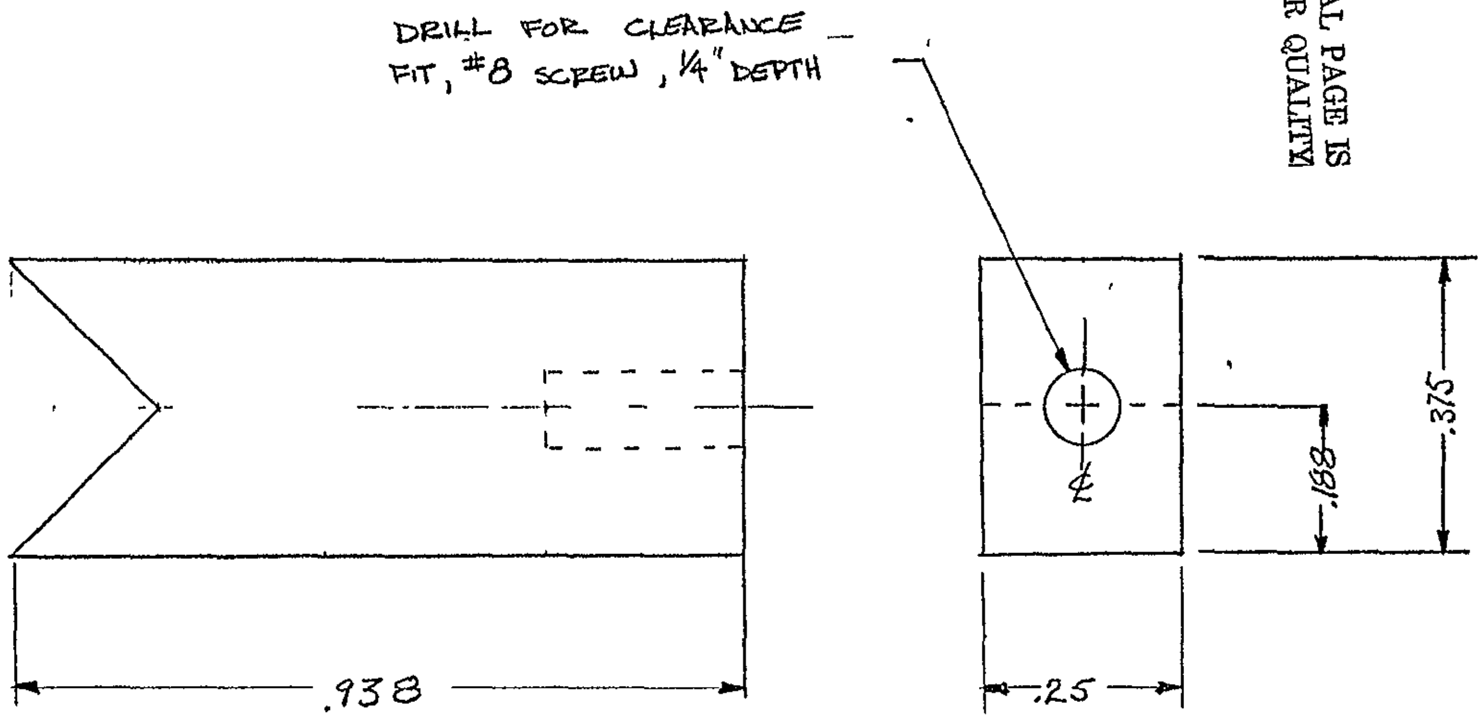

QUANTITY: 3

TOLERANCES (EXCEPT AS NOTED)	REVISIONS NO	DATE	BY
DECIMAL ±	1		
	2		
FRACTIONAL ±	3		
ANGULAR ±	4		
	5		

MARS ROVER

LENS FEET

DRAWN BY R.A.L.	SCALE 1" = 1/4"	MATERIAL ALUM
CHK'D	DATE 3-17-78	DRAWING NO
TRACED	APP D	

TELEDYNE POST 18AE-01E—8½X11

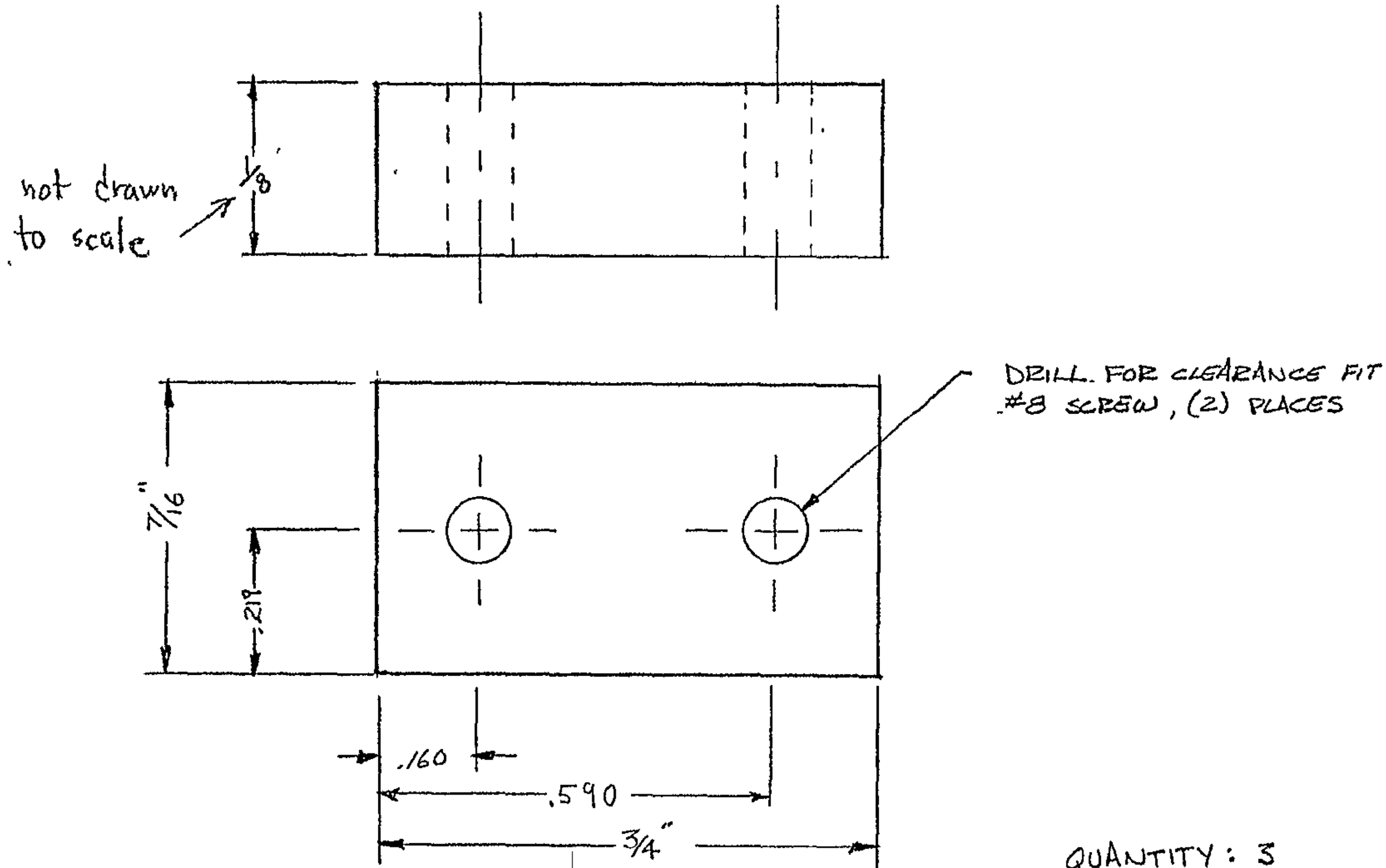

QUANTITY: 3

TOLERANCES (EXCEPT AS NOTED)	REVISIONS			MARS ROVER		
	NO	DATE	BY	FEET HOLDER		
DECIMAL ±	1			DRAWN BY RAL	SCALE 1" = 1/4"	MATERIAL ALUM
	2			CHK'D	DATE 3-17-78	DRAWING NO
FRACTIONAL ±	3			TRACED	APP'D	
ANGULAR ±	4					
	5					

TELEDYNE POST 18AE-01E—8½X11

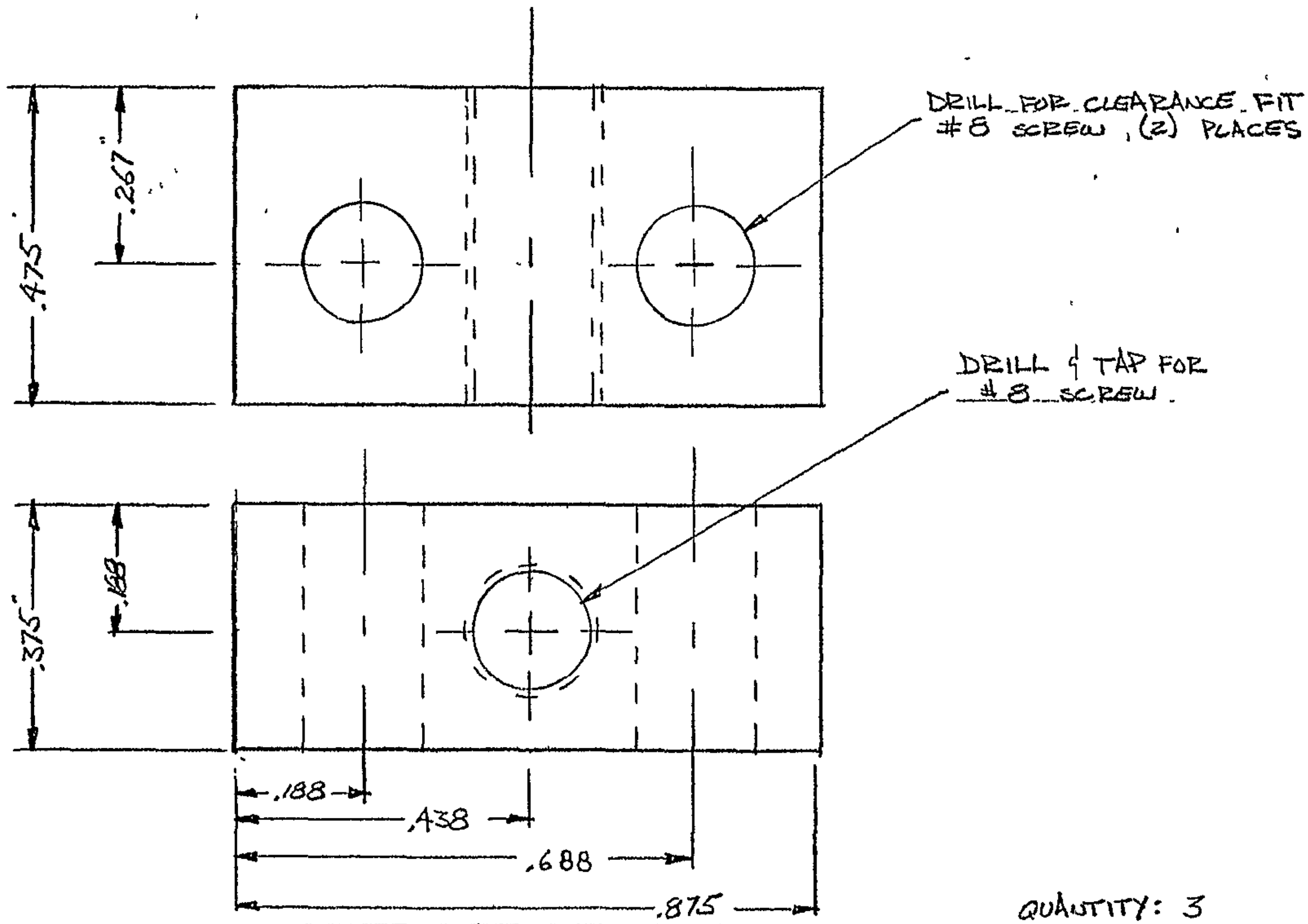

QUANTITY: 3

TOLERANCES (EXCEPT AS NOTED)	
DECIMAL	±
FRACTIONAL	±
ANGULAR	±

REVISIONS		
NO	DATE	BY
1		
2		
3		
4		
5		

MARS ROVER

ADJUSTING SUPPORT

DRAWN BY RAL	SCALE 1" = 1/4"	MATERIAL ALUM
CHK'D	DATE 3-24-78	DRAWING NO
TRACED	APP'D	

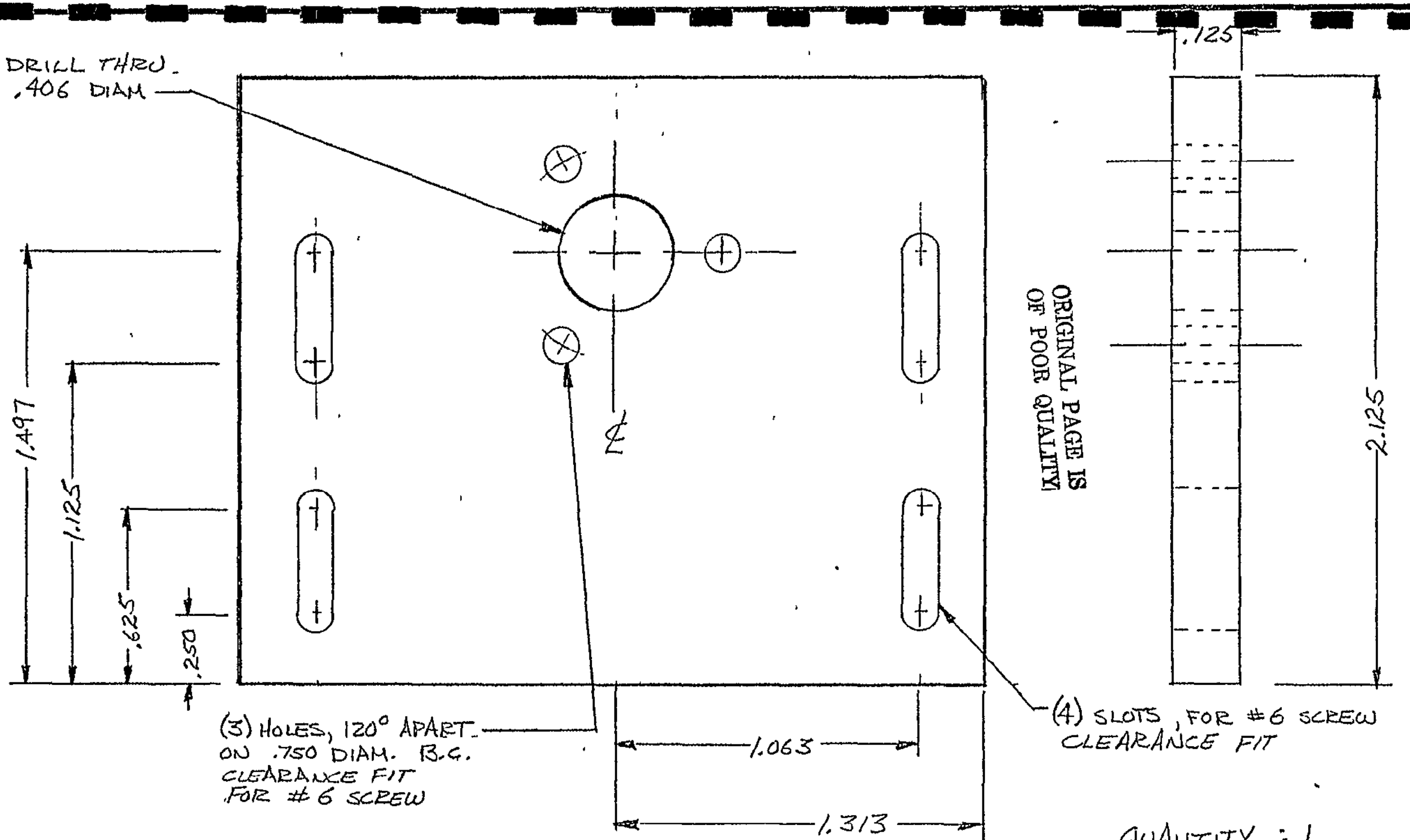

QUANTITY : 1

TOLERANCES (EXCEPT AS NOTED)	REVISIONS NO	DATE	BY	MARS ROVER		
DECIMAL ±	1			LASER MOUNTING PLATE		
FRACTIONAL ±	2					
	3			DRAWN BY RAL	SCALE 1" = 1/2"	MATERIAL Aluminum
ANGULAR ±	4			CHK'D	DATE 4-7-75	DRAWING NO
	5			TRACED	APP D	

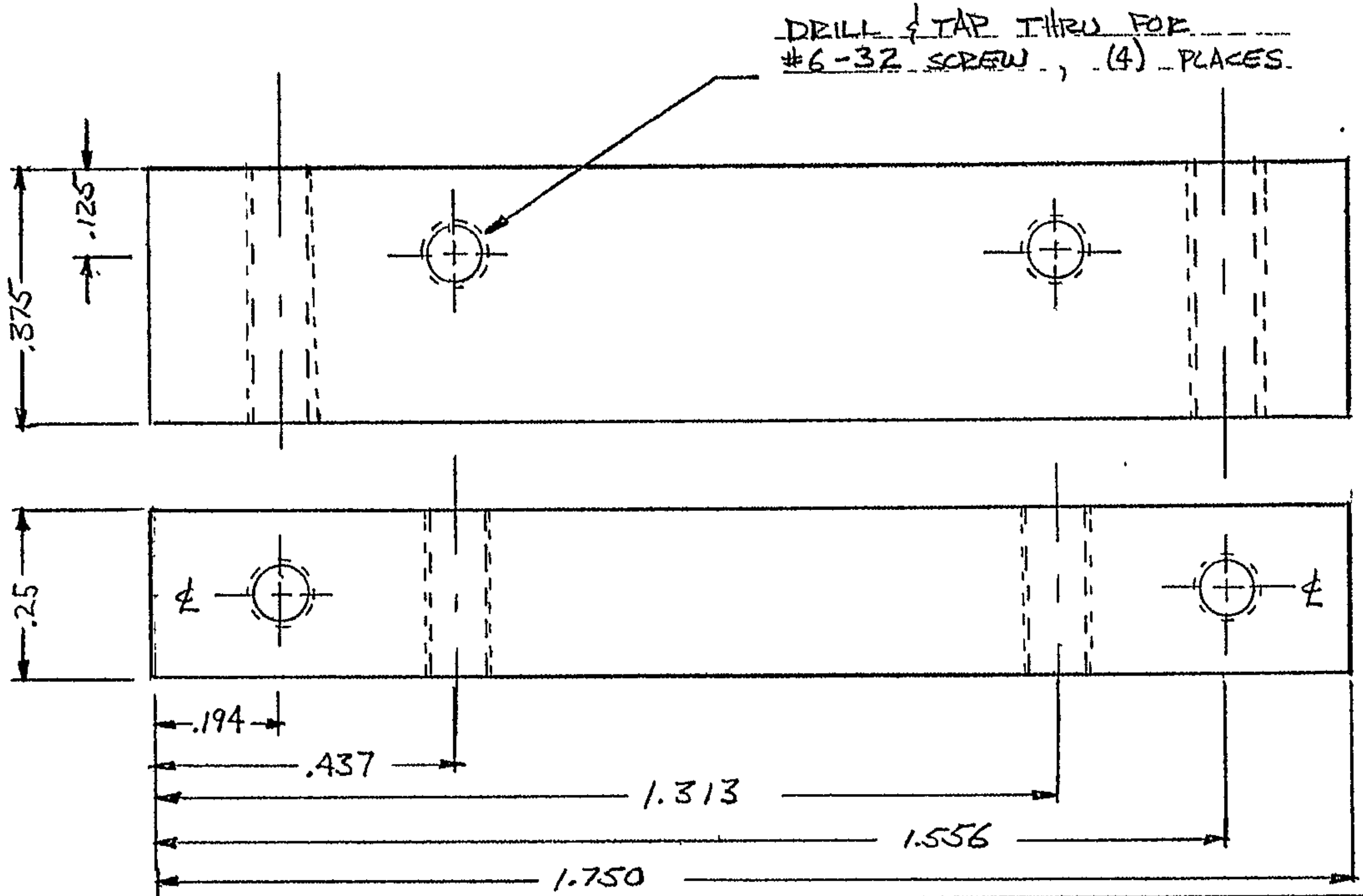

QUANTITY = 2

TOLERANCES (EXCEPT AS NOTED)	REVISIONS		
	NO	DATE	BY
DECIMAL	1		
±	2		
FRACTIONAL	3		
±	4		
ANGULAR ±	5		

MARS ROVER

LASER MOUNTING FR. SUPPORT

DRAWN BY RAL	SCALE 1" = 1/4"	MATERIAL ALUM
CHK D	DATE 3-28-78	DRAWING NO
TRACED	APP D	

TELEDYNE POST 18AE-01E–8½X11

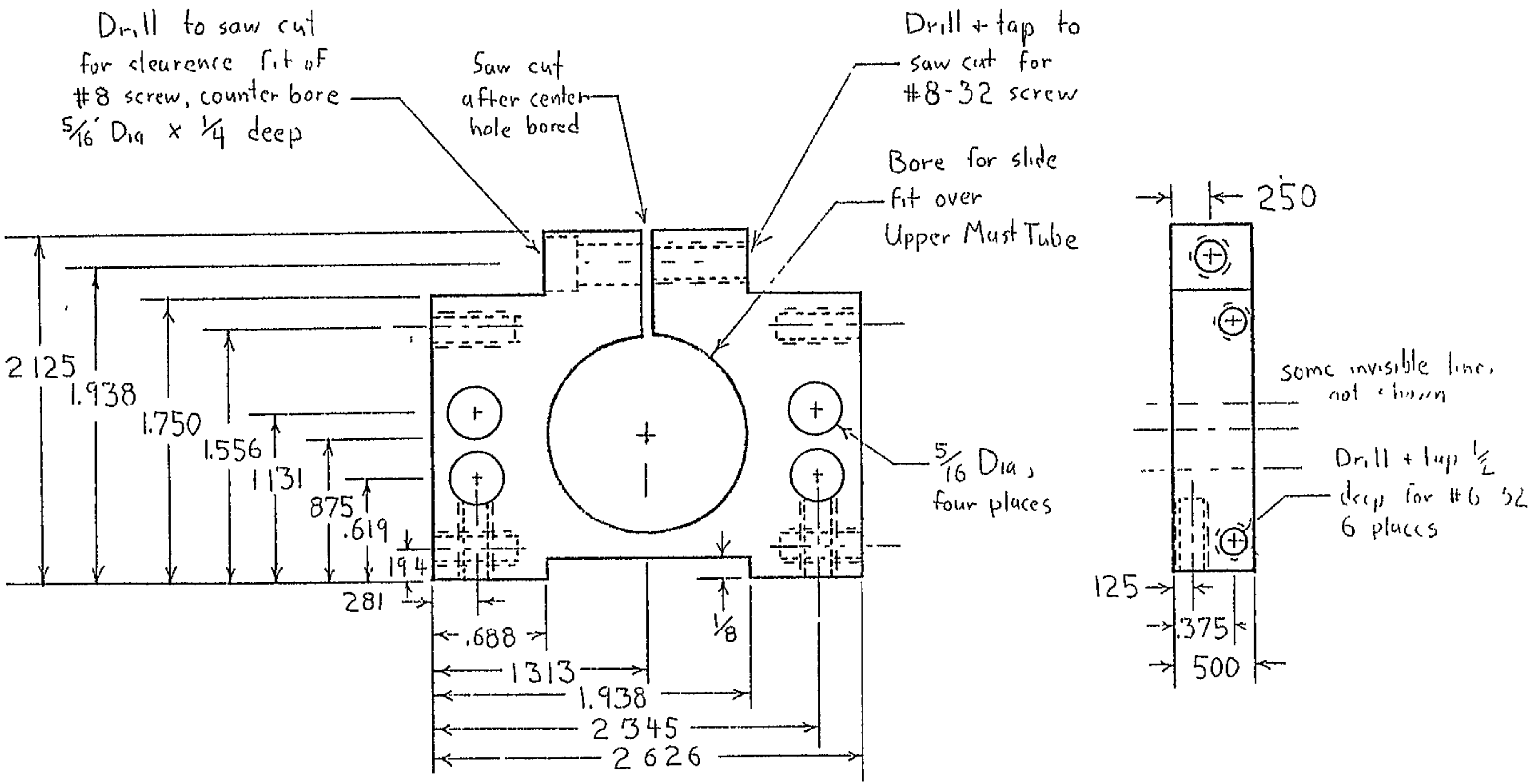

QUANTITY . 2

TOLERANCES (EXCEPT AS NOTED)	REVISIONS		
	NO	DATE	BY
DECIMAL ±	1		
	2		
FRACTIONAL ±	3		
	4		
ANGULAR ±	5		

MAST CLAMP

MARS ROVER

DRAWN BY D Knaub	SCALE 1 1	MATERIAL Alum.
CHK'D	DATE 4-17 78	DRAWING NO
TRACED	APP'D	

TELEDYNE POST 18AE-01E–8½X11

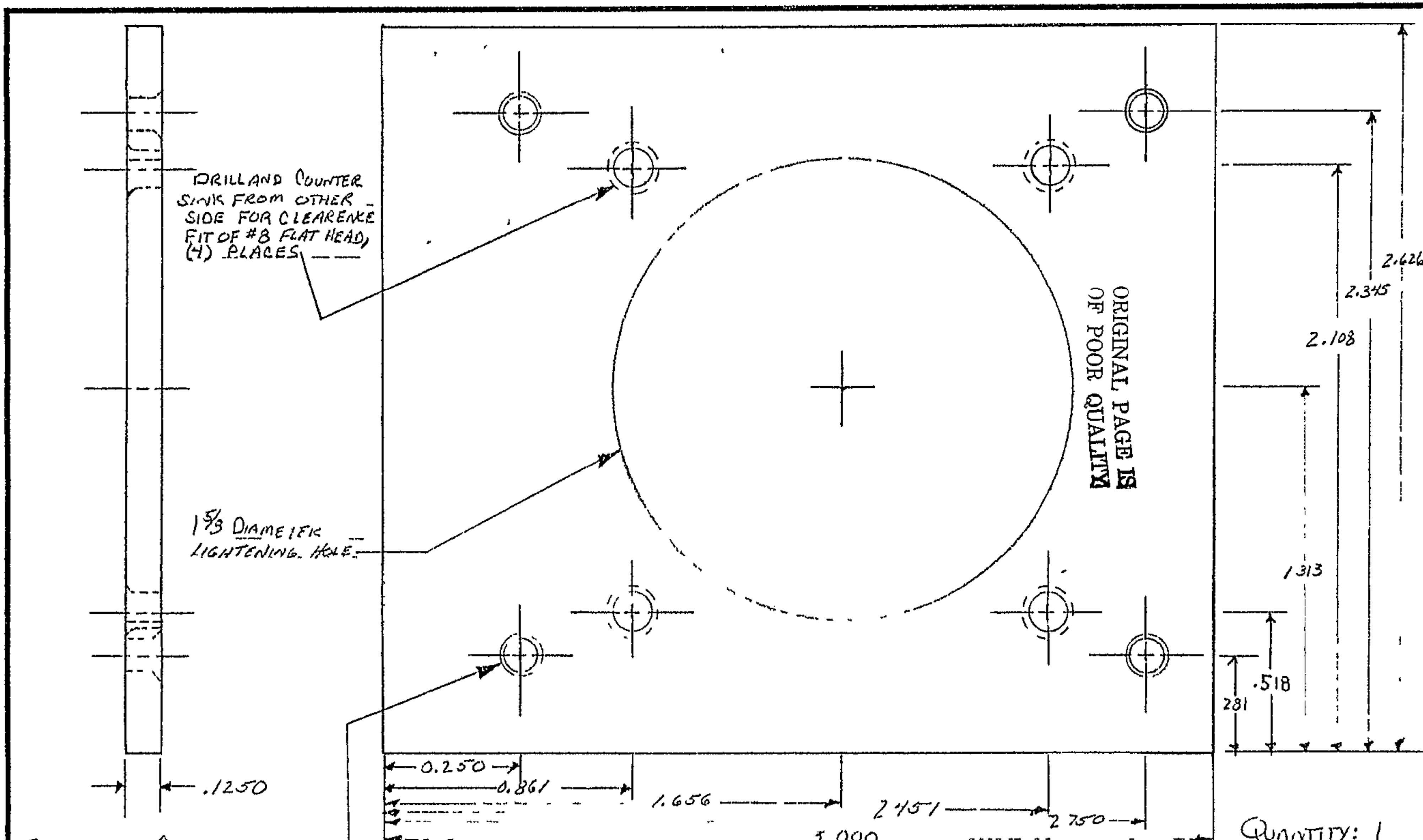

TOLERANCES (EXCEPT AS NOTED)	REVISIONS NO.	DATE	BY
DECIMAL ±	1		
	2		
FRACTIONAL ±	3		
ANGULAR	4		
±	5		

MARS ROVER

ENCODER ELECTRONICS MOUNTING PLATE

DRAWN BY	SCALE	MATERIAL
SFM	NOT TO SCALE	ALUMINUM
CHK D	DATE 5/8/78	DRAWING NO
TRACED	APP D	

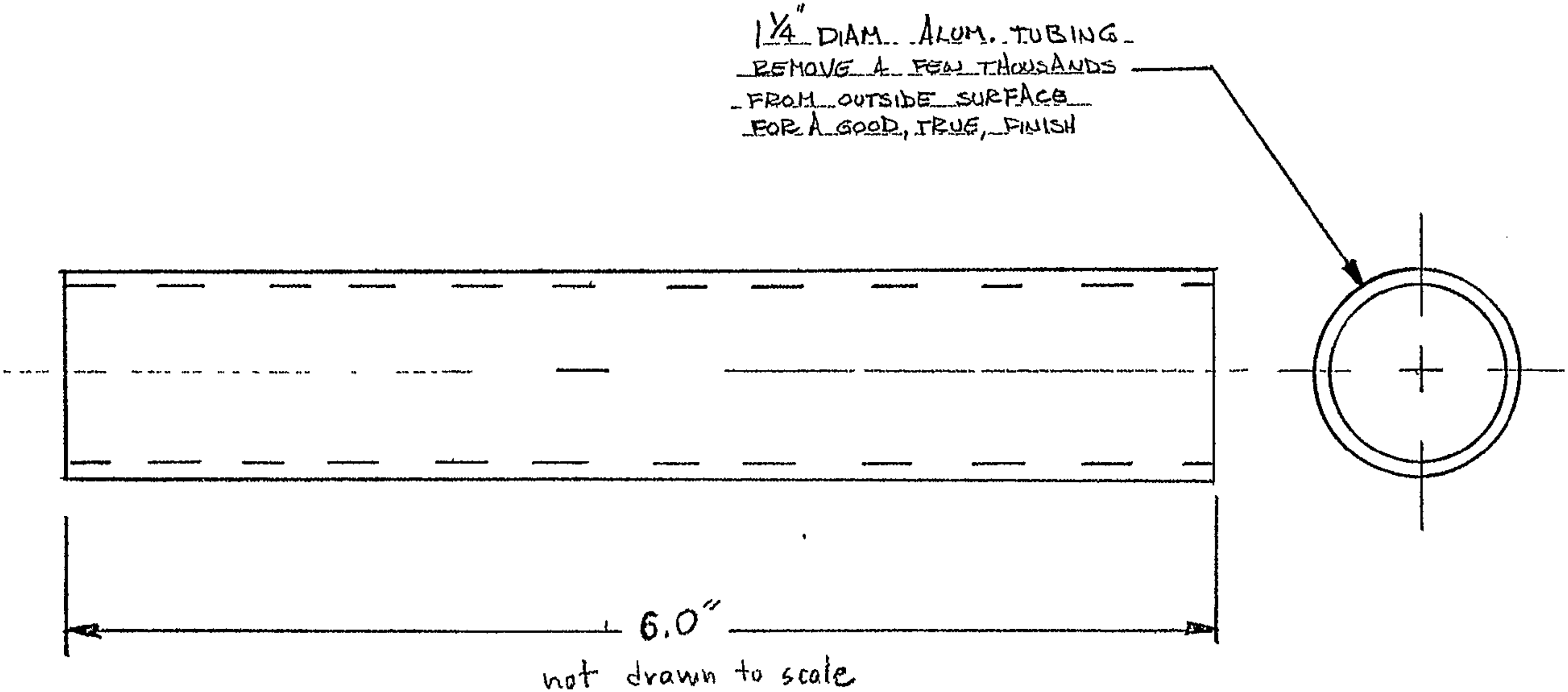

TUBING SUPPLIED

QUANTITY: 1

TOLERANCES (EXCEPT AS NOTED)	REVISIONS NO	DATE	BY	MARS ROVER		
DECIMAL ±	1			UPPER MAST TUBE		
	2					
FRACTIONAL ±	3			DRAWN BY RAL	SCALE 1" = 1"	MATERIAL ALUM.
	4			CHK'D	DATE 3-26-78	DRAWING NO
ANGULAR ±	5			TRACED	APP D	

TELEDYNE POST 18AE 01E—8½X11

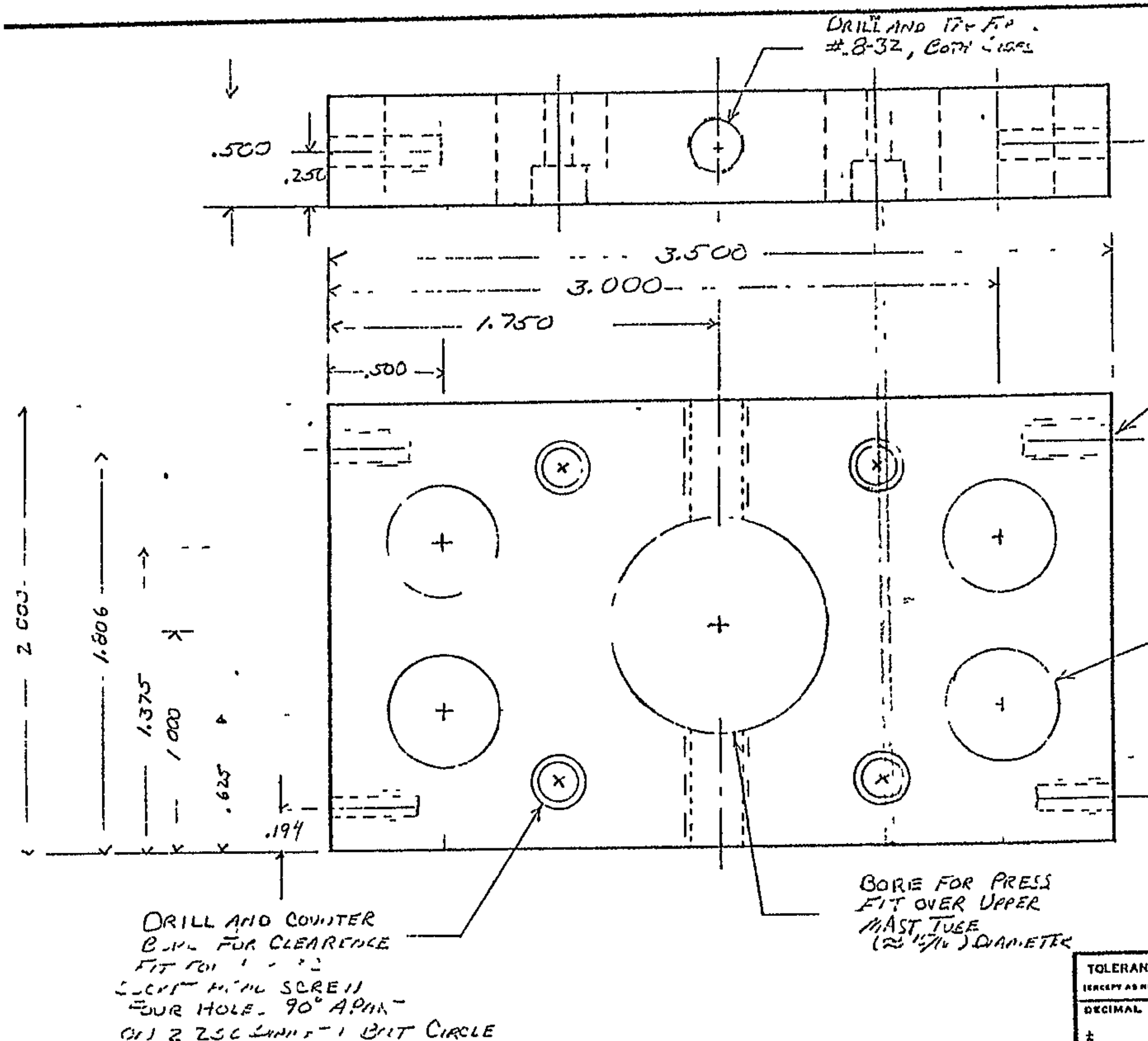

TOLERANCES (EXCEPT AS NOTED)	REVISIONS		
	NO	DATE	BY
DECIMAL ±	1		
	2		
FRACTIONAL ±	3		
	4		
ANGULAR ±	5		

Maps

Upper Deflection Frame

DRAWN BY	SCALE	MATERIAL
FR	1" – 1/2"	Alum
CHK'D	DATE 2	DRAWING NO
TRACED	APP'D	

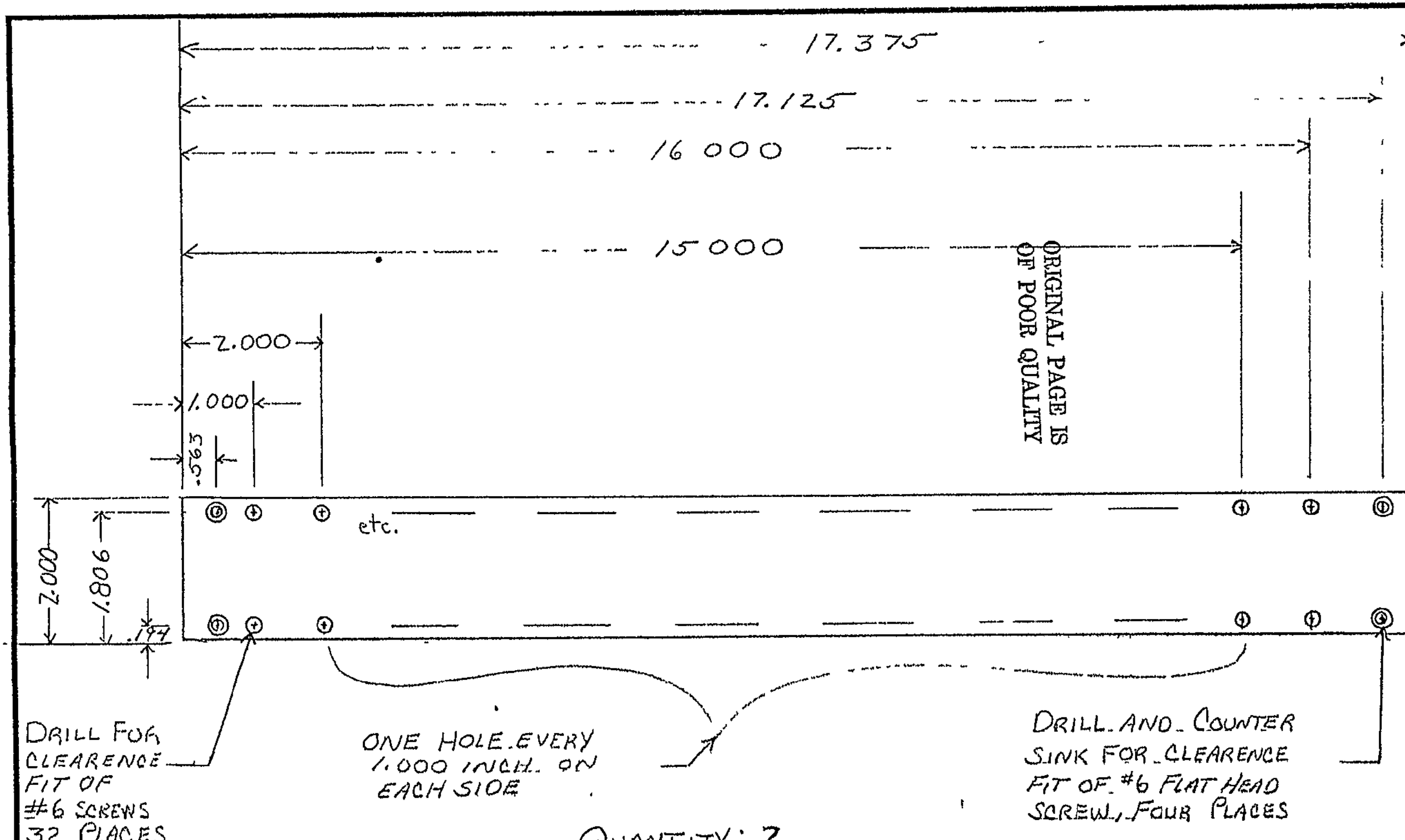

QUANTITY: 2

TOLERANCES (EXCEPT AS NOTED)	REVISIONS NO	DATE	BY	DETECTOR FRAME		
DECIMAL ±	1					
	2					
FRACTIONAL ±	3			DRAWN BY SFM	SCALE 1" = ½"	MATERIAL 1/8" ALUMINUM PLATE
	4			CHK'D	DATE 7/17/78	DRAWING NO
ANGULAR ±	5			TRACED	APP'D	

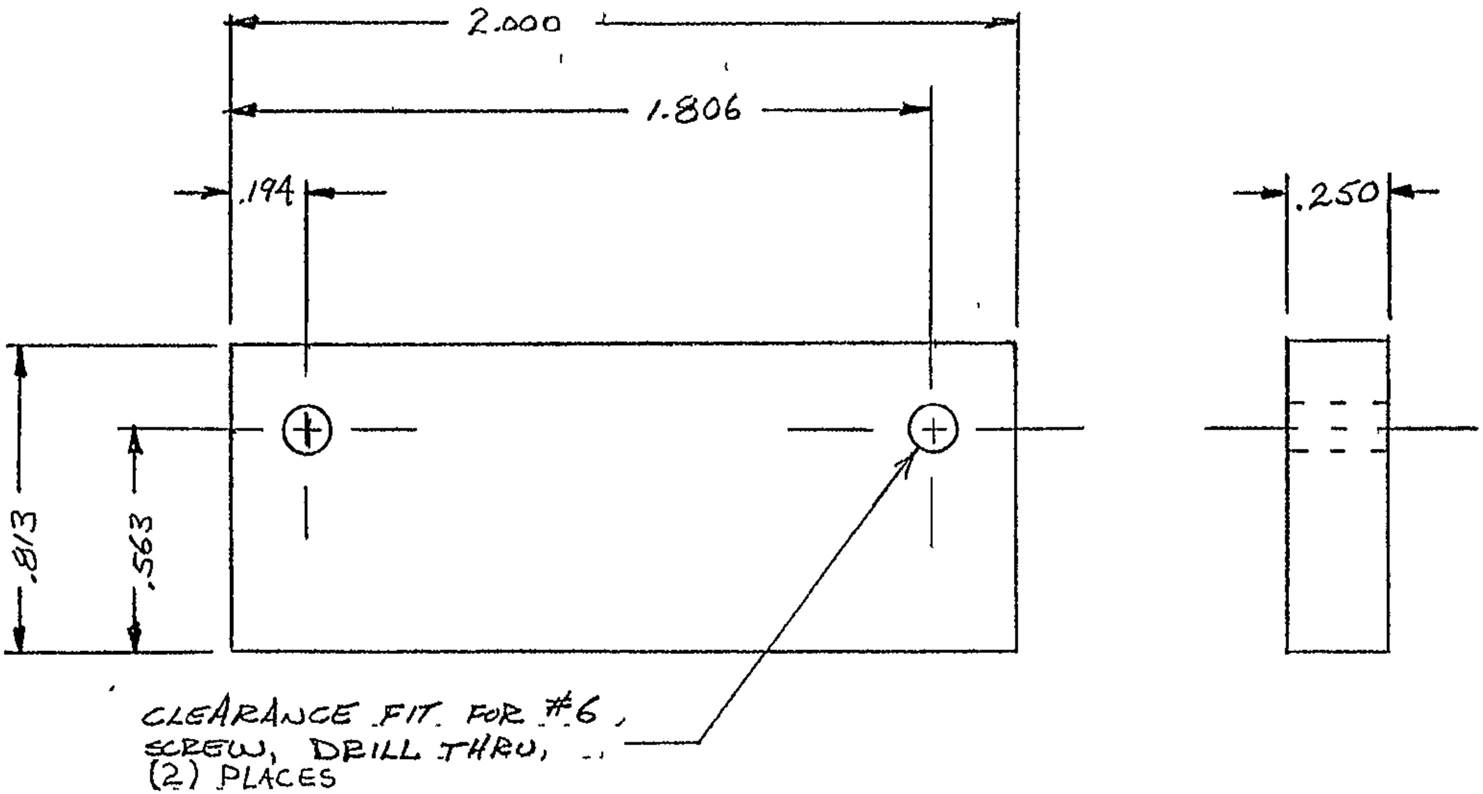

QUANTITY: 4

TOLERANCES (EXCEPT AS NOTED)	REVISIONS			MARS ROVER		
	NO	DATE	BY			
DECIMAL ±	1			DETECTOR FRAME SPACER		
	2					
FRACTIONAL ±	3			DRAWN BY RAL	SCALE 2" = 1"	MATERIAL ALUM
	4			CHK'D	DATE 5-1-78	DRAWING NO
ANGULAR ±	5			TRACED	APP D	

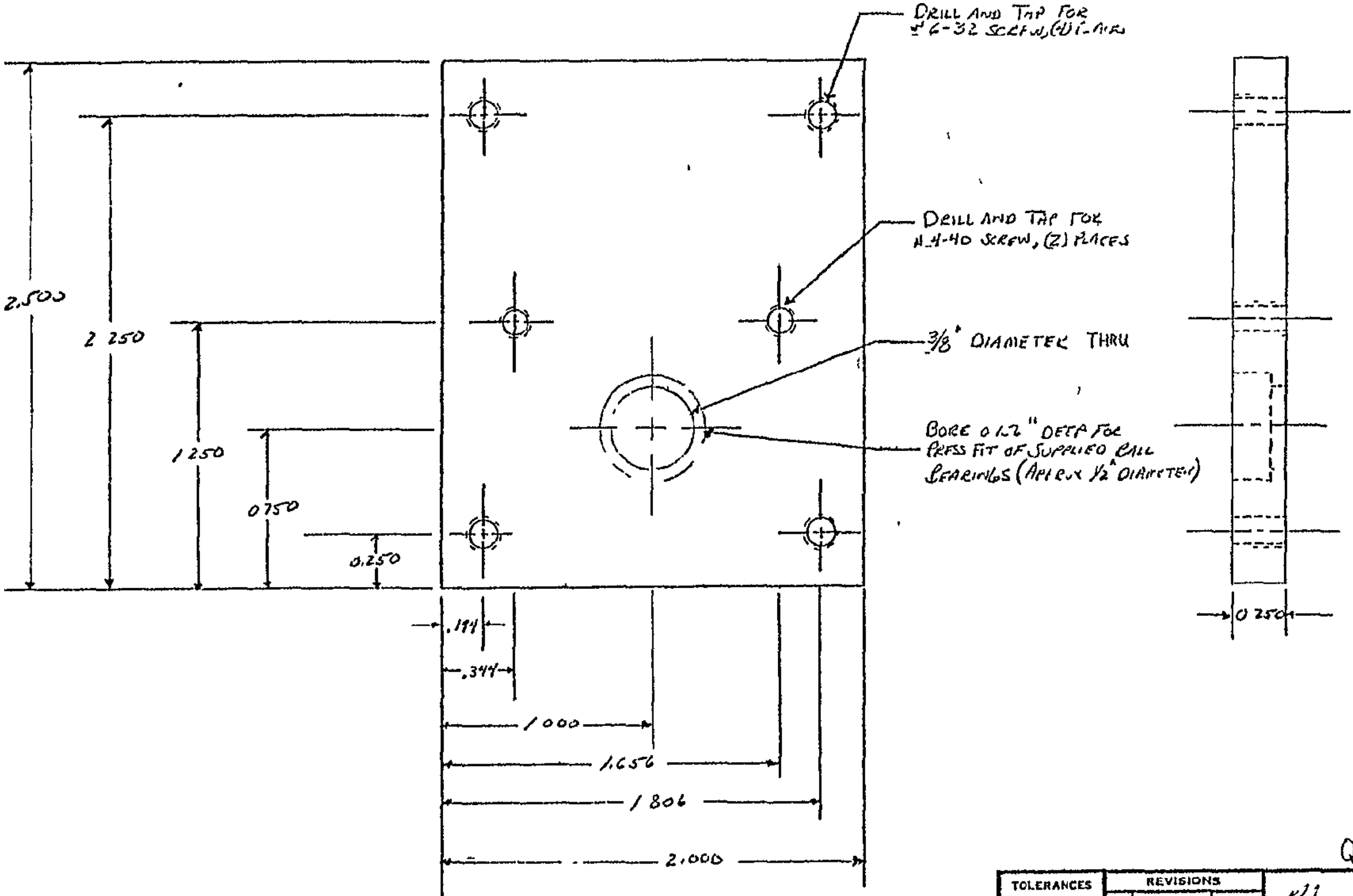

Quantity : 1

TOLERANCES (EXCEPT AS NOTED)	REVISIONS			MARS ROVER		
	NO	DATE	BY	RIGHT DETECTOR BEARING PLATE		
DECIMAL ±	1			DRAWN BY SFM	SCALE 1 = 1/2	MATERIAL ALUMINUM
FRACTIONAL ±	2					
	3			CHK'D	DATE 4/20/75	DRAWING NO
ANGULAR ±	4			TRACED	APP'D	
	5					

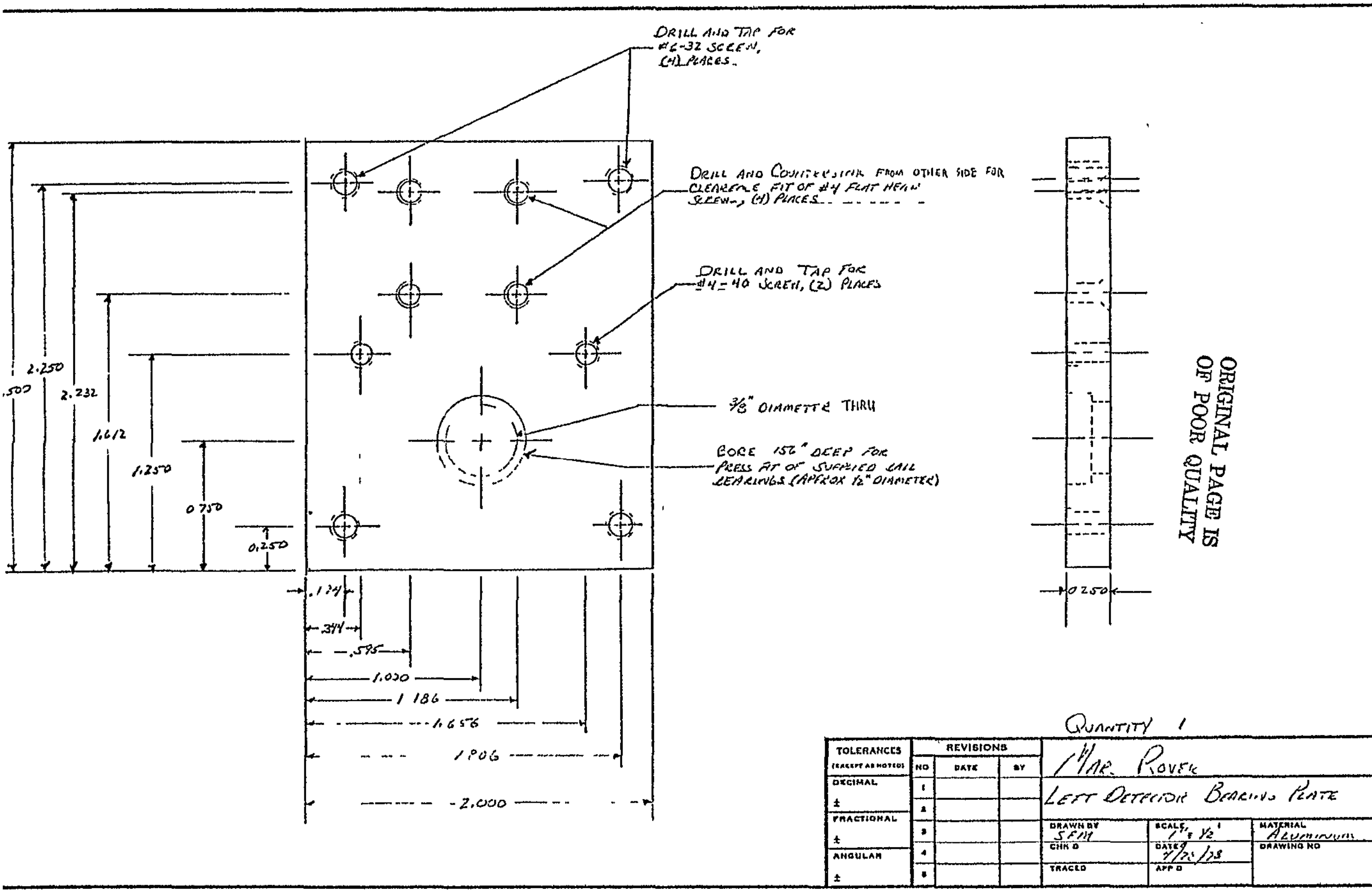
DRILL AND TAP FOR #6-32 SCREW, (4) PLACES.
DRILL AND COUNTERSINK FROM OTHER SIDE FOR CLEARANCE FIT OF #4 FLAT HEAD SCREW, (4) PLACES
DRILL AND TAP FOR #4-40 SCREW, (2) PLACES
3/8" DIAMETER THRU
BORE .156" DEEP FOR PRESS FIT OF SUPPLIED BALL BEARINGS (APPROX 1/2" DIAMETER)
2.500
2.250
2.232
1.612
1.250
0.750
0.250
.124
.344
.595
1.020
1.186
1.656
1.906
2.000
0.250
QUANTITY 1
TOLERANCES (EXCEPT AS NOTED)
DECIMAL ±
FRACTIONAL ±
ANGULAR ±
REVISIONS
NO DATE BY
1 2 3 4 5
Mar. Rover
Left Detector Bearing Plate
DRAWN BY SFM
CHK D
TRACED
SCALE 1" = 1/2"
DATE 7/25/73
APP D
MATERIAL Aluminum
DRAWING NO

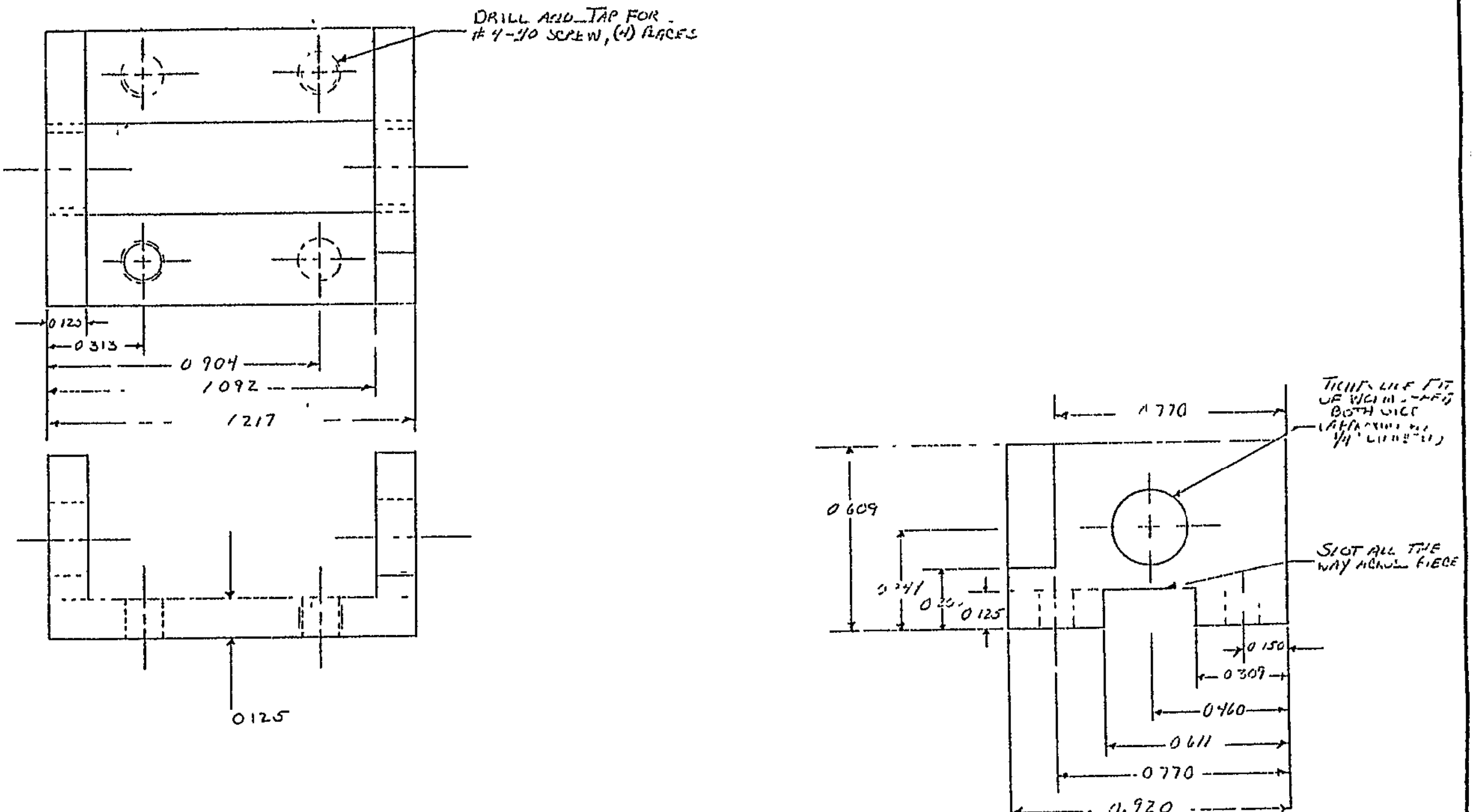

QUANTITY: 1

TOLERANCES (EXCEPT AS NOTED)	REVISIONS			MAPS ROVER		
	NO	DATE	BY	WORM SUPPORT BRACKET		
DECIMAL ±	1			DRAWN BY	SCALE	MATERIAL Aluminum
	2			CHK D	DATE 5/11/76	DRAWING NO
FRACTIONAL ±	3			TRACED	APP D	
ANGULAR ±	4					
	5					

TELEDYNE POST 18AX-08E-11 X 17

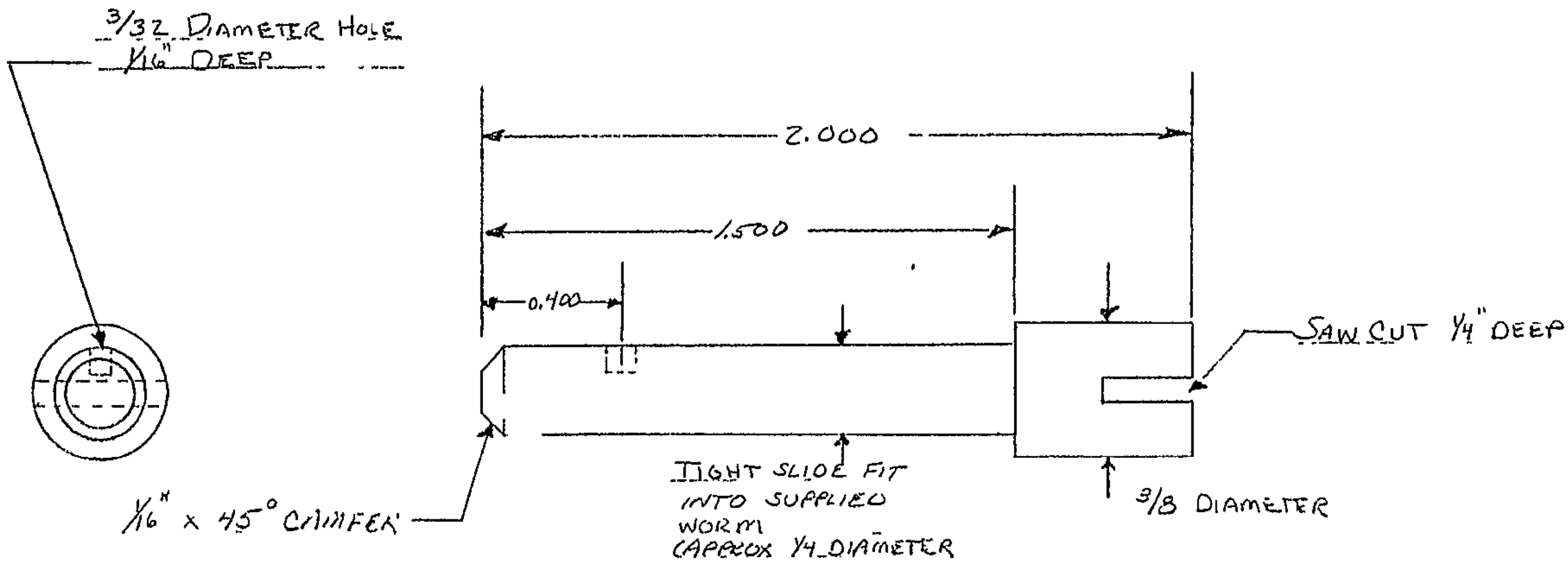

QUANTITY: 1

TOLERANCES (EXCEPT AS NOTED)	REVISIONS			MARS ROVER		
	NO	DATE	BY			
DECIMAL ±	1			WORM SHAFT		
	2					
FRACTIONAL ±	3			DRAWN BY SFM	SCALE 1" = 1/2"	MATERIAL STEEL
ANGULAR	4			CHK'D	DATE 5/4/78	DRAWING NO
±	5			TRACED	APP'D	

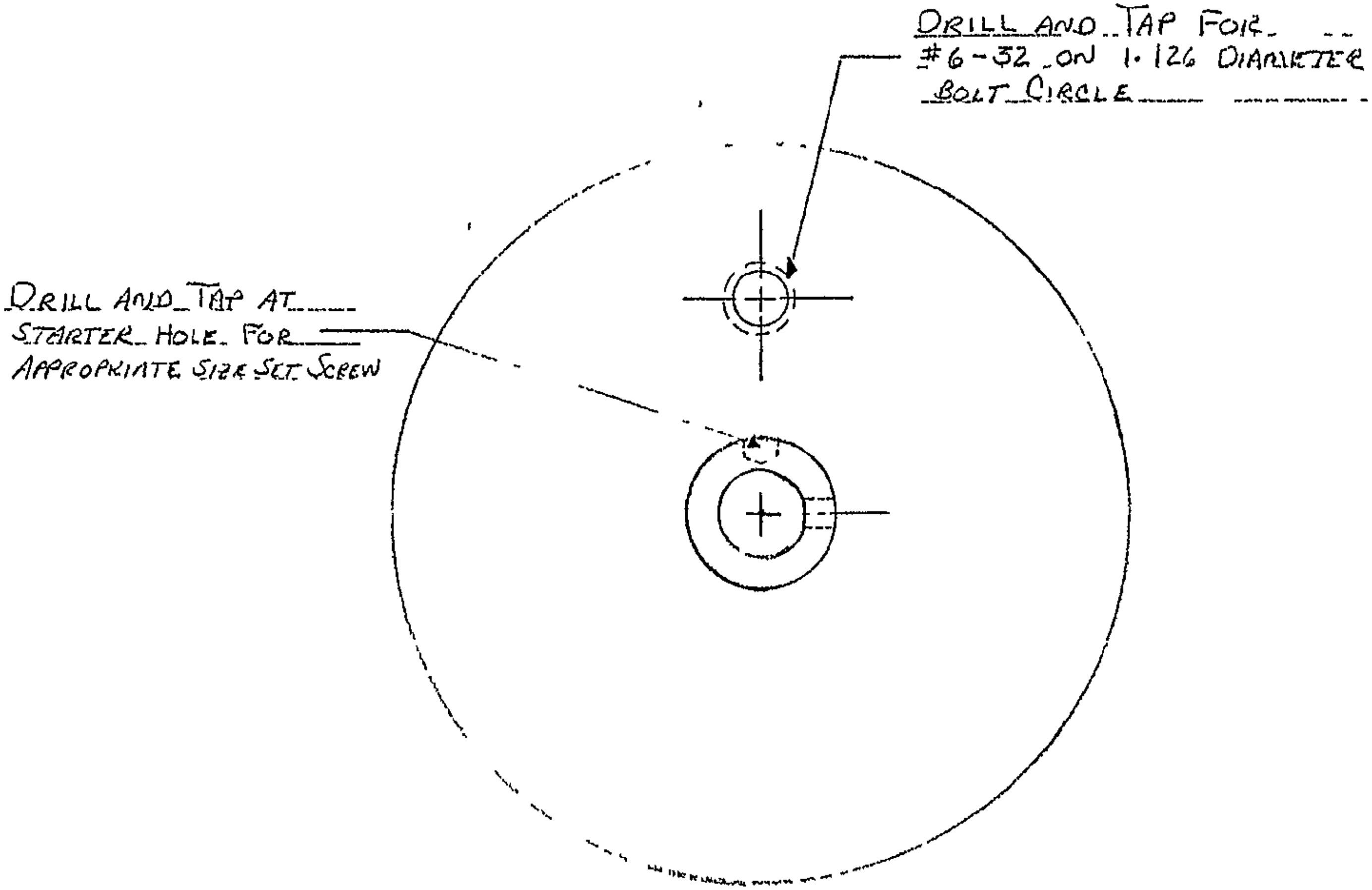

Gear Supplied
QUANTITY. 1

TOLERANCES (EXCEPT AS NOTED)	REVISIONS NO	DATE	BY	
				MARS ROVER
DECIMAL ±	1			DETECTOR WORM GEAR MODIFICATION
	2			
FRACTIONAL ±	3			DRAWN BY SFM / SCALE 1" = ½" / MATERIAL W.M BERG W64R21-S120
ANGULAR ±	4			CHK'D / DATE 5/3/78 / DRAWING NO.
	5			TRACED / APP D / BRONZE WORM GEAR

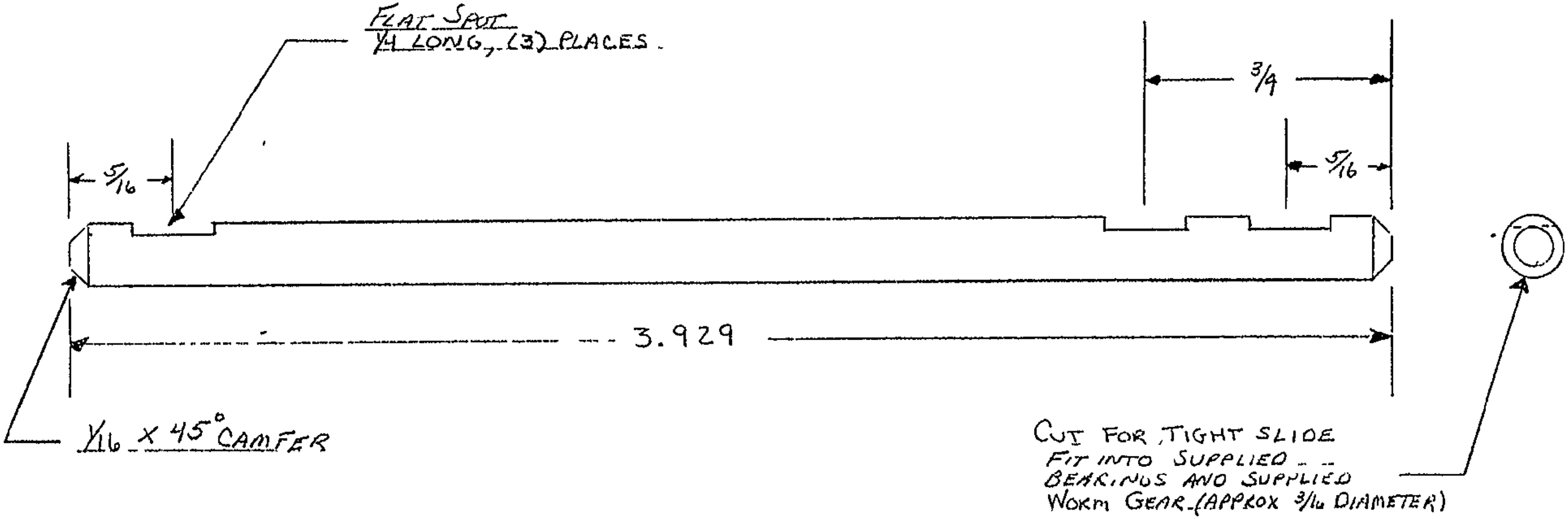

QUANTITY. 1

TOLERANCES (EXCEPT AS NOTED)	REVISIONS NO	DATE	BY	
DECIMAL	1			MARS ROVER
±	2			DETECTOR SHAFT
FRACTIONAL	3			DRAWN BY SFM; SCALE 1" = 1/2"; MATERIAL STEEL
±				
ANGULAR	4			CHK'D; DATE 5/4/78; DRAWING NO
±	5			TRACED; APP D

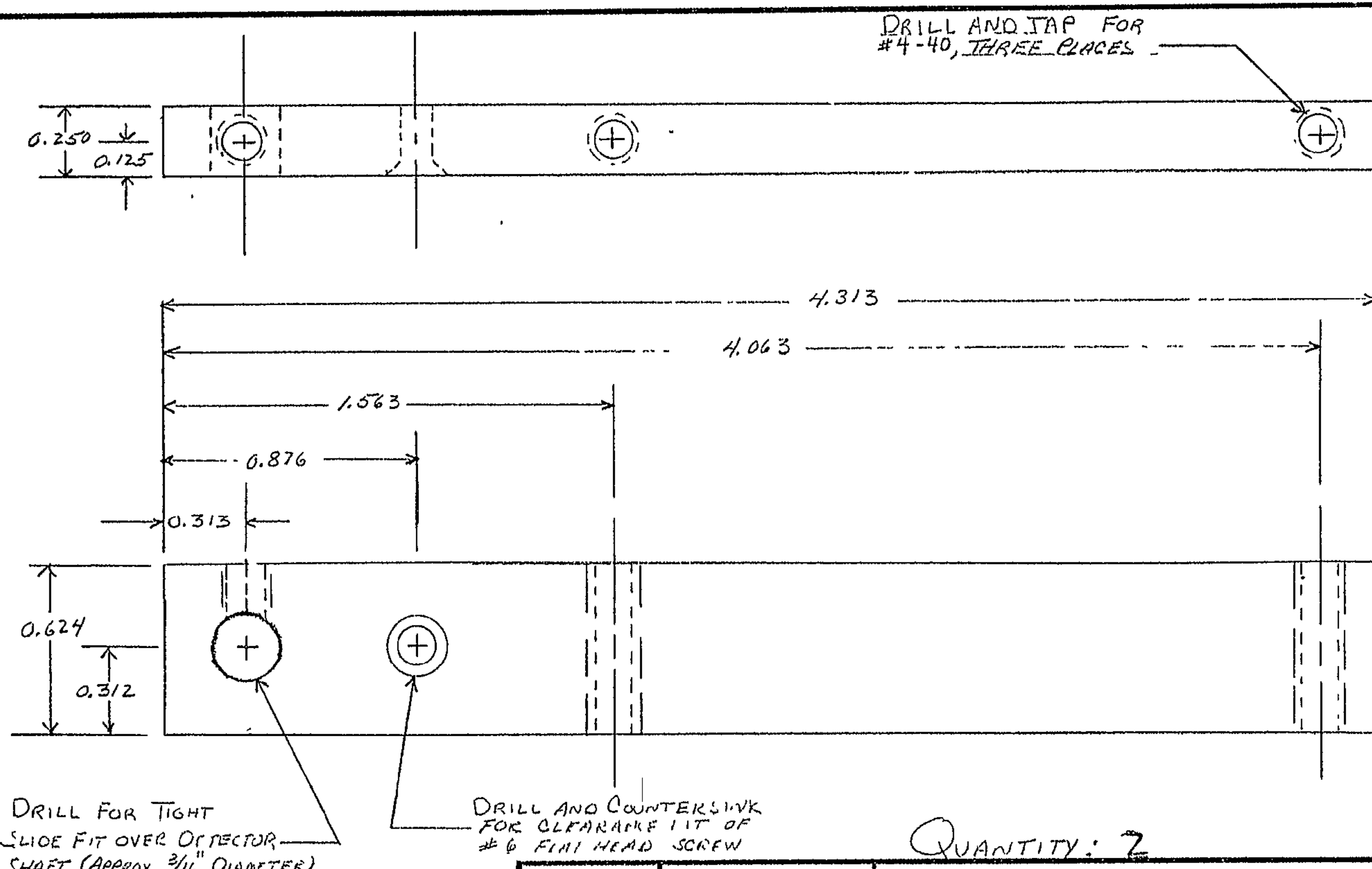

QUANTITY: 2

TOLERANCES (EXCEPT AS NOTED)	REVISIONS			MARS ROVER		
	NO	DATE	BY	DETECTOR FACE PLATE HOLDER "A"		
DECIMAL ±	1			DRAWN BY SFAI	SCALE 1" = 1/2"	MATERIAL Aluminum
	2			CHK'D	DATE 4/26/73	DRAWING NO
FRACTIONAL ±	3			TRACED	APP'D	
ANGULAR ±	4					
	5					

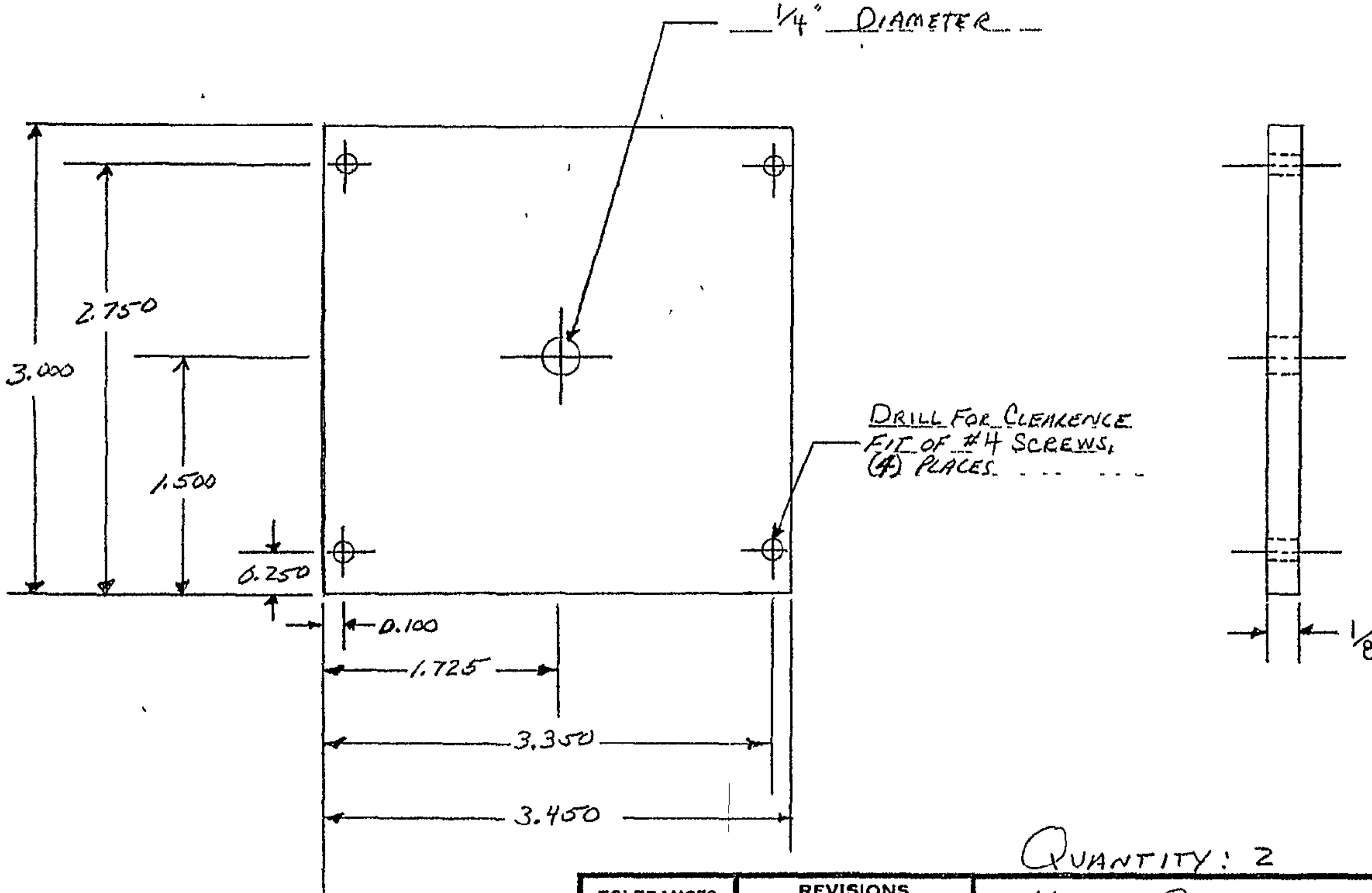

ORIGINAL PAGE IS OF POOR QUALITY

QUANTITY: 2

TOLERANCES (EXCEPT AS NOTED)	REVISIONS NO	DATE	BY	
DECIMAL ±	1			MARS ROVER
	2			DETECTOR FACE PLATE "A"
FRACTIONAL ±	3			DRAWN BY SFM; SCALE NOT TO SCALE; MATERIAL Aluminum
	4			CHK'D; DATE 4/28/78; DRAWING NO
ANGULAR ±	5			TRACED; APP'D

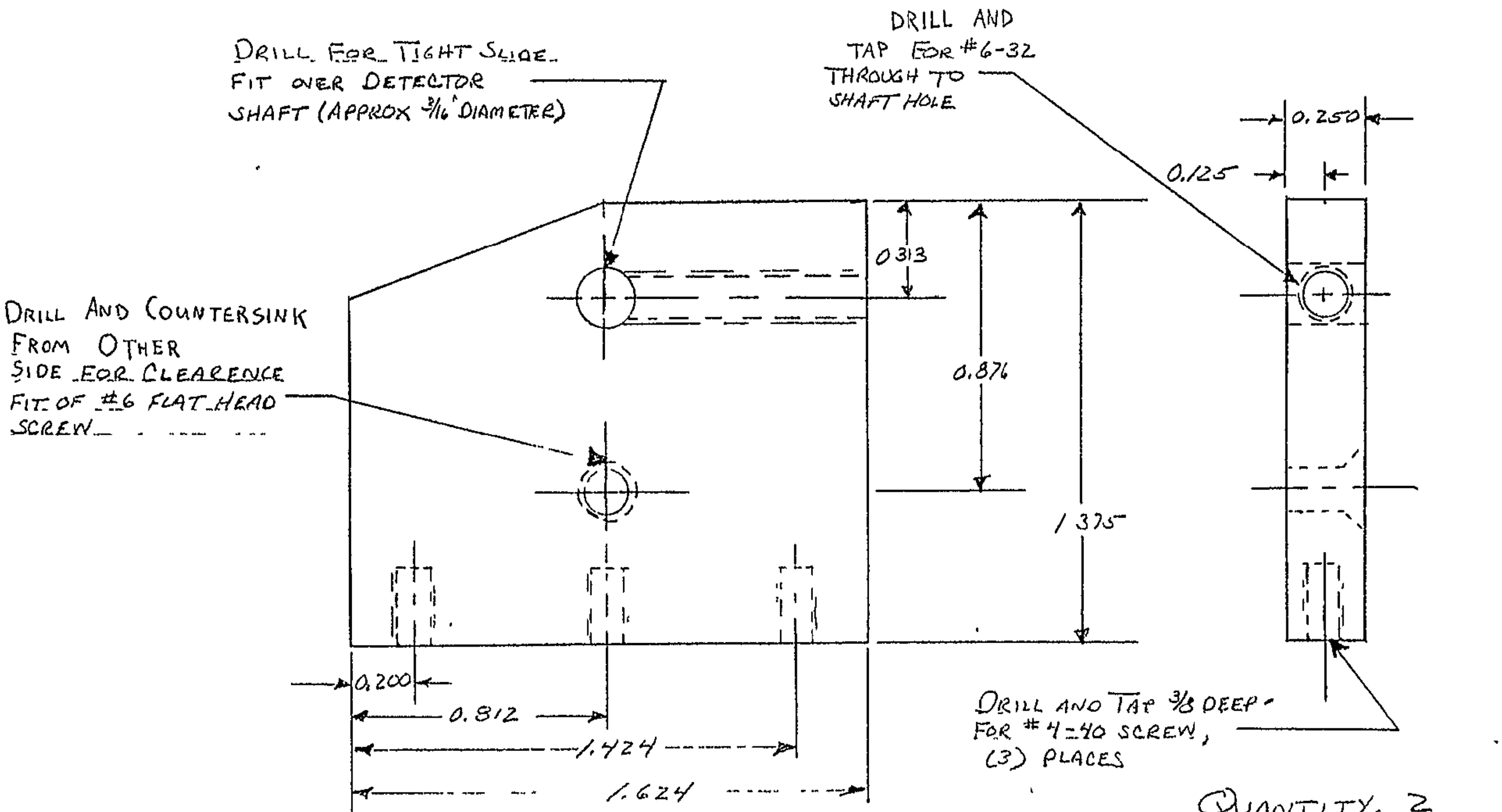

QUANTITY 2

TOLERANCES (EXCEPT AS NOTED)	REVISIONS		
	NO	DATE	BY
DECIMAL ±	1		
	2		
FRACTIONAL ±	3		
	4		
ANGULAR ±	5		

MARS ROVER

DETECTOR FACE PLATE HOLDER "B"

DRAWN BY	SCALE	MATERIAL
SFM	1" = 1/2"	ALUMINUM
CHK'D	DATE 5/8/78	DRAWING NO
TRACED	APP'D	

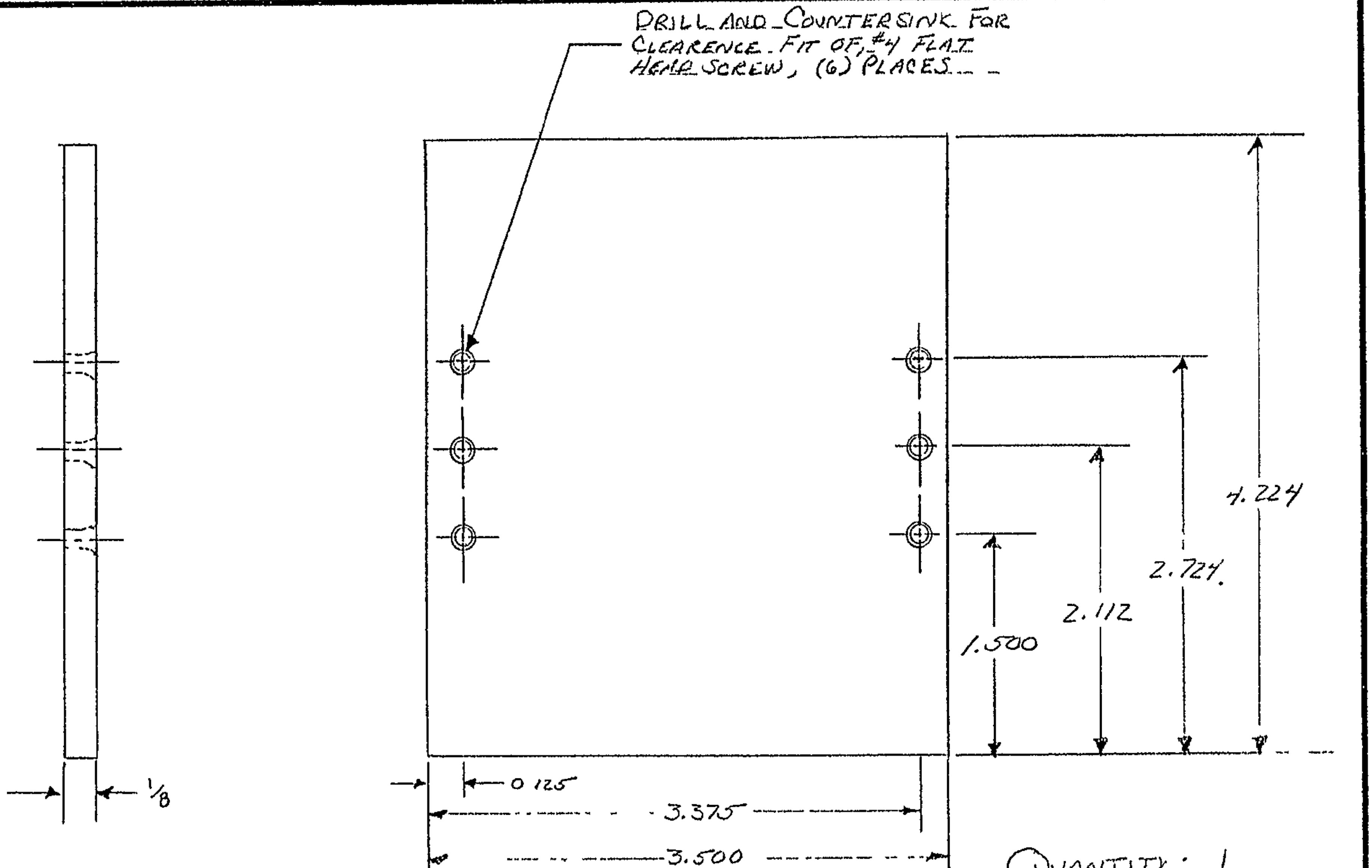

QUANTITY: 1

TOLERANCES (EXCEPT AS NOTED)	REVISIONS NO	DATE	BY	MARS ROVER		
DECIMAL ±	1			DETECTOR FACE PLATE "B"		
	2					
FRACTIONAL ±	3			DRAWN BY JFM	SCALE —	MATERIAL ALUMINUM
ANGULAR	4			CHK'D	DATE 5/3/73	DRAWING NO
±	5			TRACED	APP D	

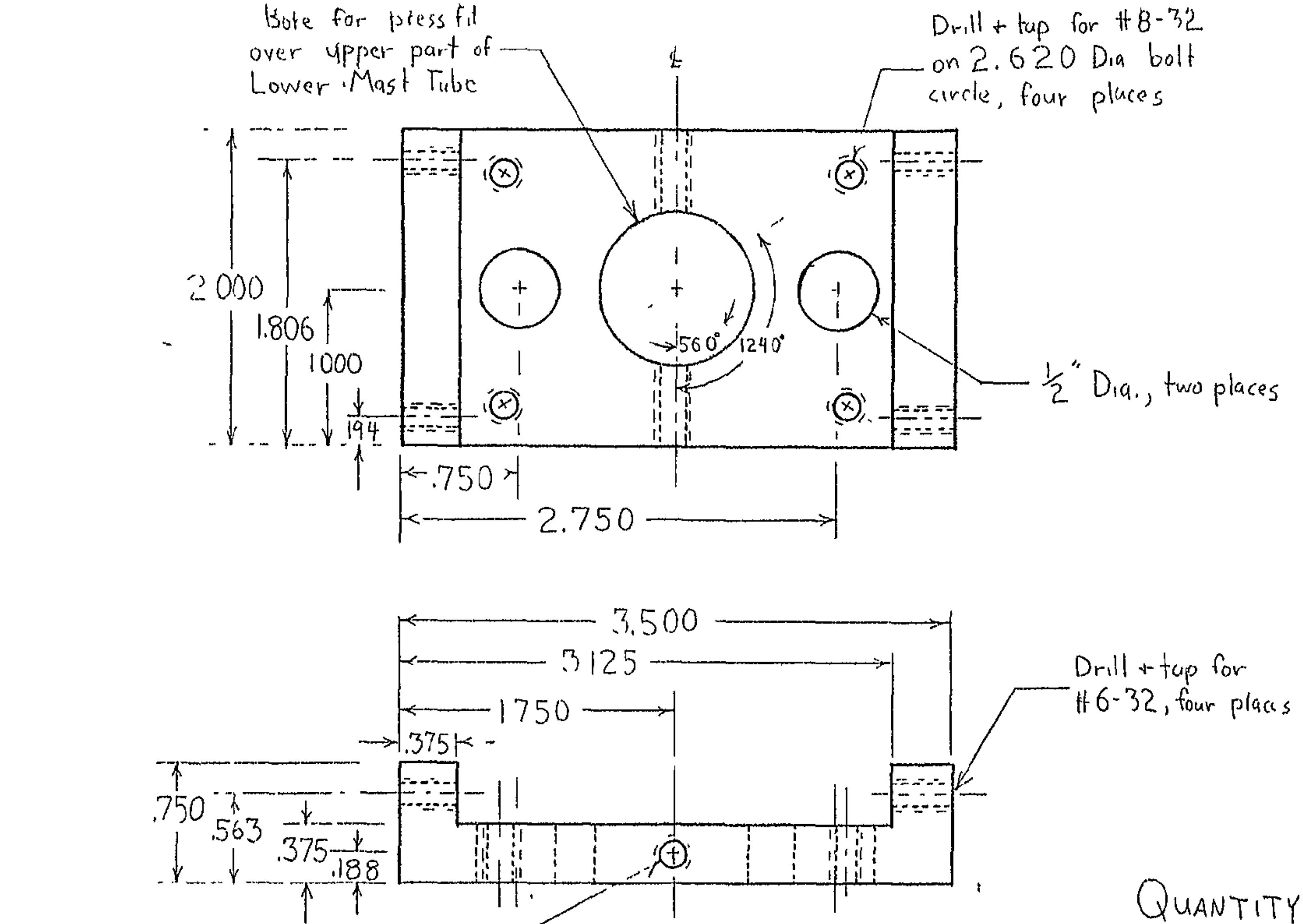

QUANTITY : 1

TOLERANCES (EXCEPT AS NOTED)	REVISIONS NO	DATE	BY	LOWER DETECTOR FRAME SUPPORT, MARS ROVER		
DECIMAL ±	1			DRAWN BY D. Knaub	SCALE 1:1	MATERIAL Alum
FRACTIONAL ±	2			CHK'D	DATE 4-16-78	DRAWING NO
ANGULAR ±	3			TRACED	APP'D	
	4					
	5					

ORIGINAL PAGE IS OF POOR QUALITY

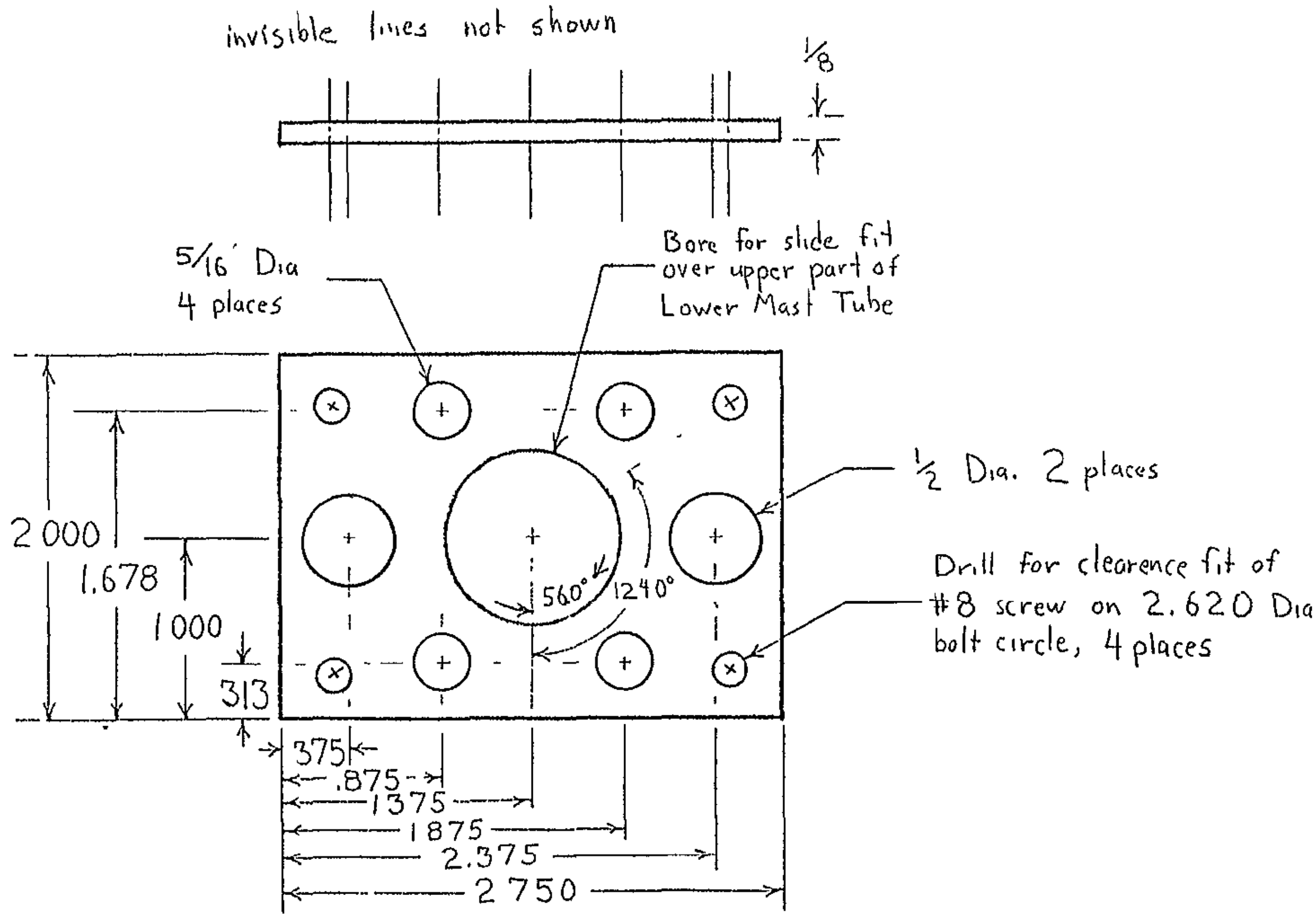

QUANTITY: 1

TOLERANCES (EXCEPT AS NOTED)	REVISIONS - NO	DATE	BY	MAST GEAR SPACER		
DECIMAL ±	1			MARS ROVER		
	2					
FRACTIONAL ±	3			DRAWN BY D Knaub	SCALE 1:1	MATERIAL Alum
ANGULAR	4			CHK'D	DATE 4-15-78	DRAWING NO

DRILL THRU 1.0" DIAM
(2) PLACES ON 2.5" DIAM B.C.
Lightening hole

BORE FOR SLIDE FIT OVER UPPER PART OF LOWER MAST TUBE, ≈ 15/16" DIAM.

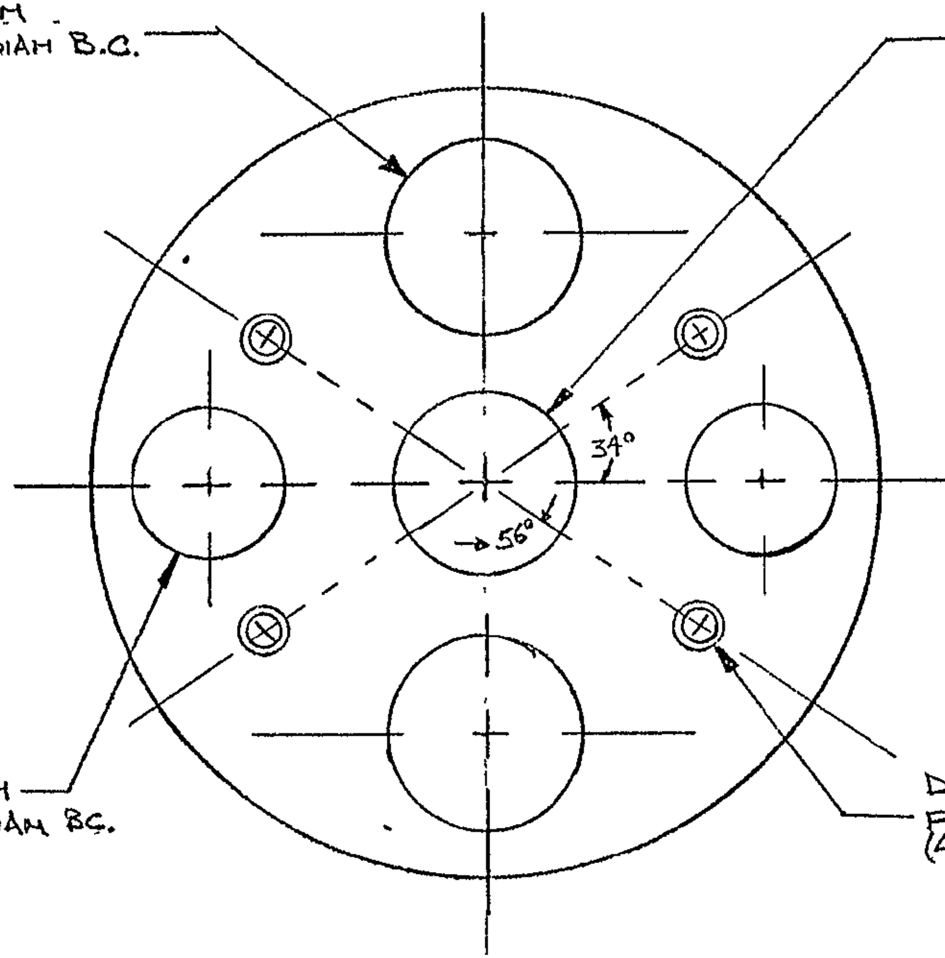

DRILL THRU, .75" DIAM
(2) PLACES ON 2.75" DIAM BC.
Lightening hole

DRILL & COUNTERSINK FOR CLEARANCE FIT OF #8 FLAT HD SCREW,
(4) HOLES ON 2.620 DIAM. B.C.

MAT'L: W. BERG F6453-256
STEEL FLAT GEAR
(SUPPLIED)
≈DIAM 4.0"

QUANTITY : 1

TOLERANCES (EXCEPT AS NOTED)	REVISIONS NO	DATE	BY	
DECIMAL ±	1			MARS ROVER
	2			MAST GEAR
FRACTIONAL ±	3			DRAWN BY RAL / SCALE 1" = 1" / MATERIAL STEEL
	4			CHK'D / DATE 4-24-78 / DRAWING NO
ANGULAR ±	5			TRACED / APP D

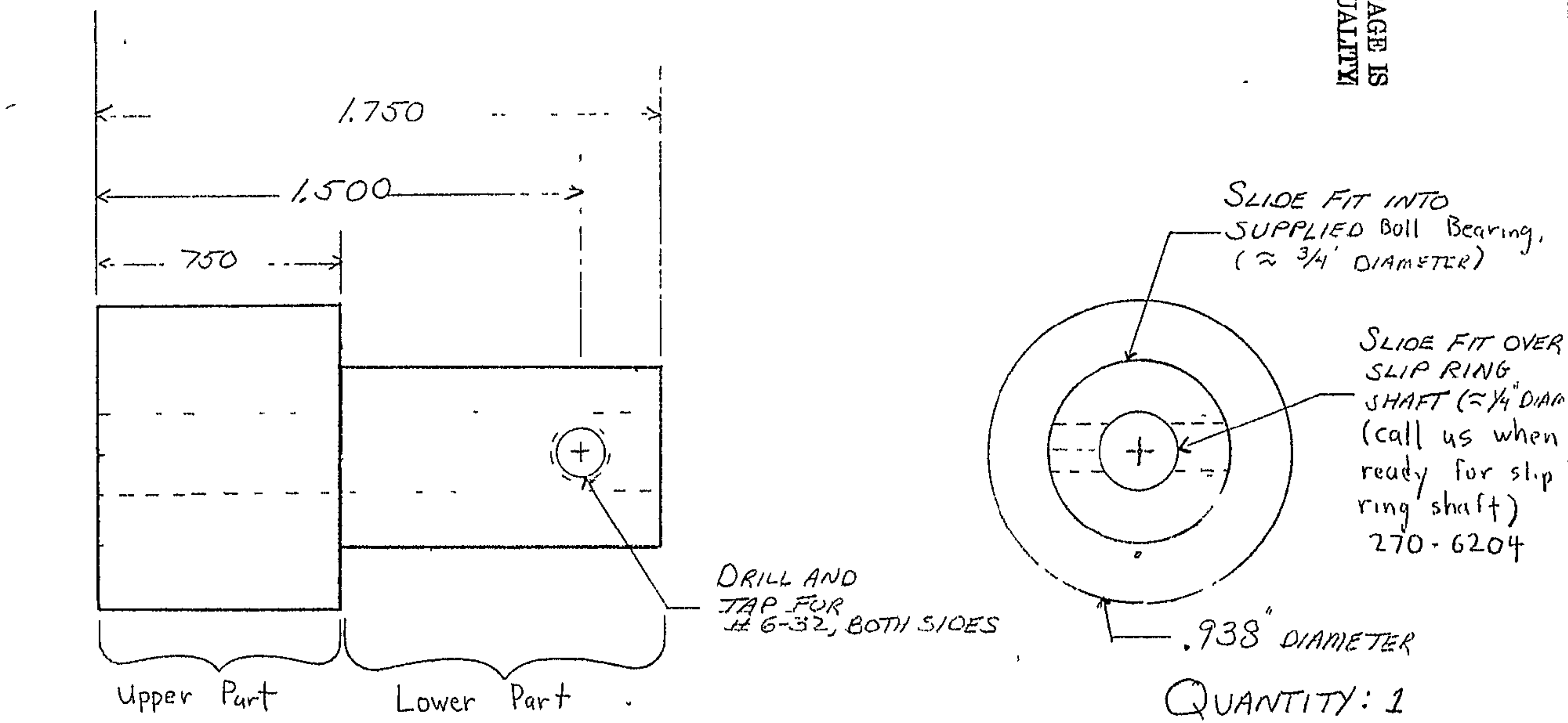

QUANTITY: 1

MATERIAL: STEEL

TOLERANCES (EXCEPT AS NOTED)	REVISIONS NO	DATE	BY
DECIMAL ±	1		
	2		
FRACTIONAL ±	3		
ANGULAR ±	4		
	5		

MARS ROVER		
LOWER MAST TUBE		
DRAWN BY SFM	SCALE 1" = 1/2"	MATERIAL STEEL
CHK'D	DATE 4/12	DRAWING NO
TRACED	APP D	

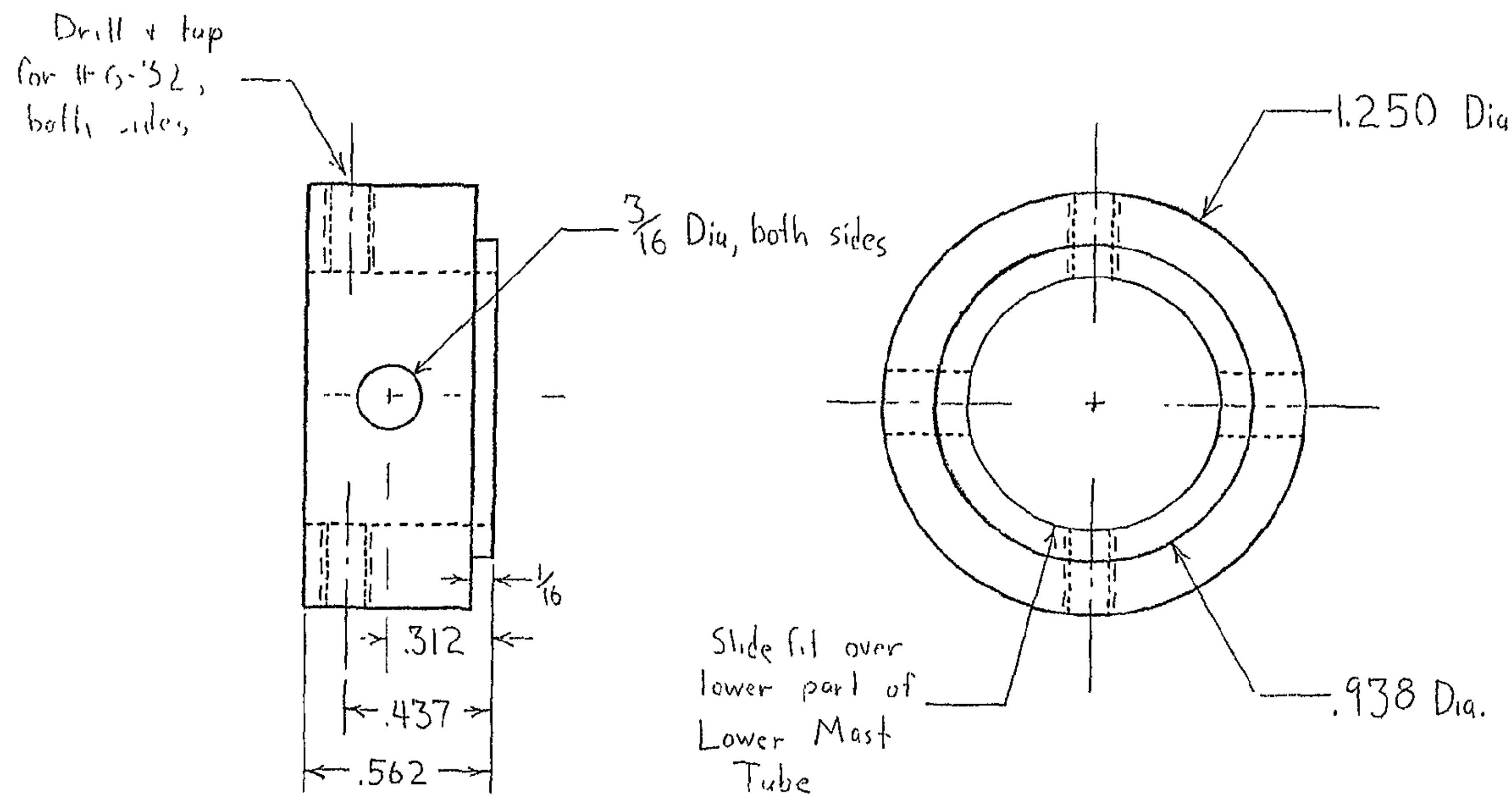

QUANTITY: 1

TOLERANCES (EXCEPT AS NOTED)	REVISIONS NO	DATE	BY	LOWER MAST TUBE SLEEVE, MARS ROVER		
DECIMAL ±	1			DRAWN BY D. [illegible]	SCALE 1 = 1/2	MATERIAL Alum
	2			CHK'D	DATE 4-16-78	DRAWING NO
FRACTIONAL ±	3			TRACED	APP'D	
ANGULAR ±	4					
	5					

When piece is finished:

a) press supplied sleeve bearing into hole

b) mill bearing ends flush with upper and lower surface of Block.

c) Make sure Upper Mast Tube rotates freely in bearing. If not, cut inside of bearing down a little.

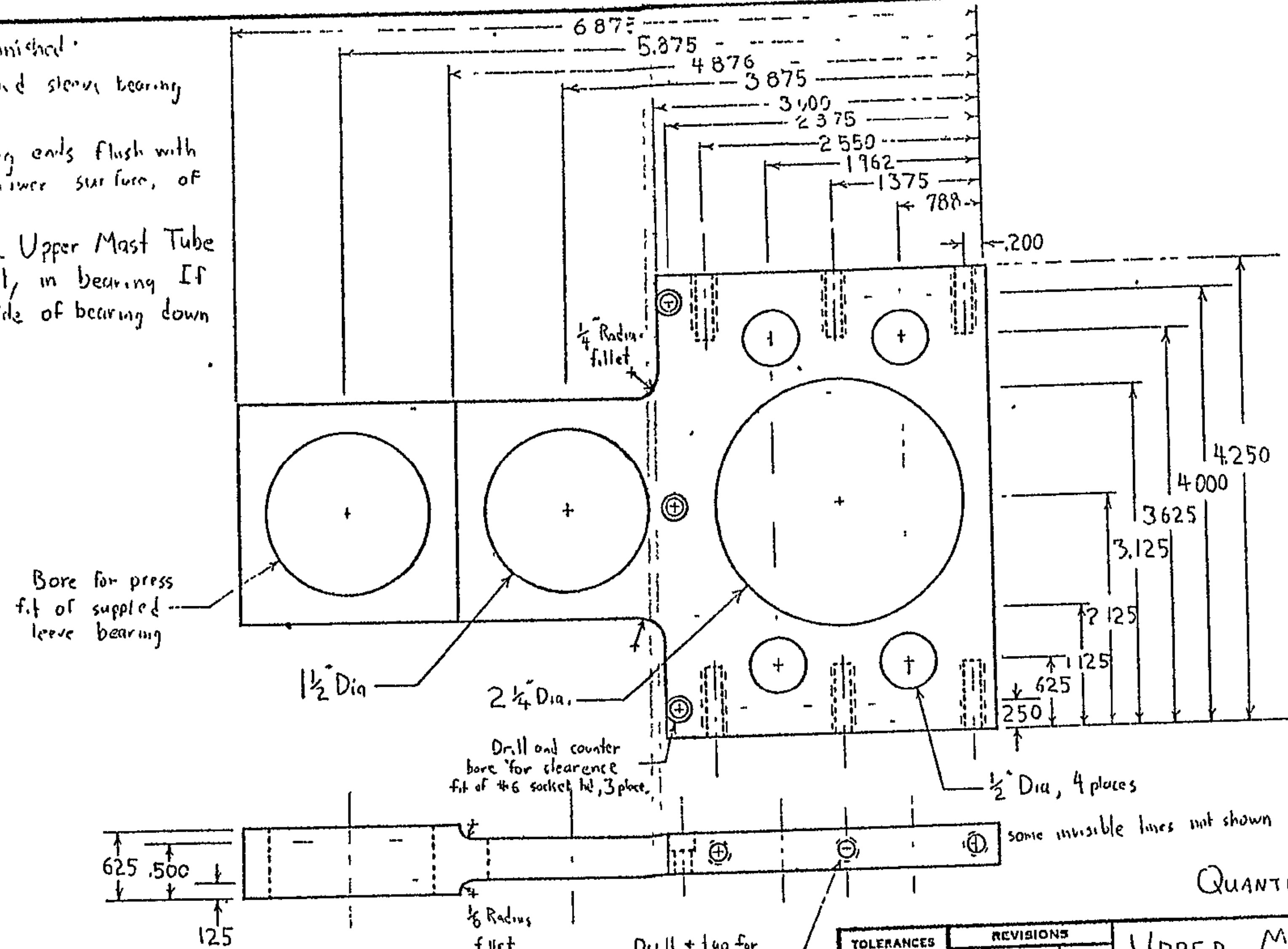

QUANTITY 1

TOLERANCES (EXCEPT AS NOTED)	REVISIONS NO	DATE	BY	UPPER MAST BEARING BLOCK, MARS ROVER
DECIMAL ±	1			DRAWN BY D. Kraub — SCALE 1:1 — MATERIAL Alum
FRACTIONAL ±	2			CHK D — DATE 2-17 — DRAWING NO
ANGULAR ±	3			TRACED — APP D
	4			
	5			

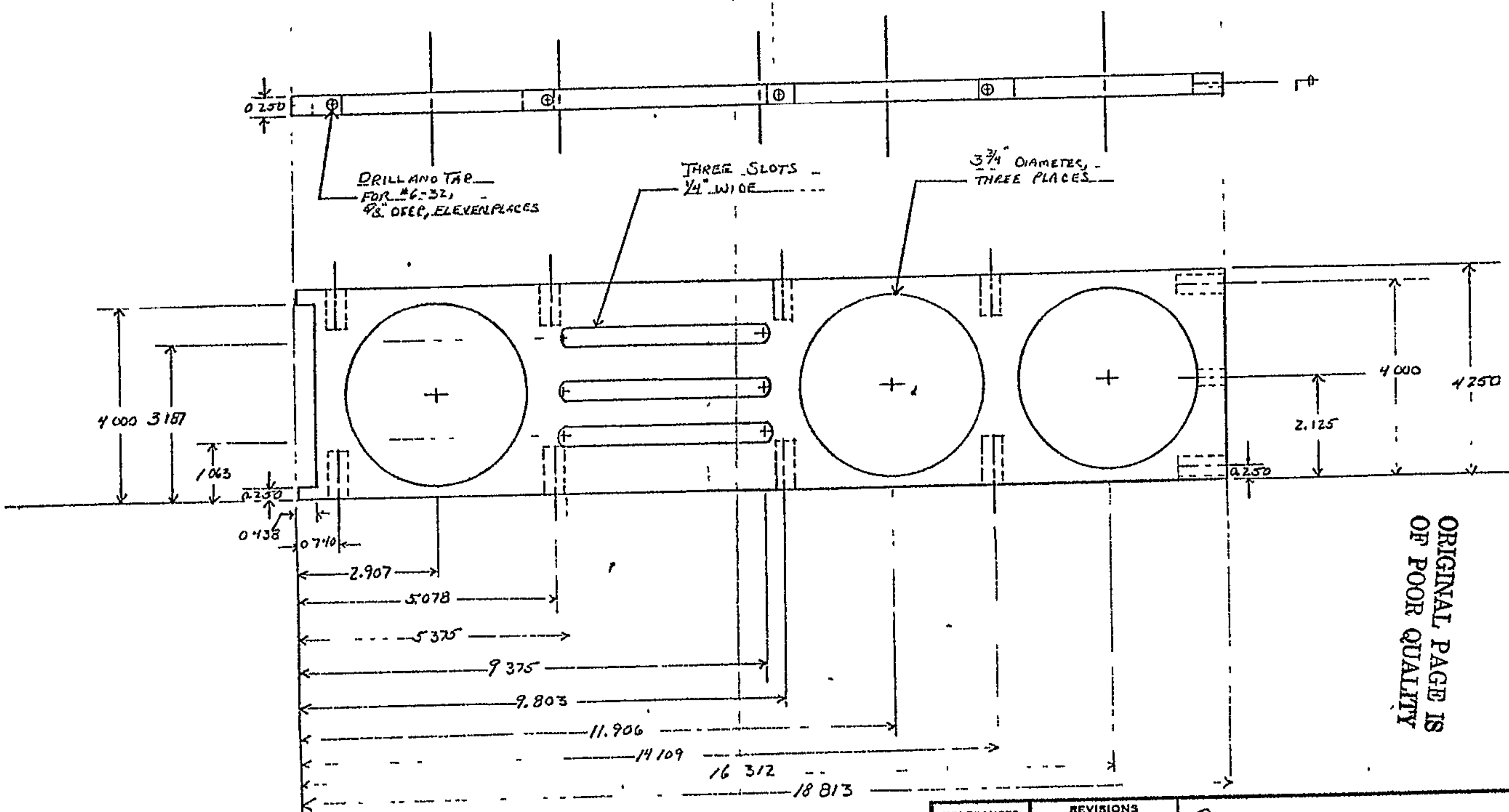

TOLERANCES (EXCEPT AS NOTED)	REVISIONS			QUANTITY: 1		
	NO	DATE	BY	FRONT MAST SUPPORT		
DECIMAL ±	1			DRAWN BY SFM	SCALE 1" = 1/2"	MATERIAL Aluminum
	2			CHK'D	DATE 4/21/73	DRAWING NO
FRACTIONAL ±	3			TRACED	APP'D	
ANGULAR ±	4					
	5					

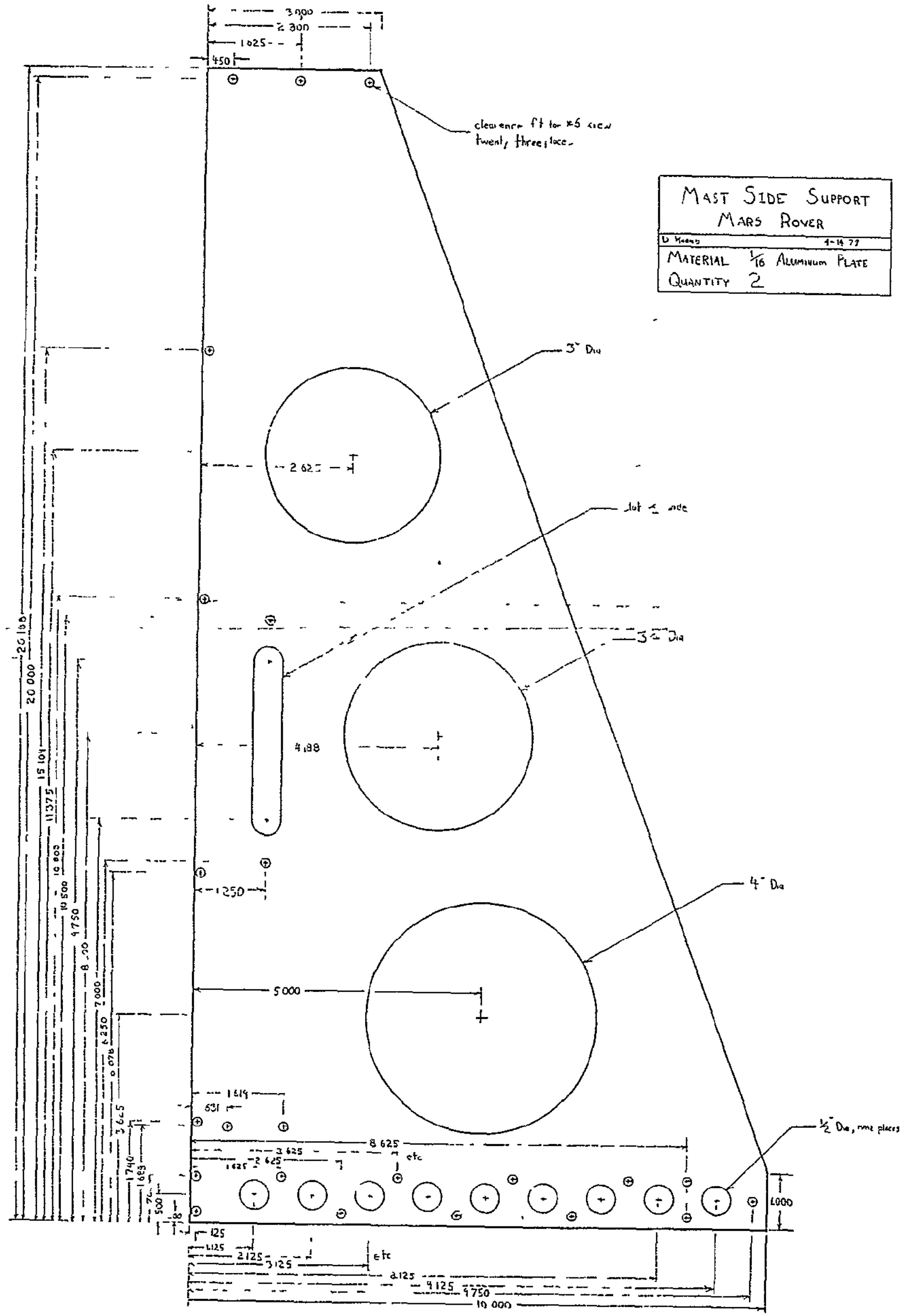

MAST SIDE SUPPORT
MARS ROVER
MATERIAL 1/16 ALUMINUM PLATE
QUANTITY 2
3" Dia
4" Dia
1/2" Dia, nine places

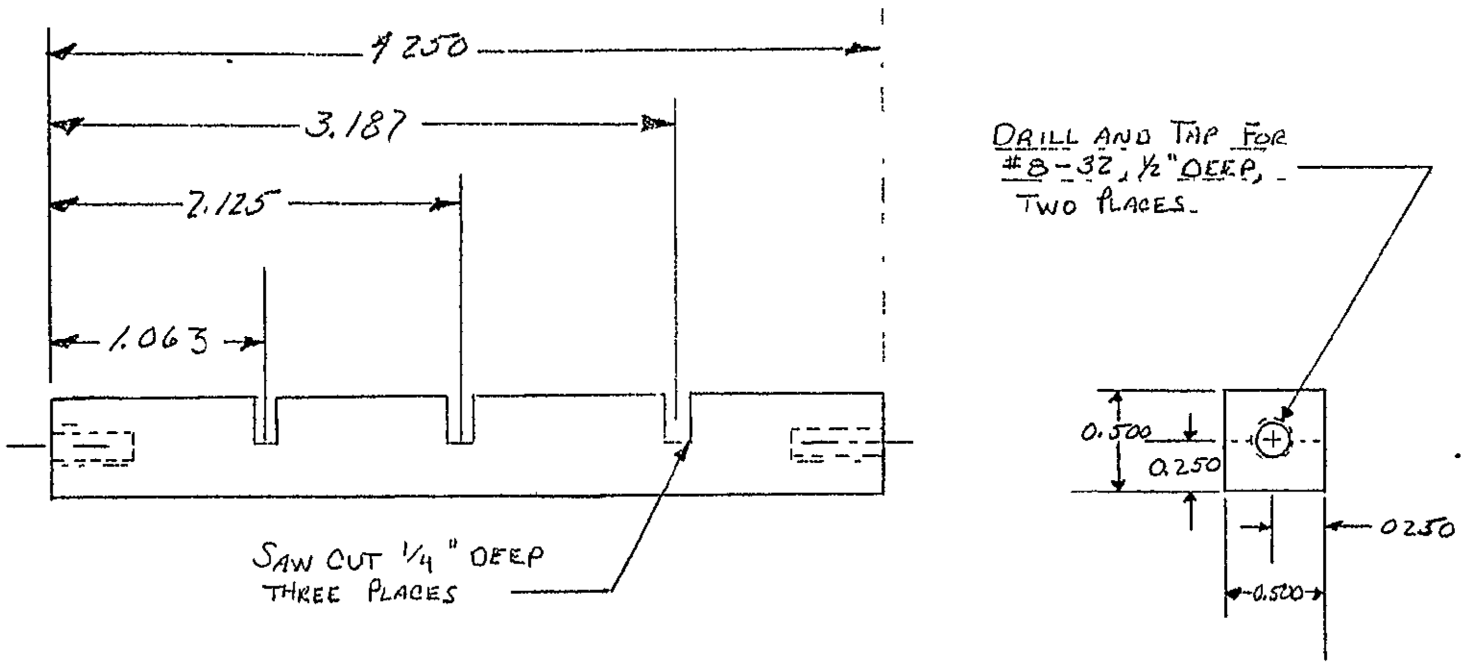

QUANTITY. 2

TOLERANCES (EXCEPT AS NOTED)	REVISIONS			
	NO	DATE	BY	MARS ROVER
DECIMAL ±	1			CIRCUIT BOARD SUPPORTS
	2			
FRACTIONAL ±	3			DRAWN BY SFM · SCALE — · MATERIAL PLEXIGLASS
ANGULAR ±	4			CHK'D · DATE 5/3/78 · DRAWING NO
	5			TRACED · APP D

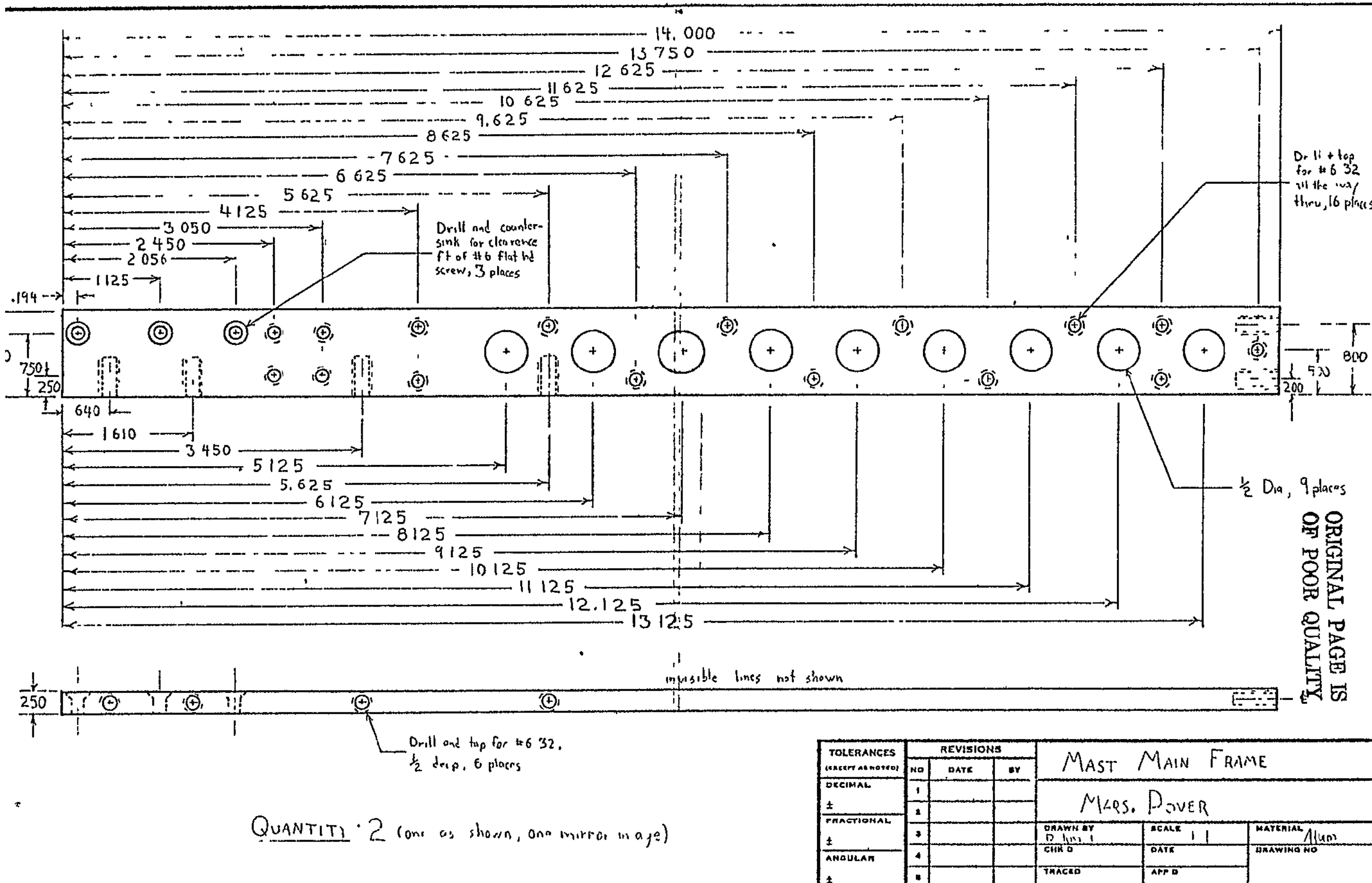
14. 000
13 750
12 625
11 625
10 625
9.625
8 625
7625
6 625
5 625
4125
3 050
2 450
2 056
1125
.194
750
250
640
1610
3 450
5125
5.625
6125
7125
8125
9125
10125
11125
12.125
13125
800
500
200
Drill and countersink for clearance fit of #6 flat hd screw, 3 places
Drill + tap for #6 32 all the way thru, 16 places
½ Dia, 9 places
invisible lines not shown
Drill and tap for #6 32, ½ deep, 6 places
QUANTITY · 2 (one as shown, one mirror image)
TOLERANCES (EXCEPT AS NOTED)
DECIMAL ±
FRACTIONAL ±
ANGULAR ±
REVISIONS
NO DATE BY
MAST MAIN FRAME
MARS. ROVER
DRAWN BY
SCALE 1:1
MATERIAL Alum
CHK'D
DATE
DRAWING NO
TRACED
APP'D

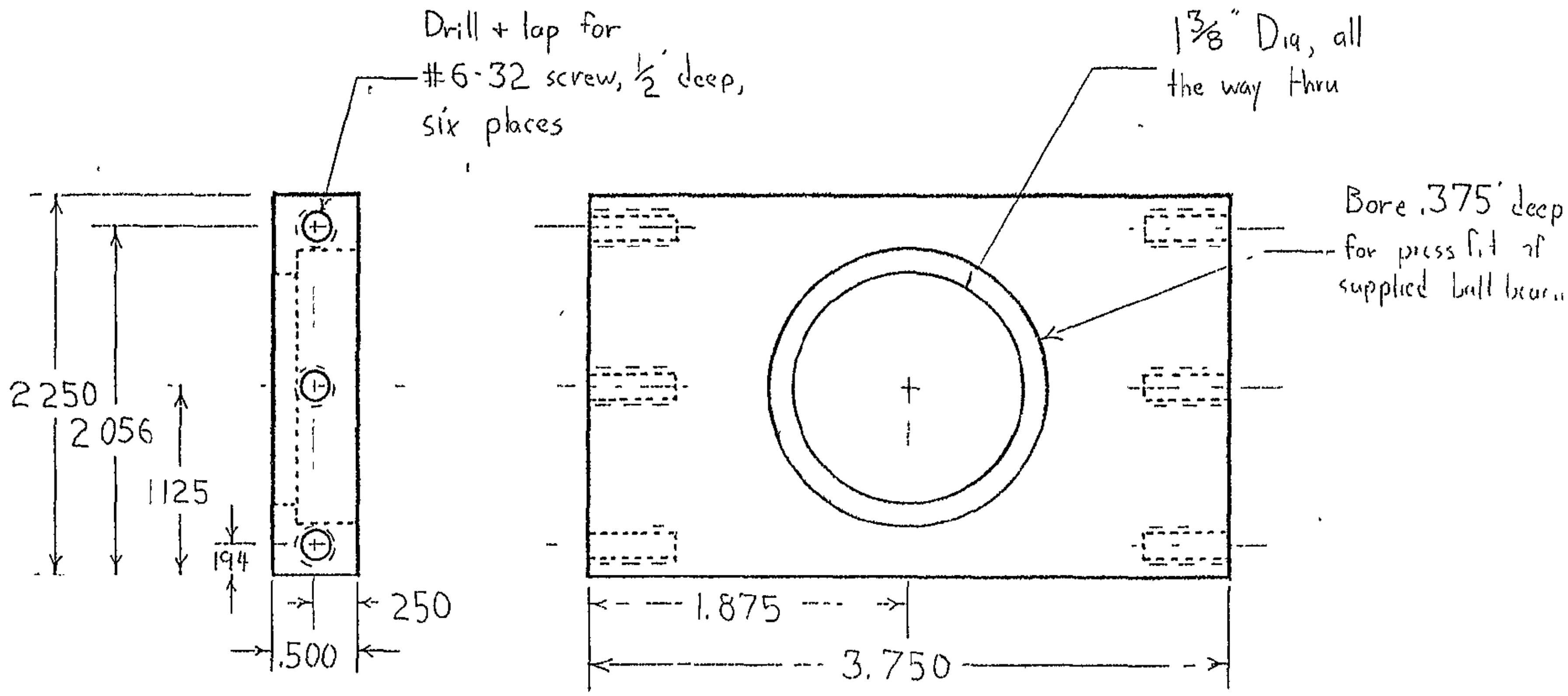

QUANTITY 1

TOLERANCES (EXCEPT AS NOTED)	REVISIONS			LOWER MAST BEARING BLOCK, MARS ROVER		
	NO	DATE	BY	DRAWN BY D. Knaub	SCALE 1:1	MATERIAL Alum
DECIMAL ±	1			CHK D	DATE 4-16-70	DRAWING NO
	2			TRACED	APP D	
FRACTIONAL ±	3					
	4					
ANGULAR ±	5					

TELEDYNE POST 18AE-01E—8½X11

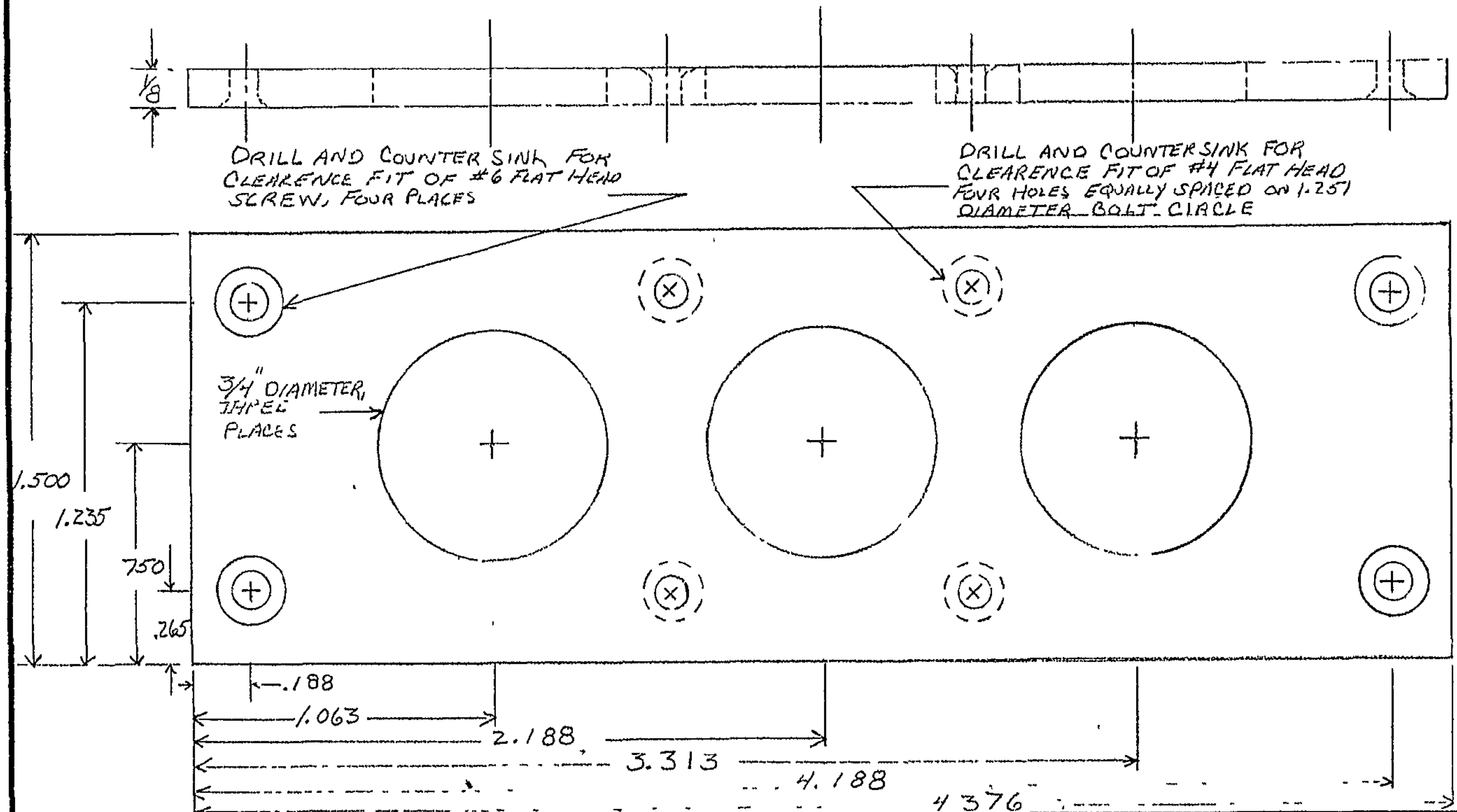

TOLERANCES (EXCEPT AS NOTED)
DECIMAL ±
FRACTIONAL ±
ANGULAR ±

REVISIONS		
NO	DATE	BY
1		
2		
3		
4		
5		

QUANTITY: 1

SLIP RING MOUNTING PLATE

DRAWN BY SFM	SCALE 1" = 1/2"	MATERIAL ALUMINUM
CHK'D	DATE 4/19/78	DRAWING NO
TRACED	APP'D	

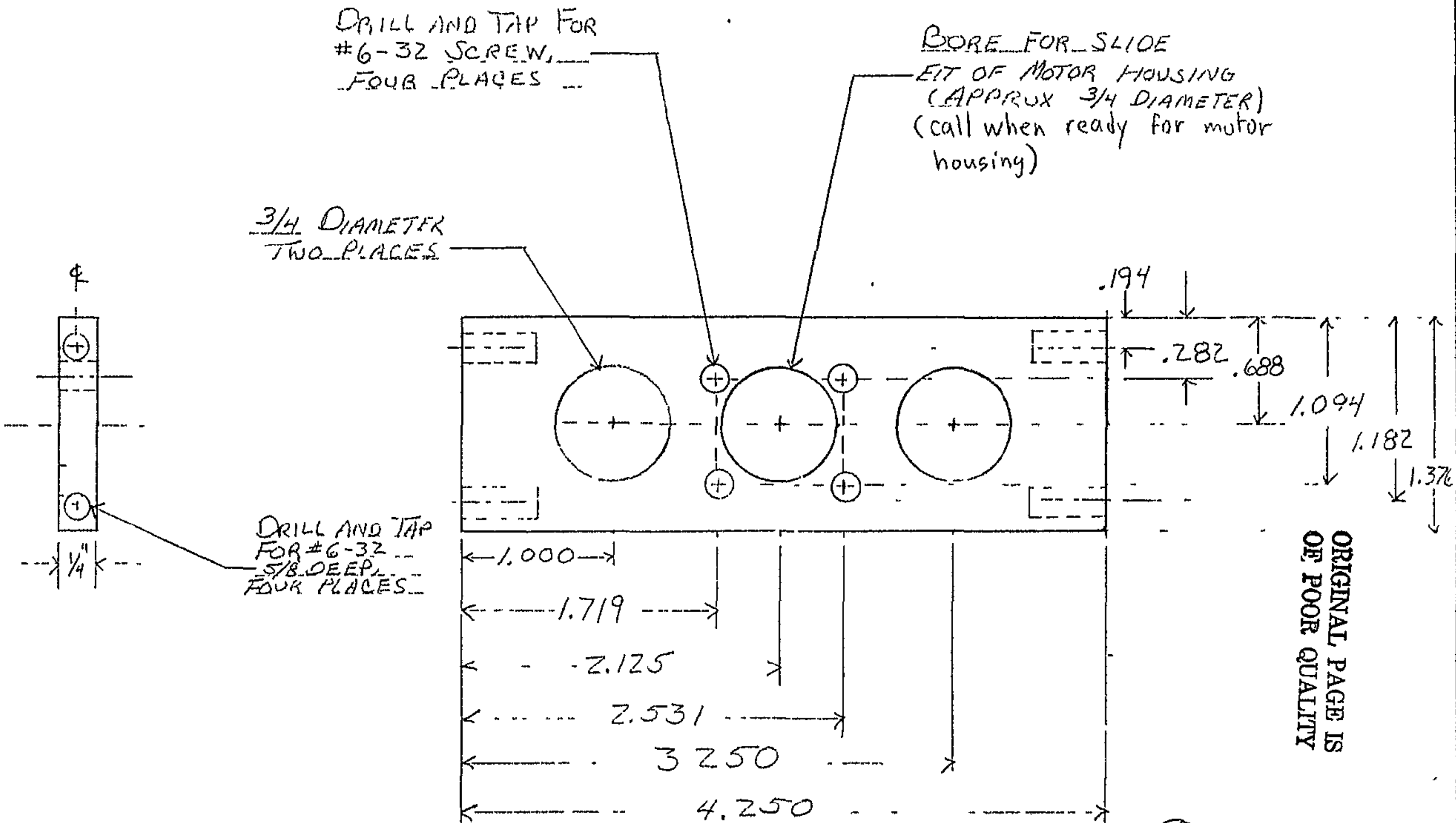

QUANTITY: 1

TOLERANCES (EXCEPT AS NOTED)	REVISIONS			MAST MOTOR MOUNTING PLATE		
	NO	DATE	BY			
DECIMAL ±	1					
	2					
FRACTIONAL ±	3			DRAWN BY SFM	SCALE	MATERIAL Aluminum
ANGULAR ±	4			CHK'D	DATE 4/17/78	DRAWING NO
	5			TRACED	APP'D	

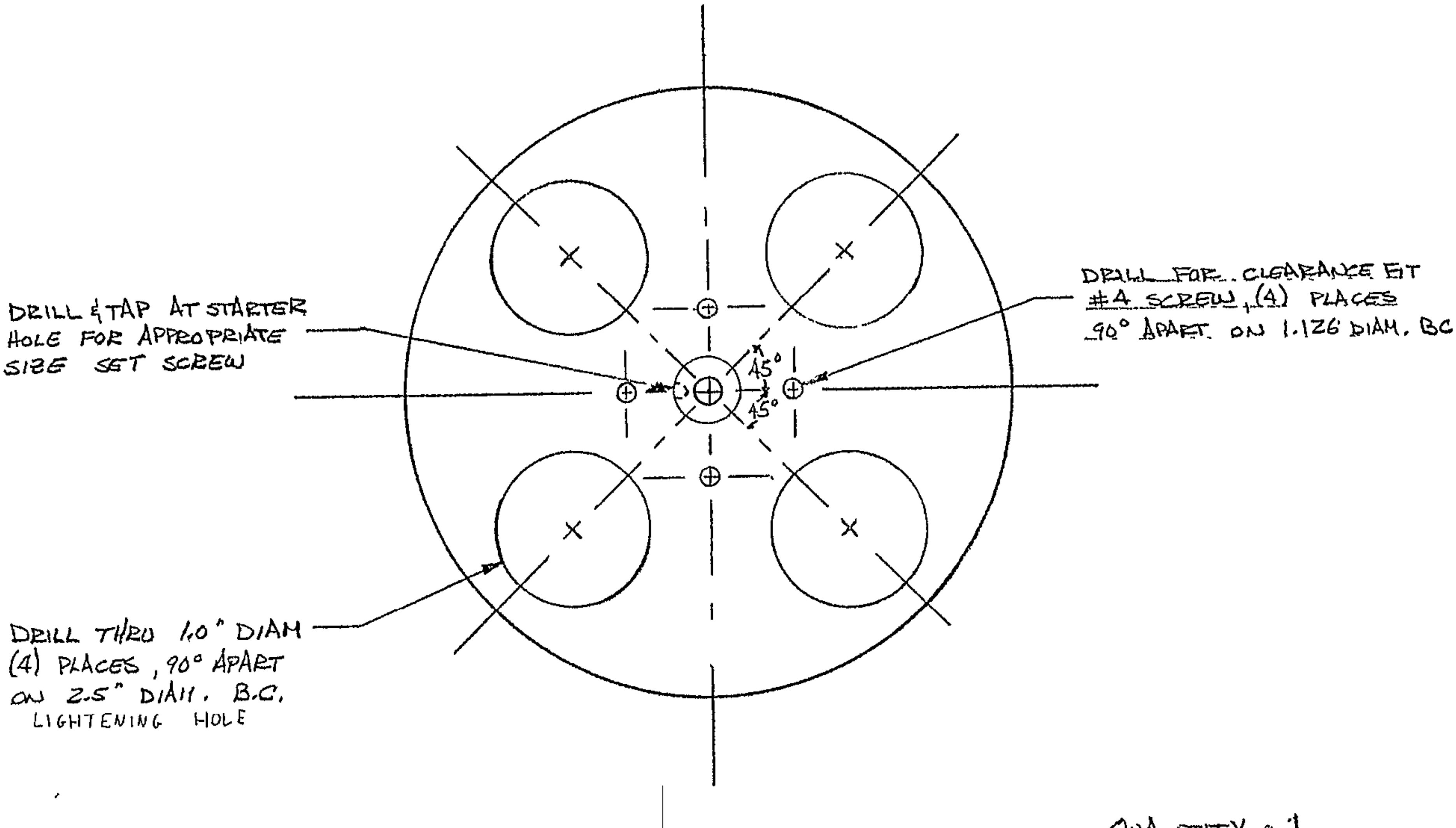

QUANTITY : 1

MAT'L: W. BERG P64519X-256
STEEL HUBBED GEAR
(SUPPLIED)
DIAM 4.0"

TOLERANCES (EXCEPT AS NOTED)	REVISIONS NO	DATE	BY			
				MARS ROVER		
DECIMAL ±	1			MOTOR GEAR		
	2					
FRACTIONAL ±	3			DRAWN BY RAL	SCALE 1:1	MATERIAL Supplied
	4			CHK D	DATE 4-25-78	DRAWING NO
ANGULAR ±	5			TRACED	APP'D	

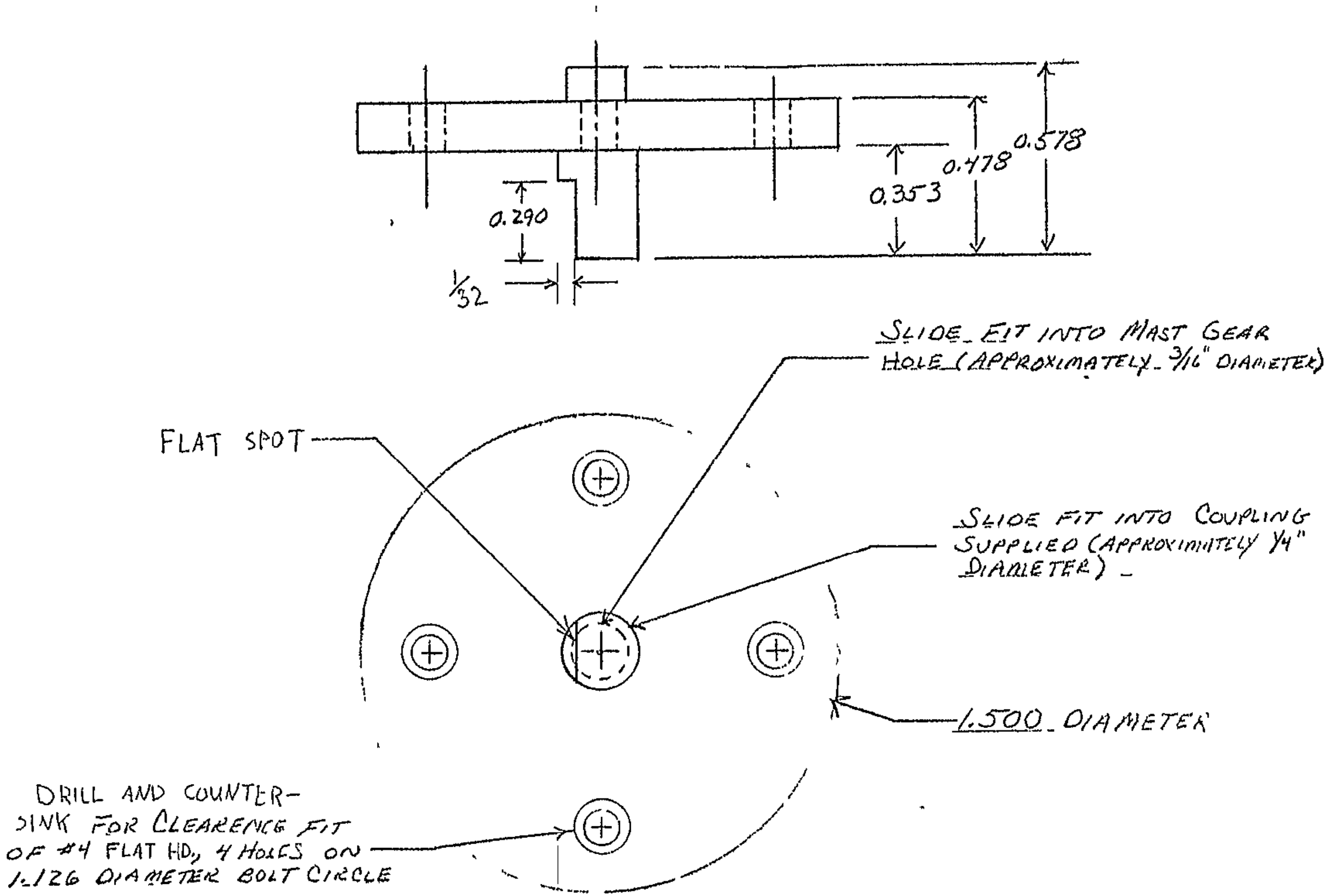

TOLERANCES (EXCEPT AS NOTED)	REVISIONS NO	DATE	BY	QUANTITY 1		
DECIMAL ±	1			MOTOR SHAFT EXTENSION		
	2					
FRACTIONAL ±	3			DRAWN BY SFM	SCALE 1" = 1/2"	MATERIAL ALUMINUM
	4			CHK D	DATE 4/24/73	DRAWING NO
ANGULAR ±	5			TRACED	APP'D	

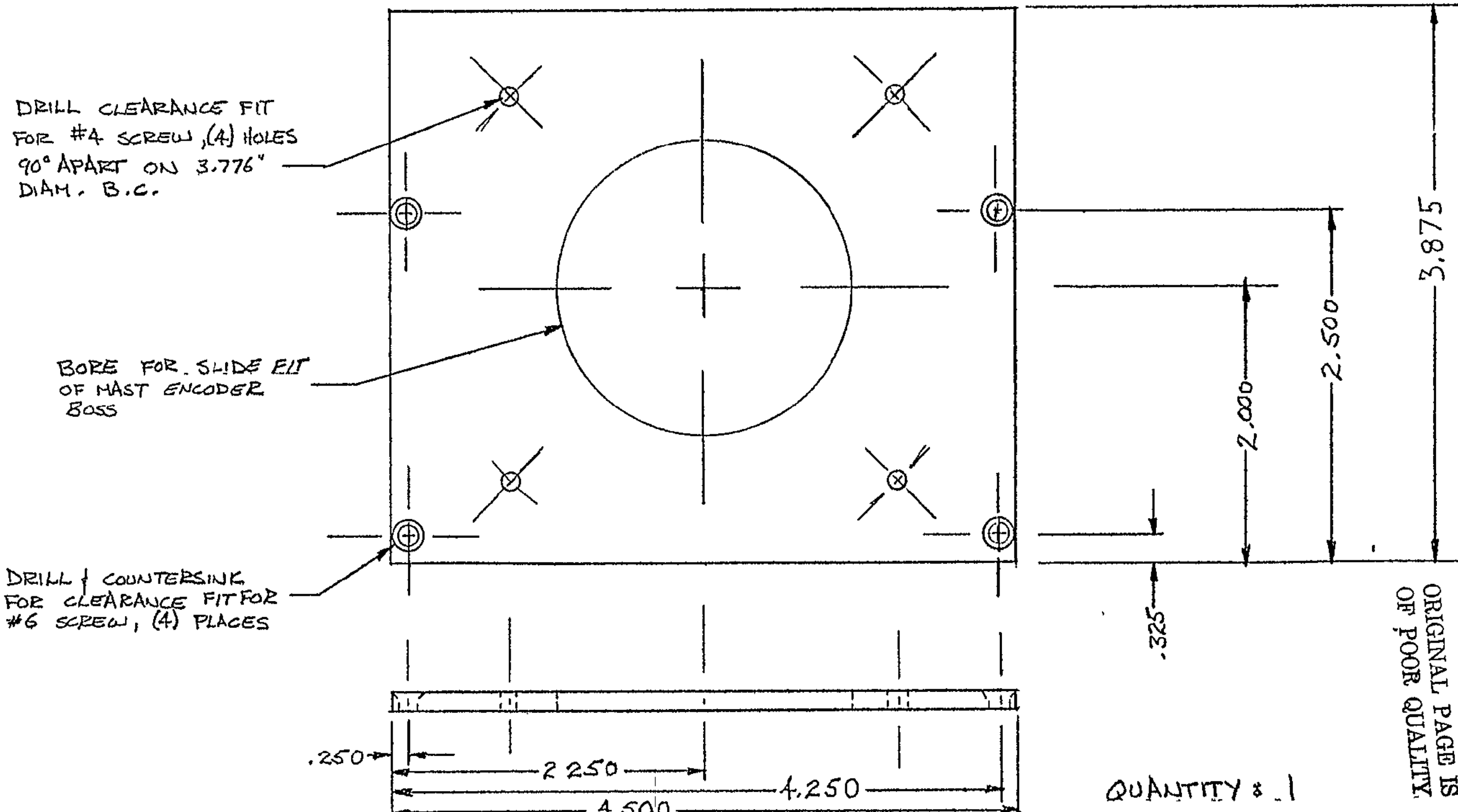

QUANTITY : 1

TOLERANCES (EXCEPT AS NOTED)	REVISIONS			MARS ROVER		
	NO	DATE	BY	MAST ENCODER MOUNTING PLATE		
DECIMAL ±	1			DRAWN BY RAL	SCALE N.T.S	MATERIAL ALUM.
	2			CHK D	DATE 4-19-78	DRAWING NO.
FRACTIONAL ±	3			TRACED	APP D	
ANGULAR ±	4					
	5					

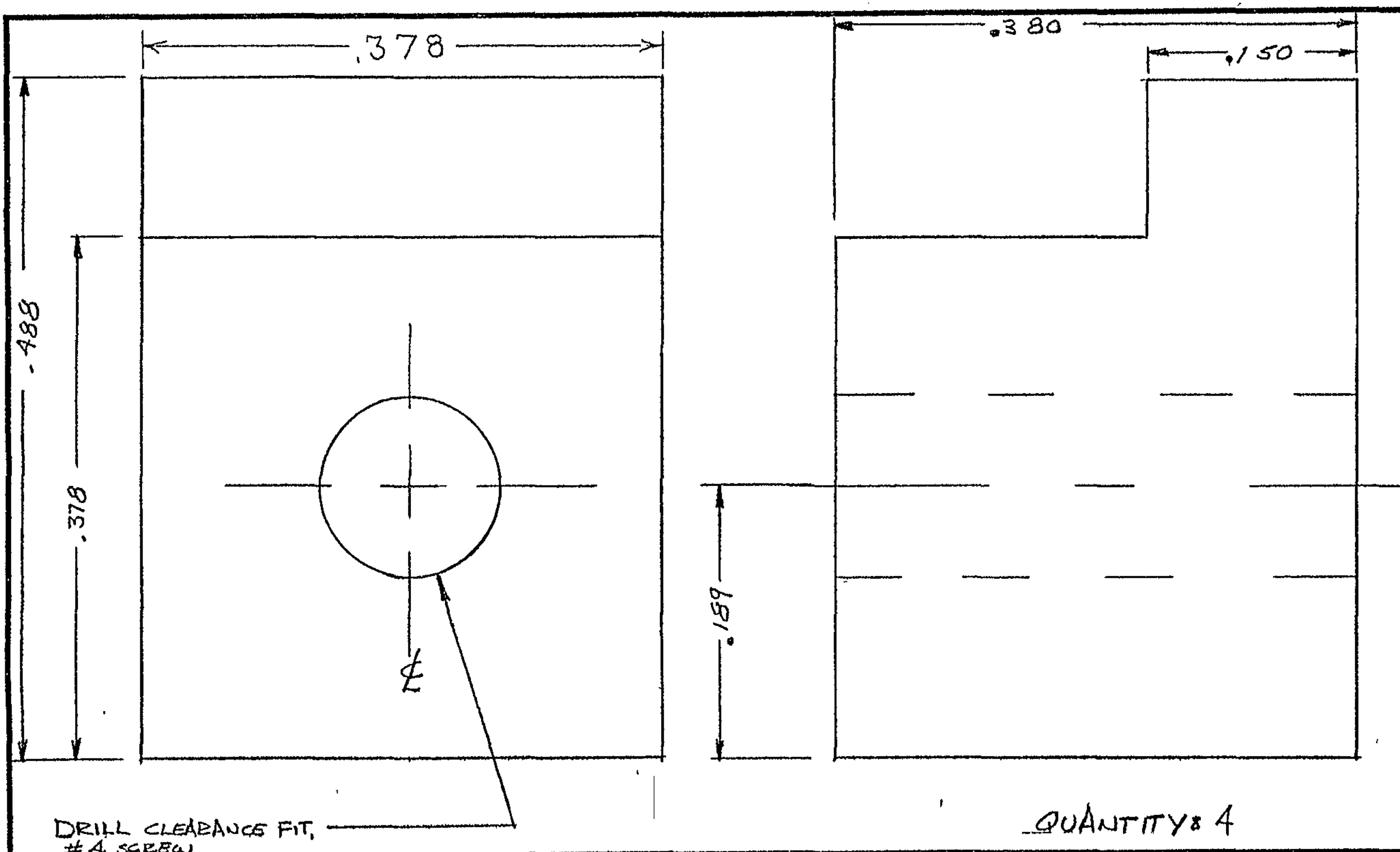

QUANTITY: 4

TOLERANCES (EXCEPT AS NOTED)	REVISIONS		
	NO	DATE	BY
DECIMAL ±	1		
	2		
FRACTIONAL ±	3		
	4		
ANGULAR ±	5		

MARS ROVER

MAST ENCODER CLAMP

DRAWN BY RAL	SCALE 10" : 1"	MATERIAL ALUM
CHK'D	DATE 4-19-78	DRAWING NO.
TRACED	APP'D	

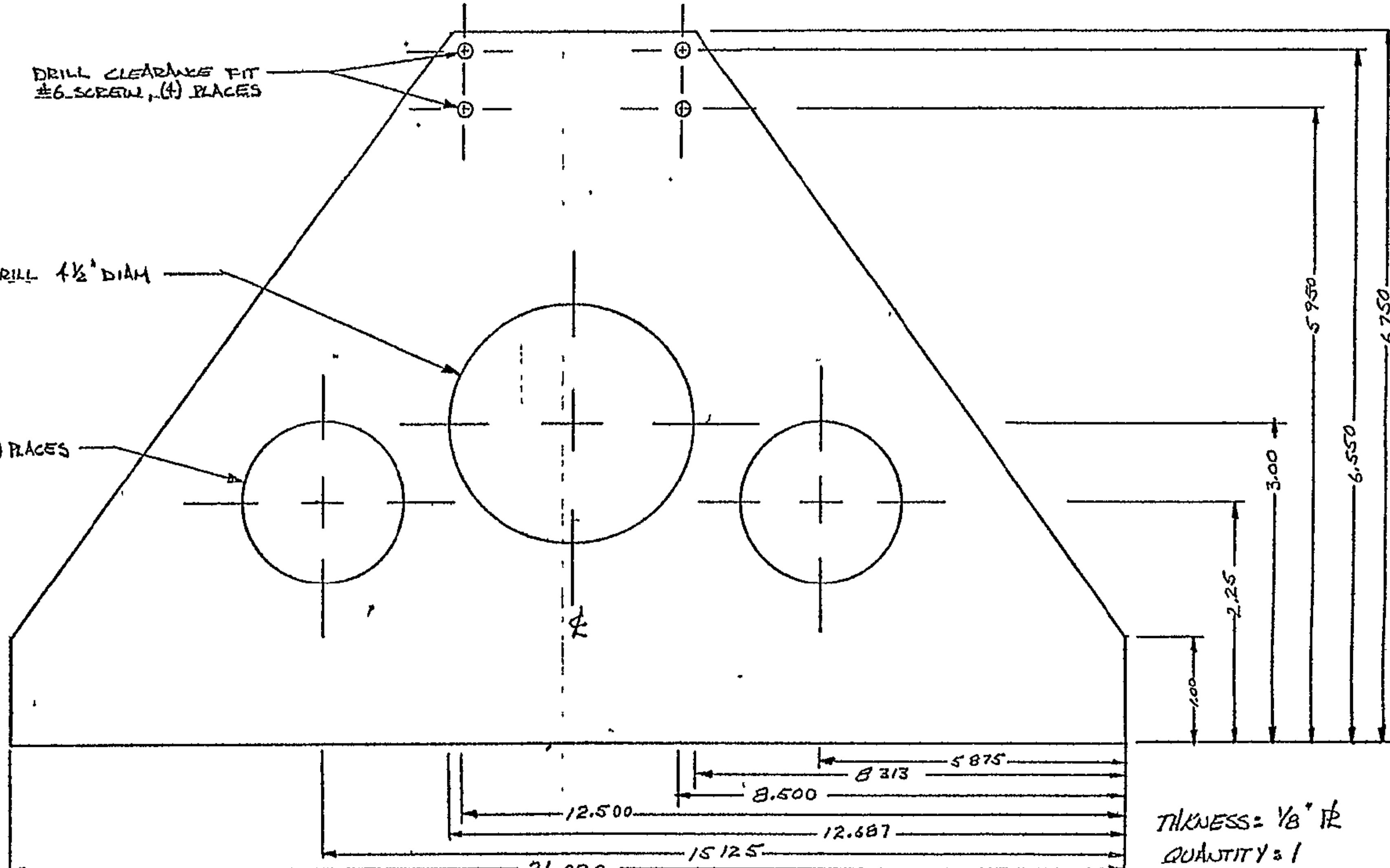

TOLERANCES (EXCEPT AS NOTED)	REVISIONS NO	DATE	BY	MARS ROVER		
DECIMAL ±	1			REAR MAIN FRAME SUPPORT		
	2			DRAWN BY KNL	SCALE N.T.S.	MATERIAL ALUM
FRACTIONAL ±	3			CHK D	DATE 4-19-73	DRAWING NO
ANGULAR ±	4			TRACED	APP D	
	5					

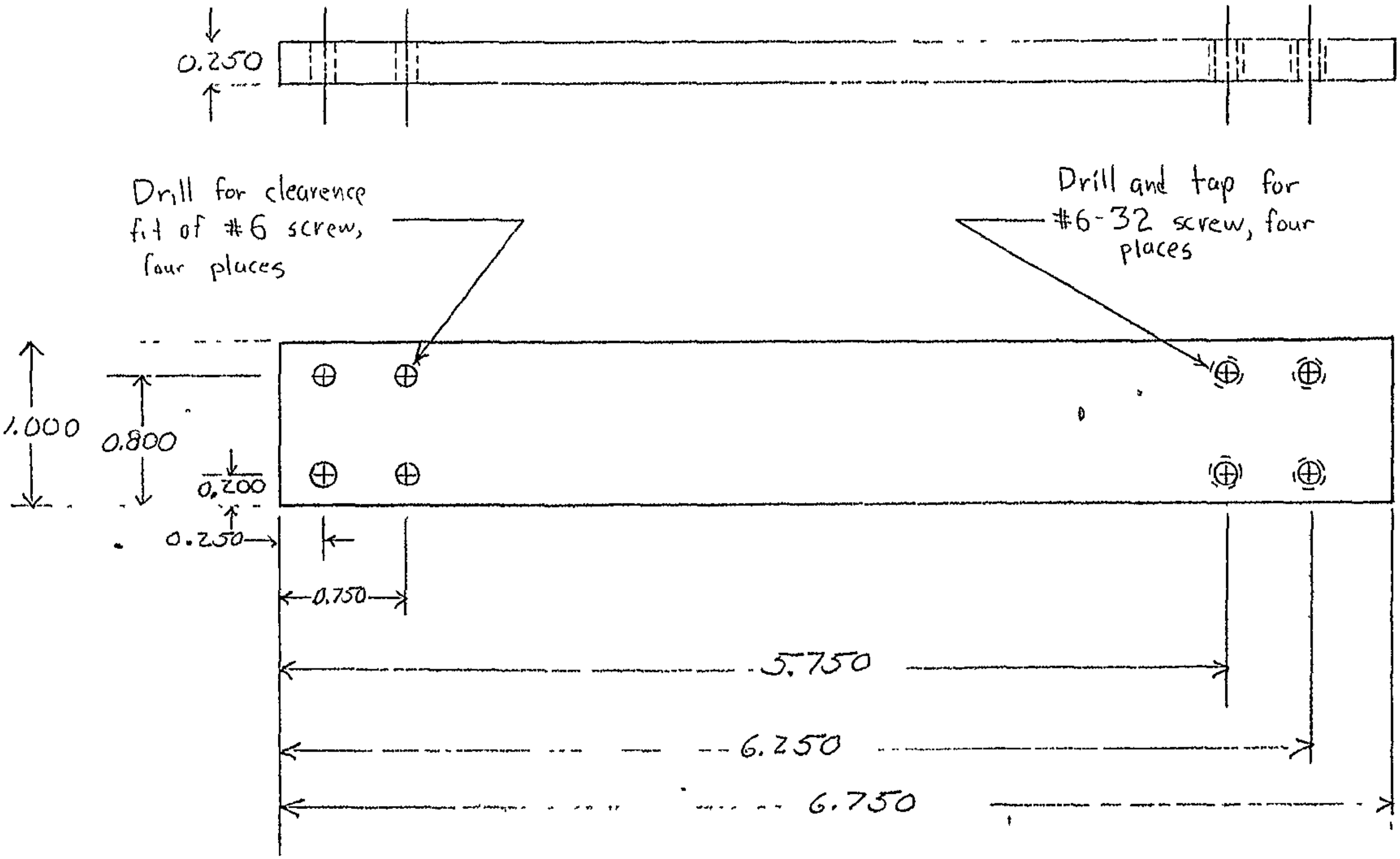

TOLERANCES (EXCEPT AS NOTED)	REVISIONS NO	DATE	BY	QUANTITY: 2		
DECIMAL ±	1			FRONT MAIN FRAME SUPPORT		
	2					
FRACTIONAL ±	3			DRAWN BY SFM	SCALE	MATERIAL Aluminum
	4			CHK'D	DATE 4/19/78	DRAWING NO
ANGULAR ±	5			TRACED	APP'D	

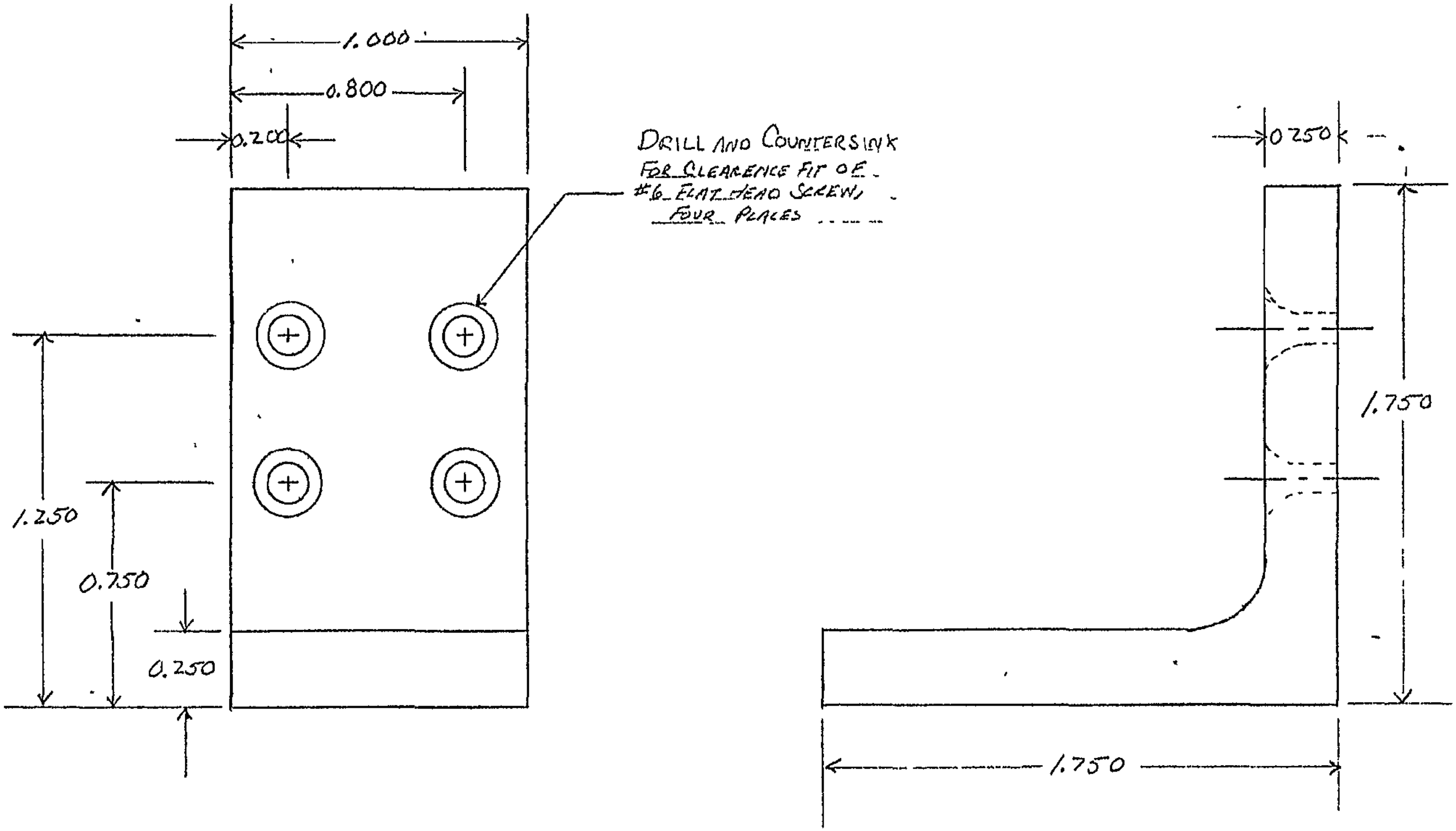

TOLERANCES (EXCEPT AS NOTED)	REVISIONS		
	NO	DATE	BY
DECIMAL ±	1		
	2		
FRACTIONAL ±	3		
	4		
ANGULAR ±	5		

QUANTITY: 2

TEMPORARY MAST SUPPORT BRACKET

DRAWN BY SFM	SCALE 1" x 1/2"	MATERIAL 1-3/4 x 1-1/4 ALUMINUM ANGLE
CHK'D	DATE 4/24/78	DRAWING NO SECTION
TRACED	APP'D	